THE THERMAL AND MOMENTUM STRUCTURE OF AN EMERGING PLUME

A Thesis

Presented to

The Faculty of the Department of Chemical Engineering

University of Houston

In partial Fulfillment

of the Requirements for the Degree

Master of Science in Chemical Engineering

by

Shun-Kwok Tse

December, 1977

ACKNOWLEDGEMENT

The author wishes to express deep appreciation to Professor H.W. Prengle, Jr. for his advice and guidance throughout this research.

Special thanks are due to Dr. Uday Mahagaokar, Professor F.L. Worley, Jr., and Dr. A.A. Siddiqi for their suggestion and inspiration during the courses of the project.

Many friends in the University helped by making the stay at U of H a pleasant and valuable experience.

The financial support from the Department of Chemical Engineering is appreciated.

Finally the author wishes to give special thanks to his family for their care and encouragement.

THE THERMAL AND MOMENTUM STRUCTURE
OF AN EMERGING PLUME

An Abstract of a Thesis

Presented to

The Faculty of the Department of Chemical Engineering

University of Houston

In Partial Fulfillment

of the Requirements for the Degree

Master of Science in Chemical Engineering

---

by

Shun-Kwok Tse

December, 1977

ABSTRACT

An analytical study of the thermal and momentum structure of a compressible, axially symmetric turbulent plume was conducted. Experimental data from the literature and recent remote sensing data were analyzed. A finite-difference numerical technique was used to solve the equations of conservation of mass, momentum, and energy for the axial decay and radial distribution of temperature and velocity. Modifications of the dynamic eddy transfer coefficient given in the literature were used in the solutions. The numerical solutions show good agreement with the literature data and the remote sensing data.

The initial exit velocity and temperature ratio were found to be the most significant properties characterizing the variations of temperature and velocity. The axial temperature and velocity were found to decay faster as the temperature ratio is increased and as the initial velocity is decreased. The flat initial radial profiles were found to change gradually to a Gaussian profile, the characteristic radius describing the temperature being greater than that for the velocity distribution. Correlations for the eddy transfer coefficient, the radial temperature and velocity distribution coefficient, and the length of the core regions were obtained.

A generalized model for the axial decay of temperature and velocity was proposed consisting of, 1) the core regions, where the exit temperature and velocity along the center line remain unchanged; and 2) the fully developed region where the behavior follows that of Priestly's model. The generalized model differs from Priestly's model by addition of the core region, and agrees well with the literature data.

The most significant parameter of the model, the spreading coefficient, was correlated.

Emissions of pollutants as a function of excess air for combustion of gas, oil, and coal were studied. Literature data indicate that the concentration of unburned fuel, and carbon monoxide decrease exponentially as excess air increases from 0-20% excess air, and above 20% most of unburned fuel and CO are negligible. NO_x concentration increases approximately linearly as a function of excess air from 5-20%, and above 25% increases very slowly or remains constant. SO_2 emissions primarily depend on the sulfur content of the fuel.

Signal processing of the remote sensing infrared interferometry-spectroscopy data was studied and improved. The well-known CO P-R infrared structure was simulated from theory, and also the spectrogram was simulated in a manner corresponding to the field experiment. Interferences, not expected from the predicted composition of the plume, were found at the edges of the radiation envelope; a new frequency range was selected to minimize this effect. A new average value for the absorption coefficient was obtained from the theoretical intensity distribution of the spectral lines. These improvements produced a 10% increase in concentration for a high CO run.

TABLE OF CONTENTS

LIST OF FIGURES

Figure		Page

Figure		Page
7-1	Infrared Emission Spectrum of Plume from Furnace Operated with Zero Excess Air	
	(a) 0 cm^{-1} -1800 cm^{-1}	97
	(b) 1800 cm^{-1} - 3600 cm^{-1}	98
7-2	The Vibration-Rotation Spectrum of CO under High Resolution	100
7-3	Simulated Spectrogram of CO	102
7-4	Simulation of Spectrogram	107
7-5	Simulated Spectrogram of CO Resembling Experimental Condition with Starting Sampled Point at	
	(a) 1993.12 cm^{-1}	109
	(b) 1993.32 cm^{-1}	110
7-6	CO Spectrogram from Experimental Data	111
A-1	The Finite-Difference Grid System	121

LIST OF TABLES

NOMENCLATURE

Upper Case

A_1, A_2	integration constants given by Eq. (3-21) and (3-22)
D	jet diameter
F	radial heat flux
M	initial jet Mach number
N_{Pr}	Prandlt number
N_{Ec}	Eckert number, defined by Eq. (2-17)
P, P_a	dimensionless density, ρ/ρ_o, and ρ_a/ρ_o respectively
R	dimensionless radial coordinate, r/D
R_m	the radial extent of the jet
T	dimensionless temperature, $(t - t_a)/(t_o-t_a)$
U_Z, U_R	dimensionless verticle and radial velocity respectively, u_z/u_o, u_r/u_o
Z	dimensionless axial coordinate, z/D
Z_{cv}, Z_{ct}	dimensionless core length for momentum and heat flux of the jet

Lower Case

c_p	heat capacity
r	radial coordinate of the plume
t, t_a, t_o	temperature, ambient temperature, and initial jet temperature
t_m	temperature at r=0., centre line
$t_{A\ rms}$	root mean square of the fluctuating temperature component
t_A	average area integrated temperature
u_r, u_z, u_o	radial, vertical, and initial jet velocity respectively

u_{zm}	vertical velocity at r=0, centre line
z	vertical coordinate of the jet
z_o	$D/2\alpha$
z'	vertical coordinate described by equation (3-19)

Greek Letters

α	spreading coefficient of the jet
α_t, α_v	spreading coefficient for temperature and velocity decay respectively
β	constant for the radial distribution of temperature in Eq. (4-1)
ΔR	finite difference step size in radial direction
Δt_m	$t_m - t_a$
Δt_o	$t_o - t_a$
ΔZ	finite different step size in axial direction
ε_v	eddy kinematic viscosity
η_L	constant for the radial distribution of velocity in Eq. (4-2)
ρ, ρ_a, ρ_o	density, ambient air density, and exit density of of the jet
τ	radial shear stress

CHAPTER I

INTRODUCTION AND PURPOSE

In recent years considerable interest has been shown in the monitoring of gaseous pollutants from stationary emission sources by the use of electro-optical techniques. Prengle and coworkers [17] have conducted investigations of remote sensing infrared radiometry-spectroscopy (IRRS) techniques using Fourier transform spectroscopic equipment to determine the temperature and concentration of pollutants in an emerging plume.

A subject of great relevance to meterologists, engineers and physicists studying the behavior of gaseous pollutants is the thermal and momentum structure of an emerging plume into the atmosphere. Of particular interest is the problem of determining the mechanism by which the energy in the hot gases dissipates and contributes to the dispersion of pollutants into the atmosphere.

So far it has been extremely difficult to make thermal and momentum measurements on actual plumes of substantial size, and essentially impossible to follow the temperature and velocity gradients, axially and radially. Some measurements using a helicopter have been attempted, but these results have definite limitations since the process of measurement alters the flow pattern of the plume [10,28,6]. Hence no body of information exists on the phenomena involved, except on emerging laboratory jets in which the flow is also disturbed by the measuring device [20].

Mahagaokar and Prengle [14] by the application of the aforementioned IRRS technique were able to obtain some preliminary results consisting of axial gradients, radial gradients, and turbulent temperature fluctuations within the plume.

Several models exist in the literature for the theoretical treatment of the behavior of a continuous plume of bouyant gas of smoke moving through various types of atmospheres. A thorough review and critique of these theoretical investigations has been done by Briggs [5] in the light of the usefulness of these treatments for calculating the height to which plumes in different conditions will rise.

The first analysis of this problem was done by Schmidt [25] who studied the behavior of convective plumes of air above steady point and line sources of heat in a uniform incompressible atmosphere. Schmidt observed that a turbulent plume is physically confined to a conical region and found the distribution of temperature and velocity by balancing the horizontal turbulent transfer of heat and momentum against the vertical transfer by convection making an allowance for the effect of buoyance. Schmidt assumed geometrical and mechanical similarity of the processes in horizontal sections of the plume, and used

Prandlt's mixing length theory of turbulence to find the complete forms of the velocity and temperature profiles. He experimentally verified the calculated results for the point source by using small electrically heated grids in air.

Later Rouse, Yip, and Humphreys [22] treated the same problem for heated plumes in calm air by assuming eddy viscosity diffusion of the buoyance and momentum by a process analogous to molecular diffusion. The treatments by Schmidt and Rouse, et al. resulted in solutions in which the radius of the plume $r(z)$ is proportional to the distance z from the source, the vertical velocity u_z on the plume axis is proportional to $z^{-1/3}$, and the temperature excess (on the plume axis) above the ambient temperature Δt is proportional to $z^{-5/3}$.

About the same time, Sutton [26] developed a simple theory for a buoyant in a calm atmosphere. As in Schmidt's theory, Sutton assumed the excess temperature in the jet, Δt, to be small compared to the absolute temperature of the air as a whole and took the missing length to be proportional to the radius of the jet at any level. He departed from the Prandtl theory by supposing that the velocity fluctuations in the jet are proportional to the rate of decrease of velocity downstream. The rate of entrainment of air by turbulent mixing on the boundary of the jet is expressed as a function of the exposed area, the velocity fluctuation and the mixing length. Sutton obtained an analytical solution in terms of an unknown constant which he determined from experimental observations, on smoke clouds. Contrasted with Schmidt's solution, $r(z)$ is proportional to $z^{0.88}$, u_z is proportional to $z^{-0.29}$ and Δt is proportional to $z^{-1.46}$. Sutton showed that his solution fits the experimental data of Schmidt slightly better than Schmidt's original solution.

The problem of convection from a point source was also studied by Batchelor [3] who used dimensional analysis and included the phenomenon of stratification of the environment, i.e., variation of the atmospheric temperature with height above the source. He found power law expressions for the mean plume velocity and temperature as functions of height in an unstable atmosphere whose potential temperature gradient is also approximated by a power law. Batchelor observed that the mass flow across a section of the plume is proportional to $z^{5/3}$ and this increasing mass flow is provided by entrainment of stationary air at the edge of the plume. He found that the required horizontal mean inflow velocity is proportional to the mean vertical velocity and the ratio of the two determine the cone angle of the plume.

A generalized model for the turbulent convection from maintained and instantaneous sources under different types stratification was developed by Morton, Taylor, and Turner [15]. They used Taylor's entrainment hypothesis and assumed that the lateral profiles of vertical velocity and buoyance are similar at all heights and that the fluids are incompressible and do not change volume on mixing, and that the local variations in density throughout the motion are small compared to some reference density. The governing equations are derived in nondimensional form for the conservation of volume, momentum and buoyance where the buoyance is related to the excess temperature Δt through a coefficient of cubical expansion. A numerical solution is obtained for the case of the maintained source which leads to a prediction of the final height to which a plume of light fluid will rise in a stable stratified environment. The constant governing the rate of entrainment was estimated by comparing the theory with experimental results.

The problem of a convective plume from a finite circular source under different conditions of environmental stratification was also considered by Priestly and Ball [18]. Their treatment is similar to the one above except that Taylor's entrainment hypothesis is replaced by an energy equation involving an assumption above the magnitude and distribution of the turbulent stress.

All the above models assumed that the flow was fully developed and similarity of the profiles exists. The fact that the emerging plume only becomes fully developed at a certain number of nozzle diameters downstream from the stack exit was not considered. Mahagaokar's experimental data (average area integrated temperature) show that near the stack exit, the axial gradient is small, whereas the above models predict a large gradient.

The purpose of the work described in this thesis is: (1) to study the thermal and momentum structure of an emerging plume; and (2) to propose a model for the axial and radial temperature and velocity decay of the emerging plume.

As already mentioned, temperature and velocity data for emerging plumes are very scarce, only laboratory free jet data are available. Several sets of free jet experimental data are used to verify the solutions for the temperature and velocity distribution of the emerging plume, and used for correlations. The term "free jet" is used most of the time in place of "emerging plume," as a more appropriate and convenient term.

Chapters reporting work on 1) Emissions as Function of Excess Air, and 2) Improved IRRS Signal Processing Method are included as a matter of record.

CHAPTER II

THEORY OF EMERGING PLUME

A. Introduction

In order to compare the average area integrated temperature, t_A, of the field of view (F.O.V.), see Figure 2-1, obtained by the IRRS technique [14] with that from theoretical mathematical solutions, it is necessary to develop a good general solution for velocity and temperature variations in a free jet. Mahagaokar's [14] experimental data for the axial and radial temperature distribution are summarized in Tables 2-1 and 2-2.

A computational technique based on finite difference solution of the boundary layers forms for conservation of mass, momentum and energy, was developed to calculate both the axial velocity and temperature decay and the radial distribution of velocity and temperature. The method can be extended to a variety of boundary conditions different than the ones used in the present work. Corrsin and Uberoi's [9] and Tomich and Weger's [29] experimental data as listed in Tables 2-3, 2-4, 2-5, 2-6 were used to verify the numerical technique and for correlation purposes.

The structure of the compressible, axially symmetric free jet can be described in terms of three flow regions;

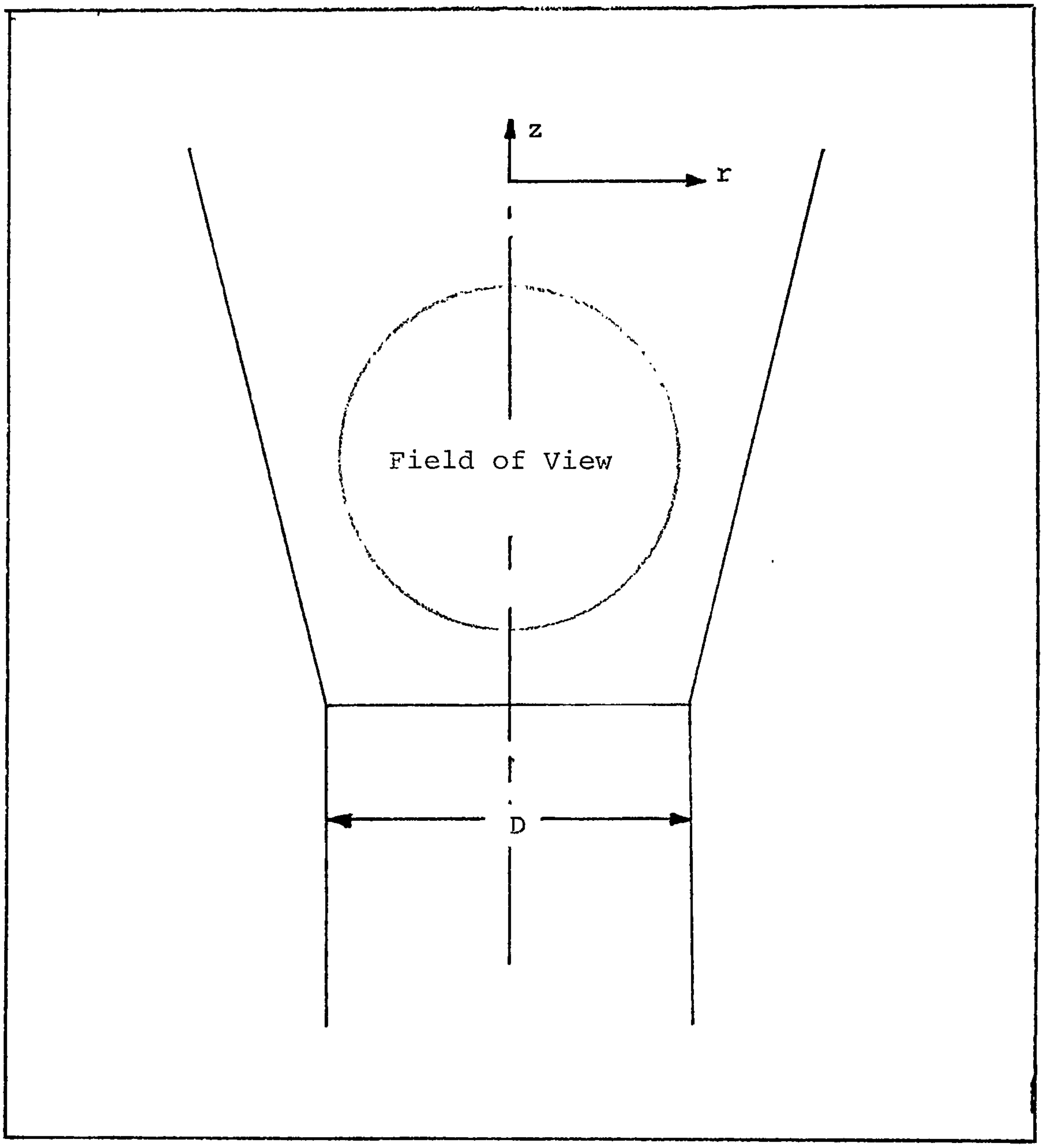

Figure 2-1. Plume Geometry and the Field of View

Table 2-1 Mahagaokar's Axial Temperature Data

$D=3.5$ ft
$u_o=37.3$ ft/sec
$t_o=511.0°K$
$t_a=292.3°K$
$t_o/t_a=1.75$

z/D	t_A (°K)	$t'_{A\ rms}$ (°K)	$\frac{t'_{A\ rms}}{t_A}$
0.47	507	7.38	0.0146
0.76	502	8.05	0.0160
1.05	488	8.29	0.0170
1.34	472	10.2	0.0216
1.63	452	21.4	0.0474
2.21	436	18.4	0.0422
2.50	425	15.4	0.0362

$D=3.5$
$u_o=37.3$ ft/sec
$t_o=511.0°K$
$t_a=292.3°K$
$t_o/t_a=1.74$

z/D	t_A (°K)	$t'_{A\ rms}$ (°K)	$\frac{t'_{A\ rms}}{t_A}$
0.47	502	7.68	0.0153
0.88	500	8.66	0.0173
1.22	476	9.58	0.0201
1.57	455	17.1	0.0376
1.92	442	20.7	0.0468
2.26	430	17.8	0.0414
2.61	421	15.7	0.0373

Table 2-2 Mahagaokar's Radial Temperature Data

$D=3.5$
$u_o=31.5$
$t_o=508°K$
$t_a=297.2°K$
$t_o/t_a=1.71$

At $z/D=0.6$

r/D	t_A (K°)	$t'_{A\ rms}$ (°K)	$\frac{t'_{A\ rms}}{t_A}$
0.359	400	15.2	0.0380
0.293	457	13.1	0.0287
0.206	479	12.9	0.0269
0.115	495	10.5	0.0212
0	500	9.14	0.0183
-0.115	490	10.6	0.0216
-0.206	477	12.3	0.0258
-0.293	453	14.1	0.0311
-0.359	403	14.2	0.0352

$D=3.5$
$u_o=29.0$
$t_o=498°K$
$t_a=296.2°K$
$t_o/t_a=1.69$

At $z/D=0.6$

r/D	t_A (K°)	$t'_{A\ rms}$ (°K)	$\frac{t'_{A\ rms}}{t_A}$
0.359	406	13.8	0.0340
0.293	454	14.2	0.0313
0.206	475	11.2	0.0236
0.115	486	11.1	0.0228
0	491	9.36	0.0191
-0.115	488	11.6	0.0238
-0.207	477	13.4	0.0281
-0.282	451	13.2	0.0293
-0.368	401	15.6	0.0389

Table 2-3 Corrsin and Uberoi's Axial Temperature and Velocity Data

$D = 1''$
$u_o = 78$ ft/sec
$t_o = 291$ °K
$t_o/t_a = 2.02$

z/D	$\frac{t - t_a}{t_o - t_a}$	$\frac{u_z}{u_o}$
0	1.0	1.0
1.0	1.0	1.0
2.0	1.0	1.0
3.0	0.96	1.0
4.0	0.90	0.97
6.0	0.67	0.80
8.0	0.50	0.60
10.0	0.40	0.48
12.0	0.32	0.39
14.0	0.26	0.33

$D = 1''$
$u_o = 78$ ft/sec
$t_o = 291$ °K
$t_o/t_a = 1.05$

z/D	$\frac{t - t_a}{t_o - t_a}$	$\frac{u_z}{u_o}$
0	1.0	1.0
1.0	1.0	1.0
2.0	1.0	1.0
3.0	1.0	1.0
4.0	0.96	1.0
6.0	0.80	0.94
8.0	0.60	0.80
10.0	0.50	0.67
12.0	0.41	0.58
14.0	0.32	0.48

Table 2-4 Corrsin and Uberoi's Radial Temperature and Velocity Data

$D = 1''$
$u_o = 78$ ft/sec
$t_o = 588$ °K
$t_a = 291$ °K
$t_o/t_a = 2.02$

At $z/D = 15$

r/D	$\frac{t - t_a}{t_{zo} - t_a}$	$\frac{u_z}{u_{zo}}$
0	1.0	1.0
0.5	0.95	0.87
1.0	0.78	0.70
1.5	0.60	0.42
2.0	0.42	0.35
2.5	0.25	0.14
3.0	0.15	0.04

$D = 1''$
$u_o = 78$ ft/sec
$t_o = 305$ °K
$t_a = 291$ °K
$t_o/t_a = 1.05$

At $z/D = 15$

r/D	$\frac{t - t_a}{t_{zo} - t_a}$	$\frac{u_z}{u_{zo}}$
0.	1.0	1.0
0.5	0.9	0.86
1.0	0.70	0.62
1.5	0.5	0.38
2.0	0.30	0.20
2.5	0.12	0.07
3.0	0.03	0.02

Table 2-5 Tomich and Weger's Axial Temperature and Velocity Data

D=1/4"
u_o=822 ft/sec
t_o=785 °K
t_a=293 °K
t_o/t_a=2.68

z/D	$\frac{t - t_a}{t_o - t_a}$	$\frac{u_z}{u_o}$
0	1.0	1.0
1.0	1.0	1.0
2.0	0.98	1.0
3.0	0.97	1.0
4.0	0.92	0.98
5.0	0.85	0.95
6.0	0.78	0.87
8.0	0.64	0.72
10.0	0.54	0.59
12.0	0.45	0.48

D=3/8"
u_o=687 ft/sec
t_o=797°K
t_a=293°K
t_o/t_a=2.72

z/D	$\frac{t - t_a}{t_o - t_a}$	$\frac{u_z}{u_o}$
0	1.0	1.0
1.0	1.0	1.0
2.0	1.0	1.0
3.0	0.94	0.98
4.0	0.90	0.96
5.0	0.83	0.91
6.0	0.76	0.88
8.0	0.64	0.72
10.0	0.52	0.57
12.0	0.41	0.46

Table 2-6 Tomich and Weger's Radial Temperature and Velocity Data

D=1/4", u_o=822 ft/sec, t_o=785 °K, t_a=293 °K, t_o/t_a=2.68						D=3/8", u_o=687 ft/sec, t_o=797 °K, t_a=293 °K, t_o/t_a=2.72		
At z/D=4.0			At z/D=11.0			At z/D=11.0		
r/D	$\frac{t - t_a}{t_{zo} - t_a}$	$\frac{u_z}{u_{zo}}$	r/D	$\frac{t - t_a}{t_{zo} - t_a}$	$\frac{u_z}{u_{zo}}$	r/D	$\frac{t - t_a}{t_{zo} - t_a}$	$\frac{u_z}{u_{zo}}$
0.0	1.0	1.0	0.0	1.0	1.0	0.0	1.0	1.0
0.1	0.99	0.99	0.30	0.95	0.90	0.30	0.96	0.92
0.2	0.96	0.99	0.60	0.82	0.70	0.50	0.85	0.77
0.3	0.93	0.92	0.95	0.63	0.49	0.80	0.72	0.59
0.4	0.89	0.61	1.30	0.50	0.30	1.10	0.57	0.42
0.6	0.62	0.44	1.60	0.30	0.18	1.30	0.42	0.20
0.8	0.40	0.20	1.90	0.20	0.11	1.60	0.30	0.20
1.0	0.22	0.06	2.20	0.10	0.06	1.85	0.19	0.12
1.2	0.11	0.02	2.60	0.05	0.03	2.40	0.04	0.01

see Figure 2-2. The potential core region extends to the point where the turbulent mixing region reaches the jet axis. This region is, of course, not necessarily identical for velocity and temperature. The next region is a transition region where the spread of the jet in the radial direction and the axial decay of the center-line properties are very rapid, and is followed by the fully developed region where the radial spread of the jet is nearly linear with respect to the axial distance. The greater the compressible effects, the greater is the deviation from linearity.

There are many problems which arise in connection with any numerical approach to the problem of solving for temperature and velocity as a function of position in the compressible free jet. One is the non-existance of similarity [12] in the profiles (as distinct from the case for incompressible flow). The model must also take into account the fact that the free jet only becomes fully developed a certain number of nozzle diameters downstream from the nozzle. Therefore, a complete treatment must include the potential core region and the transition region, as well as the fully developed portion of the jet. The boundary conditions are also a source of difficulty. These include the prescribed conditions at the nozzle (i.e., flat or other types of profiles) and the conditions at an infinite radial distance (i.e., where the jet is exhausting into a moving gas stream of into quiescent surroundings).

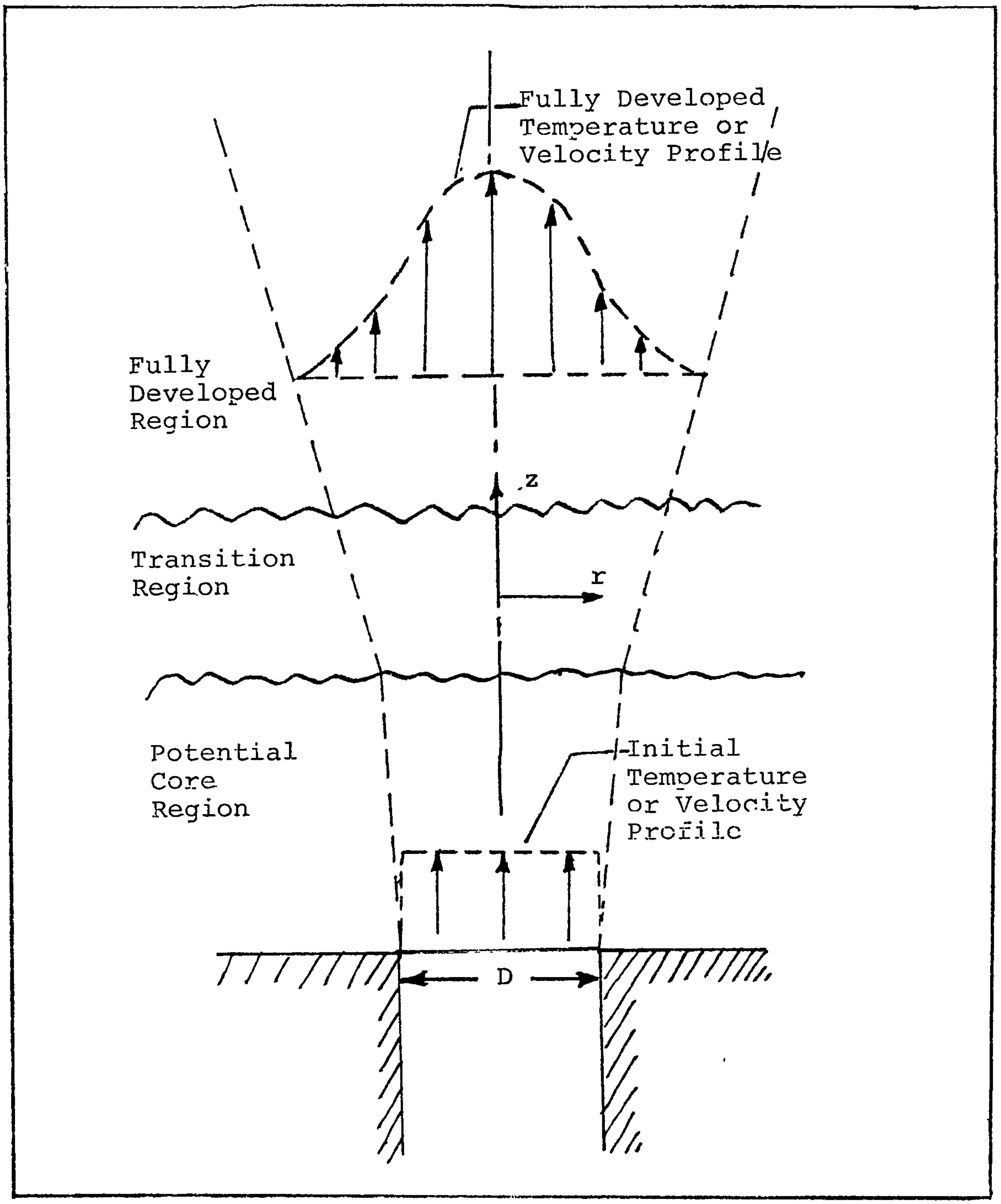

Figure 2-2. Schematic Sketch of Free Jet

Because of these problems, most of the available calculational techniques have had to make use of various simplifying assumptions which has limited their usefulness. Much of the work has been restricted to the problem of axial velocity and temperature decay, while the question of the radial variation of these quantities has not been dealt with extensively. It is the intent of this numerical technique to overcome some of these limitations.

B. Review of Literature

Hinze and van der Hegge Zijmen [11], Tollmien [50], Schlichting [24], and others have obtained solutions to the problem of determining the velocity and temperature profiles in incompressible, turbulent free jets. These solutions, however, are somewhat limited in that they do not apply to the region near the nozzle. Solutions for the velocity and temperature profiles in compressible, turbulent jets have been much less numerous than the solutions for the incompressible case.

Kleinstein [12] presented solutions for the velocity and temperature profiles in the fully developed region of a compressible, turbulent free jet. He applied von Mises transformation to the boundary layer equations and used a Taylor series expansion to linearised the equations. Kleinstein incorporated in his solution a new formulation for the eddy viscosity of a compressible free jet. The solution agreed well with experimental data [9] for the axial decay of velocity and temperature. However, radial distributions of velocity and temperature were not shown or compared with experimental data. Pai [16] solved the boundary layer equations in the form of von Mises variables by using a finite difference technique. This solution was restricted to the case of a free jet exhausting into a moving external stream. No comparison has been made between the solution and the experimental data, probably due to the lack of data for this type of flow.

Warren [31] solved for the axial variation of velocity and temperature in a compressible turbulent free jet exhausting into a media at rest using an integral method. He used universal profiles to describe the radial variation of axial velocity in the potential core region and the fully developed region. He also proposed a formulation for the eddy viscosity of a compressible free jet. The solution, which was restricted to turbulent Prandtl number of one, agreed fairly well with experimental data except for the transition region.

Szablewski [27] developed an analysis of the core region of a compressible free jet. He used a similarity parameter and numerical integration of the boundary layer equations to obtain velocity and temperature profiles, but the solution was restricted to the potential core region.

Tomich and Weger's [29] modified Kleistein's eddy transfer coefficient for the core region and the fully developed region, and solved the boundary layer equations by a finite difference technique. The solution agreed farily well with experimental data [18,29], however, their correlations for the eddy transfer coefficients and the length of the core region do not apply for lower velocities (usual plume velocity is between 20 ft/sec to 40 ft/sec), and no buoyance effect has been taken into account in their boundary layer equations. Other investigators have also treated various aspects of the compressible jet problem [28,24].

C. Mathematical Modeling and Numerical Solution

The solution of the boundary layer equations of conservation of mass, momentum and energy was obtained by using a variation of the finite difference method due to Abbott [1]. No transformations are made; solutions are obtained for free jet injection into a medium at rest where initial free jet velocity and temperature profiles are assumed to be step functions. Dynamic eddy transfer coefficients of momentum, $\rho\varepsilon_v$, and heat flux, k, are defined for the turbulent compressible flow. These transfer coefficients are modifications of those introduced by Kleinstein [16] , and Tomich and Weger [15], and are functions of axial position only.

The finite difference technique can also be used to describe jets exhausting into a uniform external stream by changing the boundary conditions, jets with initial profiles of velocity and temperature of an arbitrary shape, and jets with variable fluid properties. Also, concentration profiles can be obtained as more is learned about the structure of free turbulent shear flows, and this finite difference technique can accommodate more advanced formulations of the eddy transfer coefficients which may be functions of both axial and radial position.

A schematic diagram of the free jet showing the coordinate system used is shown in Figure 2-2. The equations were derived from the conservation of mass, momentum, and energy in the turbulent, compressible, axially symmetric steady state free jet.

Conservation of mass (continuity):

$$\frac{\partial}{\partial z}(\rho u_z) + \frac{1}{r}\frac{\partial}{\partial r}(r\rho u_r) = 0 \qquad (2\text{-}1)$$

Conservation of momentum:

$$\rho u_z \frac{\partial u_z}{\partial z} + \rho u_r \frac{\partial u_z}{\partial r} = \frac{1}{r}\frac{\partial}{\partial r}\left(r\rho\varepsilon_v \frac{\partial u_z}{\partial z}\right) + (\rho_a - \rho)g \qquad (2\text{-}2)$$

Conservation of energy:

$$\rho u_z c_p \frac{\partial t}{\partial z} + \rho u_r c_p \frac{\partial t}{\partial r} = \frac{1}{r} \frac{\partial}{\partial r} \left(rk \frac{\partial t}{\partial r}\right) + \rho \varepsilon_v \left(\frac{\partial u_z}{\partial r}\right)^2 \tag{2-3}$$

The heat capacity and the static pressure are assumed to be constant in the above equations. The assumption of constant static pressure has been shown to be a valid assumption for subsonic free jet [8]. All densities, velocities and temperatures have been time-smoothed for turbulent flow. The boundary conditions for this free jet flow are:

at $z = 0$,

$$\left.\begin{aligned} u_z &= u_o \\ t &= t_o \\ u_r &= 0 \end{aligned}\right\} \quad \text{for } r < \frac{D}{z}$$

$$\left.\begin{aligned} u_z &= 0 \\ t &= t_a \\ u_r &= 0 \end{aligned}\right\} \quad \text{for } r \geq \frac{D}{2}$$

at $r = 0$,

$$\frac{\partial u_z}{\partial r} = 0$$

$$\frac{\partial t}{\partial r} = 0 \qquad \text{for all } z$$

$$u_r = 0$$

at $r \to \infty$,

$$u_z = 0$$

$$t = t_a \qquad \text{for all } z$$

$$u_r = 0$$

Making Equations (1) - (3) dimensionless, they become:

$$\frac{\partial}{\partial Z}(PU_Z) + \frac{1}{R}\frac{1}{\partial R}(RPU_R) = 0 \tag{2-4}$$

$$PU_Z \frac{\partial U_Z}{\partial Z} + PU_R \frac{\partial U_Z}{\partial R} = \frac{1}{u_o D}\frac{1}{R} \cdot \frac{\partial}{\partial R}\left(RP\varepsilon_v \frac{\partial U_Z}{\partial R}\right)$$

$$+ \frac{Dg}{u_o^2}[P_z - P] \tag{2-5}$$

$$PU_z \frac{\partial T}{\partial Z} + PU_R \frac{\partial T}{\partial R} = \frac{1}{\rho_o u_o D}\frac{1}{R}\frac{\partial}{\partial R}\left(R \frac{k}{c_p}\frac{\partial T}{\partial R}\right)$$

$$+ \frac{u_o}{D(t_o - t_a)c_p} P\varepsilon_v \left(\frac{\partial U_Z}{\partial R}\right)^2 \tag{2-6}$$

The transformed boundary conditions are:

at $Z = 0$,

$$U_Z = 1.0$$

$$T = 1.0 \qquad \text{for } R < \frac{1}{2}$$

$$U_R = 0.$$

$$U_Z = 0.$$

$$T = 0. \qquad \text{for } R \geq \frac{1}{2}$$

$$U_R = 0.$$

at $R = 0$,

$$\frac{\partial U_Z}{\partial R} = 0$$

$$\frac{\partial T}{\partial R} = 0 \qquad \text{for all } Z$$

$$U_R = 0$$

at $R \to \infty$,

$$U_Z = 0$$

$$T = 0 \qquad \text{for all } Z$$

$$U_R = 0$$

For incompressible jets, expressions for the eddy kinematic viscosity have been obtained semi-empirically in terms of parameters of the main jet flow using either Prandtl's constant exchange coefficient theory, von Karman's hypothesis, or Taylor's vorticity theory. Solutions incorporating these expressions have agreed well with experimental data. Therefore, the expressions for eddy kinematic viscosity derived using these theories have become generally accepted for the solution of incompressible free jet flows.

For compressible free jet flows, however the mechanism of the transport phenomena has not been semi-empirically determined, and few empirical formulations have resulted in solutions which compare well with experimental data. Kleinstein [12] has stated that a "dynamic eddy transfer coefficient,' $\rho\varepsilon_v$, must be used as a measure of the transport phenomena for compressible flows. Furthermore, Kleinstein, using an empirical approach to deduce this result, states that this transfer coefficient is a function of axial position only. Kleinstein's momentum transfer coefficient is as follows:

$$\rho\varepsilon_v = 0.0183 \ (\rho_o \rho_a)^{1/2} \ u_o \frac{D}{2} \tag{2-7}$$

Tomich and Weger [29] modified Kleinstein eddy transfer coefficient to provide a better agreement with experimental data:

$$P\varepsilon_v = F(M) P_a^{1/2} P_m u_o D f v(Z) \tag{2-8}$$

where $F(M) = 0.00954 - 0.00782M + 0.00325M^2$ (2-9)

(M = Mach number)

$$fv(Z) = 0.2 \quad \text{for } Z \le Z_{cv}$$

$$= 1.0 \quad \text{for } Z > Z_{cv}$$

$$Z_{cv} = 4.73 \quad P_a^{-1/2} \tag{2-10}$$

And they also suggested that if the turbulent Prandtl number is only a function of axial position, the eddy thermal conductivity may be expressed as

$$k = F(M) \; C_p \; P_a^{1/2} \; P_m \; \rho_o u_o D \; f_t(Z)/N_{p_r} \tag{2-11}$$

where

$$f_t(Z) = 0.2 \quad \text{for } Z \le Z_{ct}$$

$$= 1.0 \quad \text{for } Z \ge Z_{ct}$$

$$Z_{ct} = 3.43 \quad P_a^{1/2} \tag{2-12}$$

$$N_{p_r} = 1.0 \quad \text{for } Z \le Z_{ct}$$

$$= 0.715 \quad \text{for } Z > Z_{ct}$$

The extent of the core regions for velocity and temperature (Z_{cv} and Z_{ct}, respectively) were defined by Kleinstein, but it was verified by Tomich and Weger that Kleinstein transfer coefficients are much too large in the core regions which he did not treat in his analysis. They introduced the functions $f_v(z)$ and $f_t(z)$, which modify the transfer coefficient for the fully developed region to fit the core regions. Also the turbulent Prandtl number in the temperature core region is unity, indicating equal turbulent transport rates of momentum and energy. The turbulent Prandtl number for the remainder flow field has been found to be roughly constant and very nearly equal to the laminar Prandtl number [9,12]. F(M) was the best value found for each experimental Mach number [9,29], and a least squares method was used to obtain F(M) as a polynomial in Mach number.

Substituting Equations (2-8) and (2-11) into Equations (2-5) and (2-6), we have

$$PU_z \frac{\partial U_Z}{\partial Z} + PU_R \frac{\partial U_R}{\partial R} = A_V \frac{1}{R} \frac{\partial}{\partial R} \left(R \frac{\partial U_Z}{\partial R}\right) + \frac{D_g}{u_o^2} [P_A - P] \qquad (2\text{-}13)$$

where

$$A_v = \frac{P_{\varepsilon_v}}{u_o D} = F(M)\ P_a^{1/2}\ P_m\ f_v(Z) \tag{2-14}$$

$$PU_Z \frac{\partial T}{\partial Z} + PU_R \frac{\partial T}{\partial R} = A_t \frac{1}{R} \frac{\partial}{\partial R} (R \frac{\partial T}{\partial R})$$

$$+ N_{E_c}\ A_v\ {\frac{\partial U_Z}{\partial R^2}}^{2} \tag{2-15}$$

where,

$$A_t = \frac{k}{c_p \rho_o u_o D} = F(M) P_a^{1/2}\ P_m\ f_t(Z)/N_{P_r} \tag{2-16}$$

$$N_{E_c} = \frac{u_o^{\ 2}}{c_p (t_o - t_a)} \tag{2-17}$$

Differentiating Equations (2-4), (2-13), and (2-15), the final form of the equations used in finite difference technique are obtained,

$$\underline{U_Z} \frac{\partial P}{\partial Z} + \underline{P} \frac{\partial U_Z}{\partial Z} + \underline{U_R} \frac{\partial P}{\partial R} + \underline{P} \frac{\partial U_R}{\partial R} + \underline{\frac{PU_R}{R}} = 0 \tag{2-18}$$

$$\underline{PU_Z}\ \frac{\partial U_Z}{\partial Z} + \underline{PU_R}\ \frac{\partial U_Z}{\partial R} = A_V\ \frac{\partial^2 U_Z}{\partial R^2} + \frac{1}{R}\ \frac{\partial U_Z}{\partial R}$$

$$+ \frac{Dg}{u_o{}^2}\,[P_A - P] \tag{2-19}$$

$$\underline{PU_Z}\ \frac{\partial T}{\partial Z} + \underline{PU_R}\ \frac{\partial T}{\partial R} = A_t\ \frac{\partial^2 T}{\partial R^2} + \frac{1}{R}\ \frac{\partial T}{\partial R}$$

$$+ N_{Ec}\ A_V\ \underline{\left(\frac{\partial U_Z}{\partial R}\right)^2} \tag{2-20}$$

The finite-difference solution used here is a variation of the fully implicit method of Abbott [15] for constant temperature, axially symmetric flows. The following finite difference approximations for derivatives at $(Z+\Delta Z, R)$ were used:

$$\frac{\partial U_Z}{\partial Z} = \frac{U_Z(Z+\Delta Z, R) - U_Z(Z, R)}{\Delta Z} \tag{2-21}$$

$$\frac{\partial U_Z}{\partial R} = \frac{U_Z(Z+\Delta Z, R+\Delta R) - U_Z(Z+\Delta Z, R-\Delta R)}{2\Delta R} \tag{2-22}$$

$$\frac{\partial^2 U_Z}{\partial R^2} = \frac{U_Z(Z+\Delta Z, R+\Delta R) - 2U_Z(Z+\Delta Z, R) + U_Z(Z+\Delta Z, R-\Delta R)}{\Delta R^2} \tag{2-23}$$

Similar expressions were used for the derivatives of U_R, T and P. Another radial derivative form, which is used in the continuity equation in order to make the application of the boundary conditions easier is

$$\frac{\partial U_R}{\partial R} = \frac{U_R(Z+\Delta Z,R) - U_R(Z+\Delta Z,R-\Delta R)}{\Delta R} \tag{2-24}$$

The finite difference approximations are substituted into Equations (2-18), (2-19) and (2-20), which along with Equations (2-14), (2-16), and (2-17), and the boundary conditions, comprise the system of nonlinear algebraic equations to be solved at each point of the finite-difference net work; see Figure 2-3. The system of algebraic equations was linearlized by taking the coefficients (shown as the underlined coefficients in Equations (2-18), (2-19) and (2-20)) of the nonlinear lines at their known value on the previous line of the net work or at Z. The resulting system of simultaneous, linear algebraic equations was solved by using Gaussian elimination method [13] for initial values of U_Z, U_R and T at each point of the line $Z+\Delta Z$. The computational accuracy was then improved with an iterative procedure until the deviations of the assumed and the newly calculated was less than 5% on U_Z and T, and the solution is carried downstream to $Z+2\Delta Z$, etc. A procedure developed by Wegstein [32]:

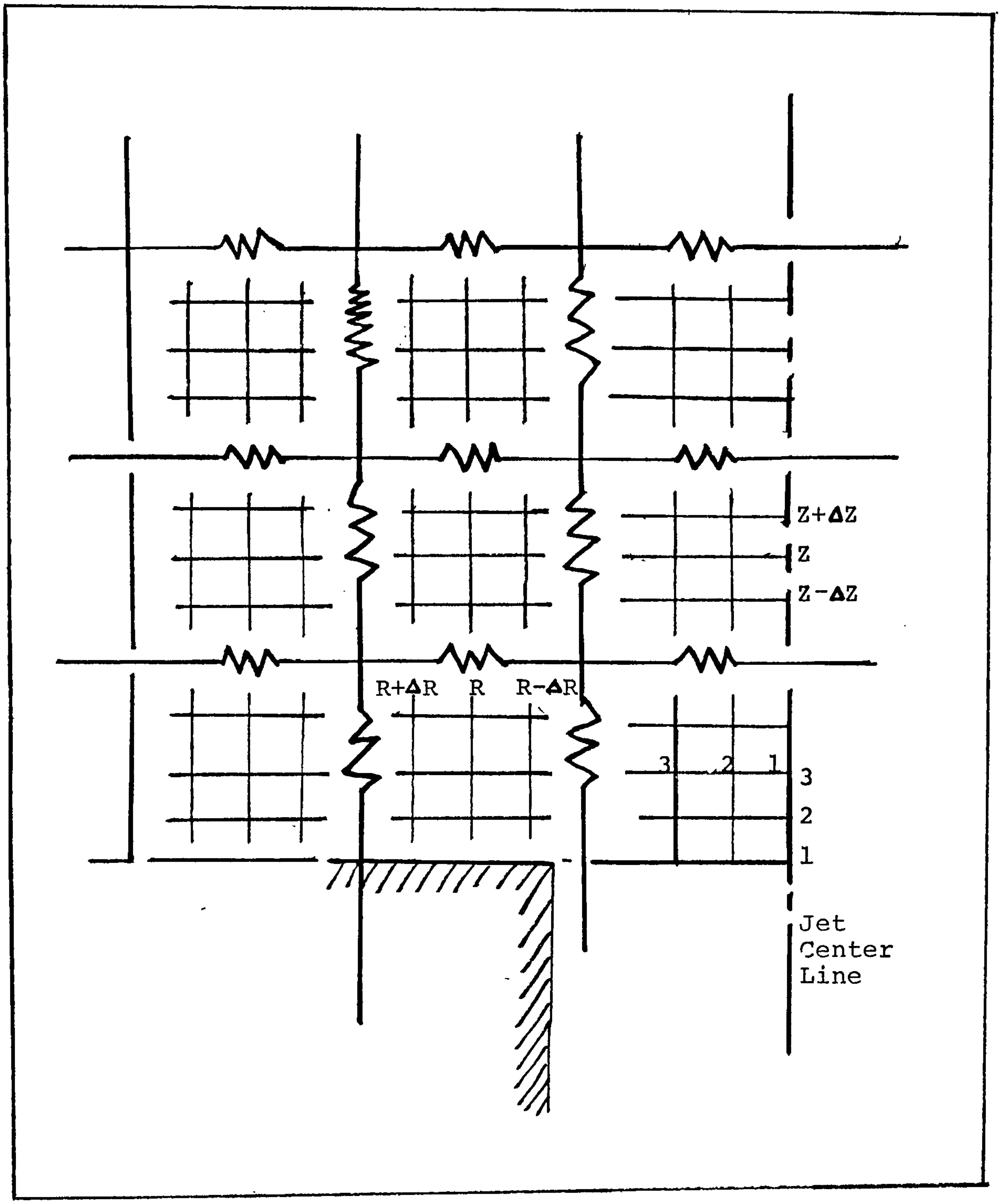

Figure 2-3 The Finite Difference Network

$$\overline{U}_Z(\text{new}) = 0.33\ U_Z(\text{old}) + 0.67\ U_Z(\text{new}) \qquad (2\text{-}25)$$

was used to accelerate the iterative process.

Near Z=0, a smaller step size was required to converge to the correction solution than was required further downstream where the gradients are much smaller. The step sizes were increased downstream in order to speed up the numerical solution. A more detail description on the development of finite-difference equations and program set up are given in Appendix A. The computer program and the results are given in Appendix B.

CHAPTER III

AXIAL TEMPERATURE AND VELOCITY DECAY

A. Analysis and Correlations

The results from the finite-difference method using Tomich and Weger's correlation P_{ε_V}, k, Z_{cv} and Z_{ct}, using Corrsin and Uberoi, and Tomich and Weger's experimental data are shown in Figures 3-1, 3-2, 3-3 and 3-4. For short distance the temperature and velocity decay at a shorter distance, as compared to the experimental data, and for long distance, the decay of temperature and velocity are about the same, which implies that the core lenghts Z_{ct} and Z_{cv} should be adjusted.

New values of Z_{ct} and Z_{cv} were determined by a trial and error fit of experimental data. Beyond these core regions, the decay of temperature and velocity begins to drop much faster as observed from the experimental data.

In order to fit Mahagaokar's experimental temperature data, the values of F(M) had to be adjusted and were determined by trial and error. The values of Z_{ct} were also determined by trial and error. Since no velocity data were presented, the values of Z_{cv} were determined using a factor of 1.28 of Z_{ct}, which is the average value of Z_{ct}/Z_{cv}, and the highest deviation is only 0.12 for the four sets of

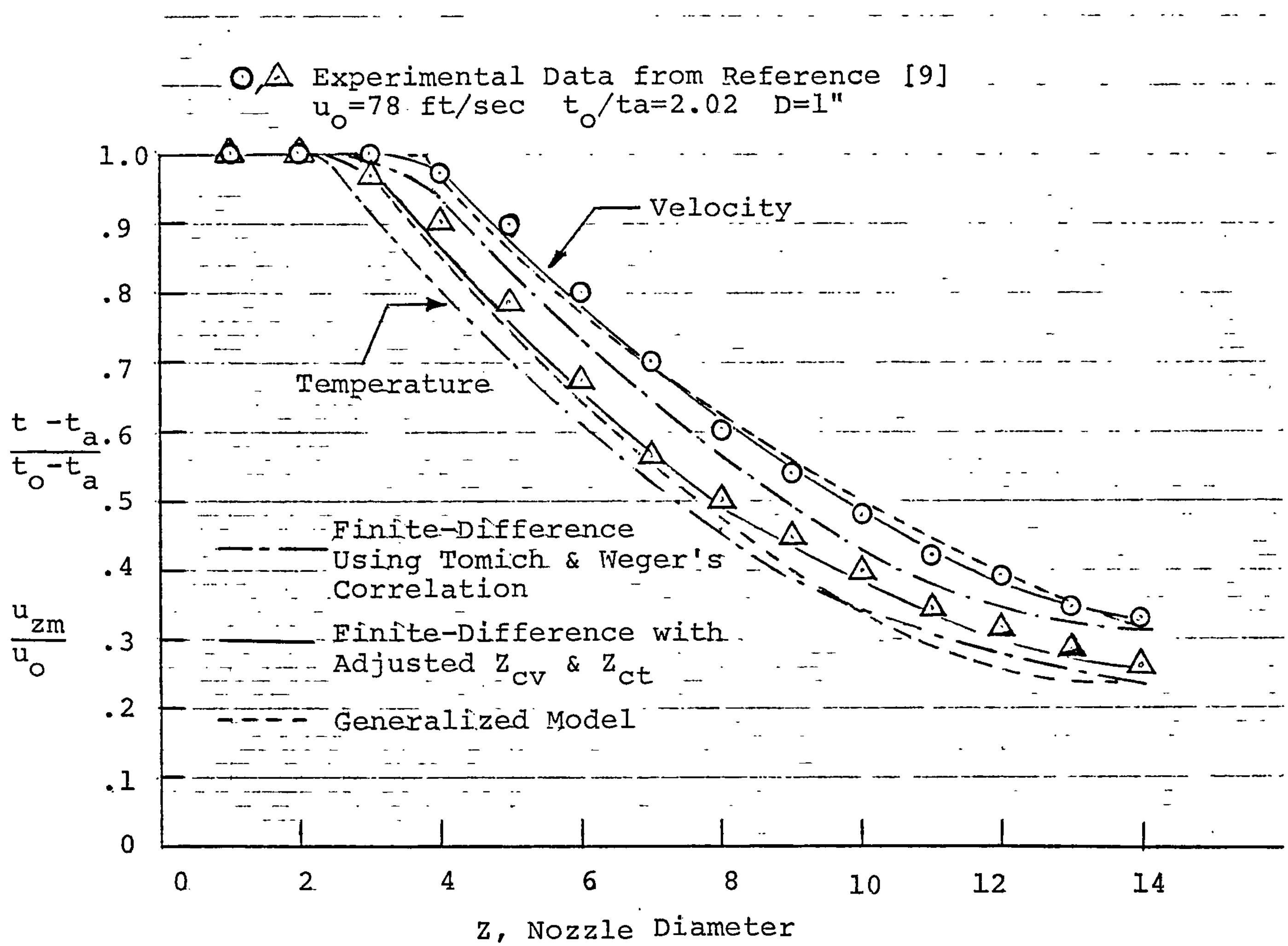

Figure 3-1. Comparision of Experimental Data [9] with Analysis for Axial Decay of Temperature and Velocity

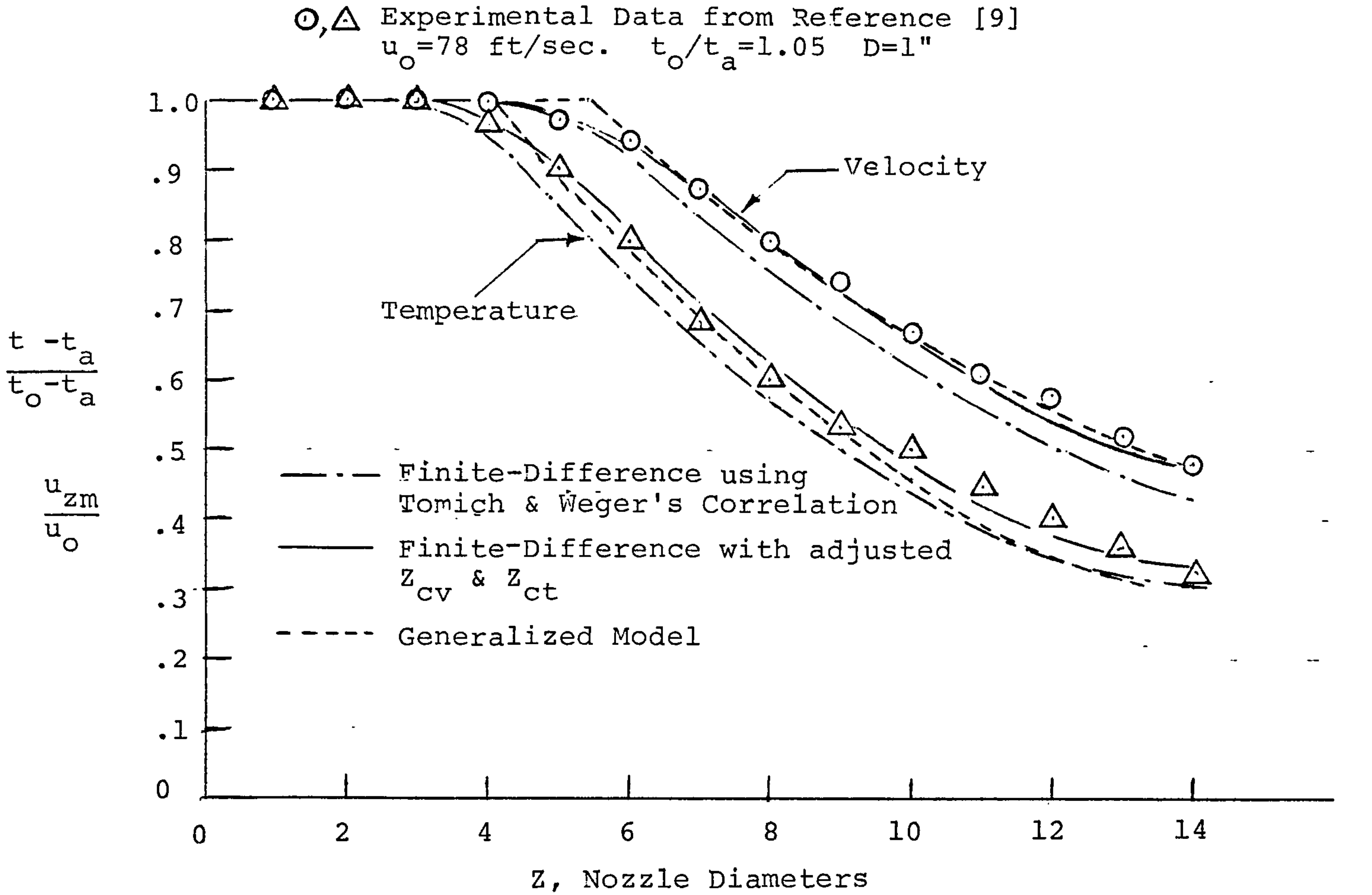

Figure 3-2. Comparision of Experimental Data [9] with Analysis for Axial Decay of Temperature and Velocity

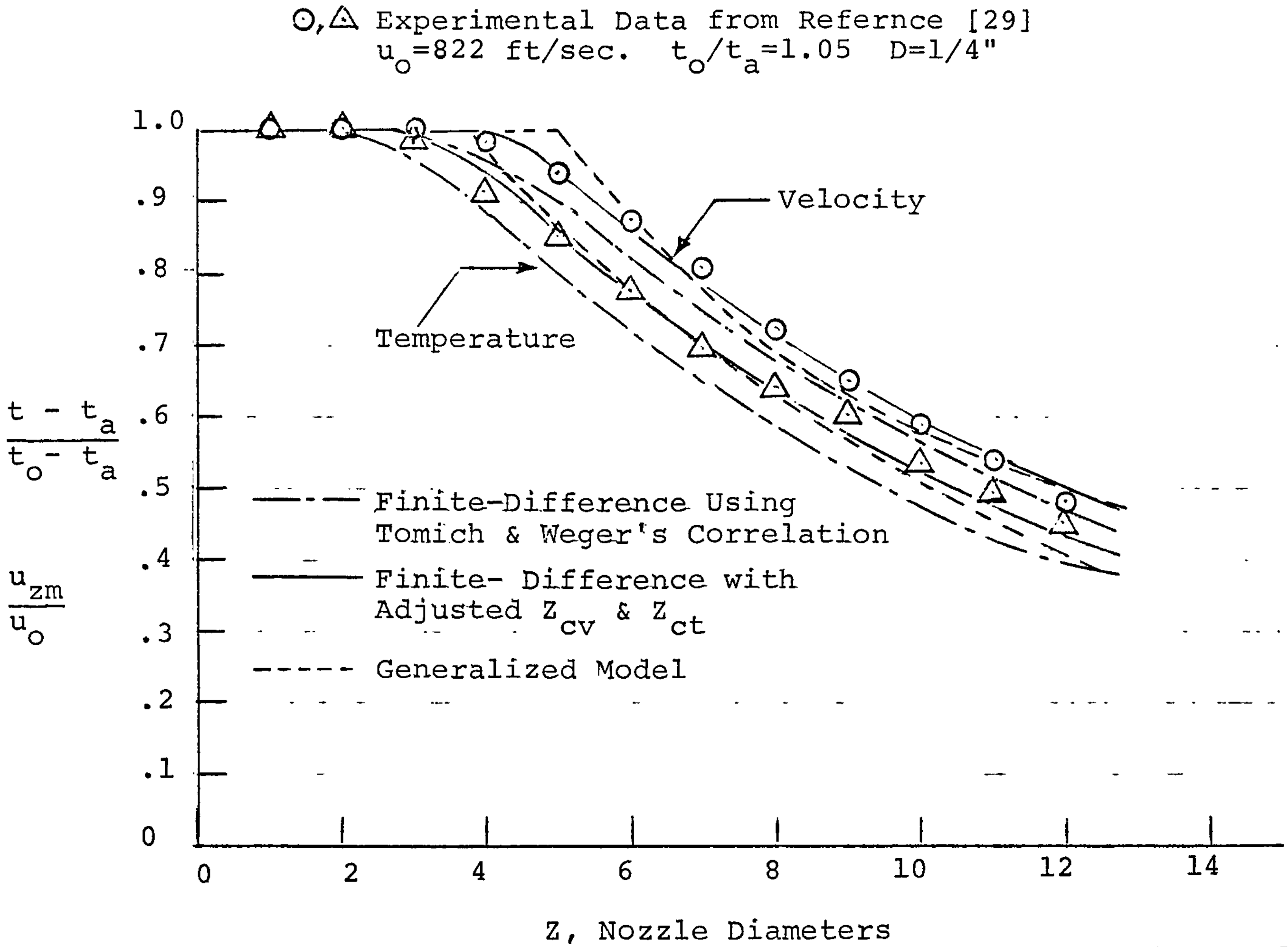

Figure 3-3. Comparision of Experimental Data [29] with Analysis for Axial Decay of Temperature and Velocity

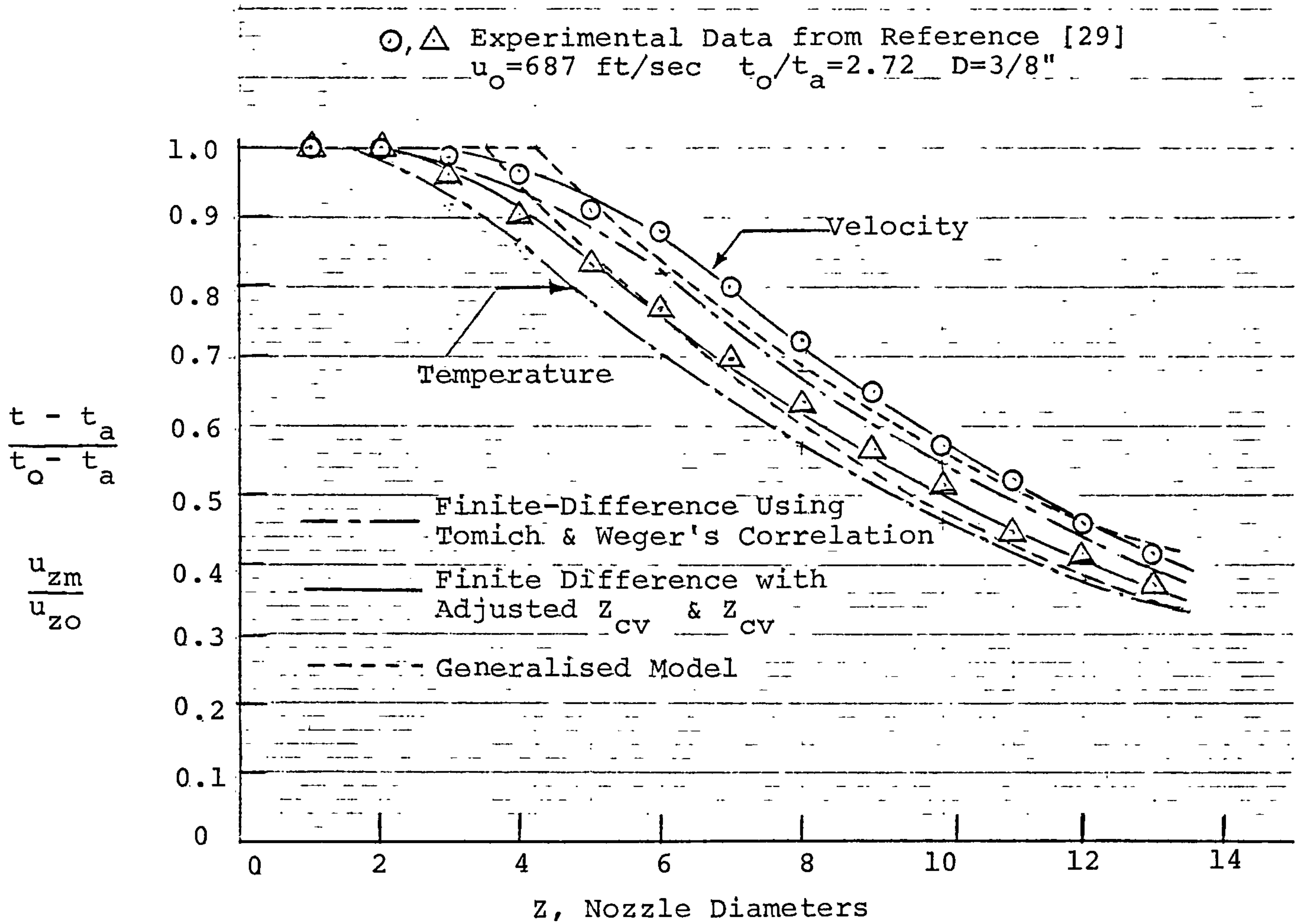

Figure 3-4. Comparision of Experimental Data [29] with Analysis for Axial Decay of Temperature and Velocity

experimental data. The axial temperature and velocity decay, and the average tamperature of the "field of view," as calculated from the radial and axial temperature distributions obtained from the finite difference program, are shown in Figures 3-5 and 3-6.

Also from Mahagoakar's axial temperature fluctuation data, Figure 3-7 and 3-8, the temperature fluctuations start to rise approximately at Z=1.2, where the values of Z_{ct} we determine are 1.4 and 1.3, respectively. From the studies of turbulent fluctuations in pipe flow [4,21], the axial velocity and mass fluctuations are about 0.020 and 0.025, respectively; Mahagoakar's temperature fluctuations in the core region are about 0.017. It can be concluded that the flow behavior of the emerging plume in the core region primarily resembles its behavior at the point of emergence. Also from the temperature fluctuation data, we can distinguish the three flow regions of the emerging plume as shown in Figures 3-7 and 3-8.

The values of Z_{ct}, Z_{cv} and F(M) determined in the present work as compared with those from Tomich and Weger's correlation are listed in Table 3-1. Correlations were derived for F(M), Z_{ct} and Z_{cv} using the results obtained in this work.

A least squares procedure was used to correlate F(M):

$$F(M) = 0.0168 - 0.155M + 0.388M^2 - 0.267M^3 \quad (3\text{-}1)$$

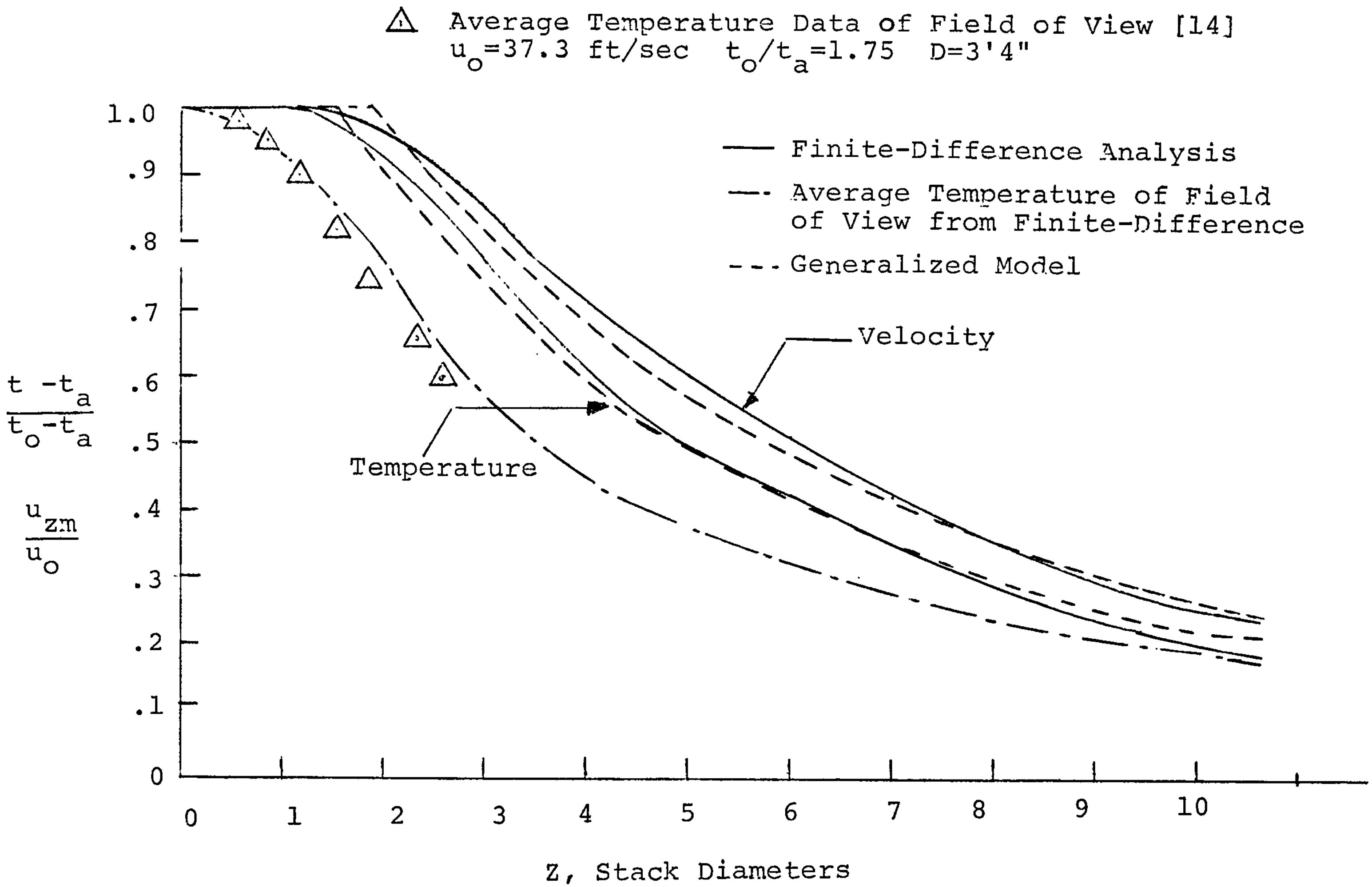

Figure 3-5. Comparision of Experimental Data [14] with Analysis for Axial Decay of Temperature and Velocity

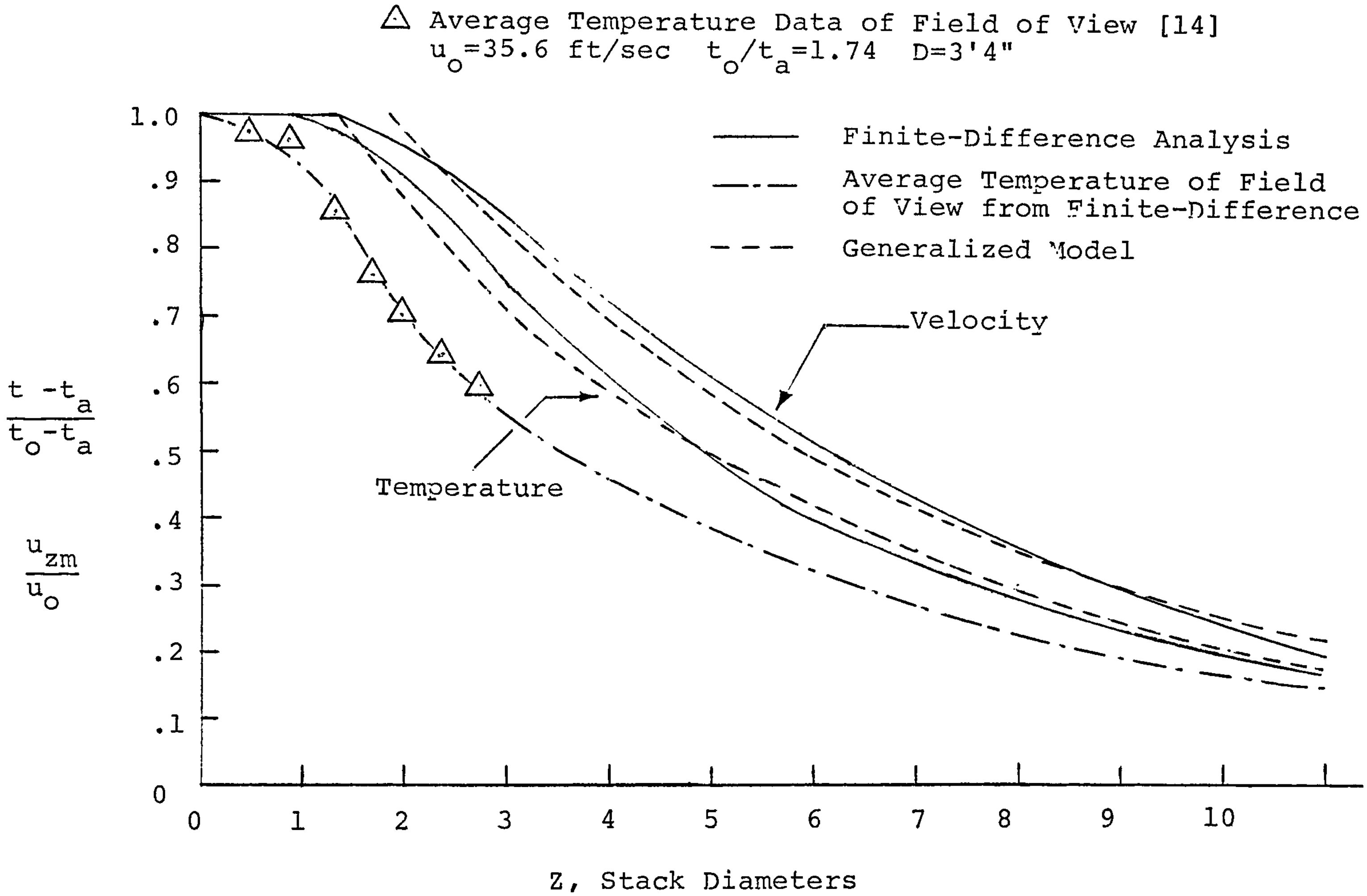

Figure 3-6. Comparision of Experimental data [14] with Analysis for Axial Decay of Temperature and Velocity

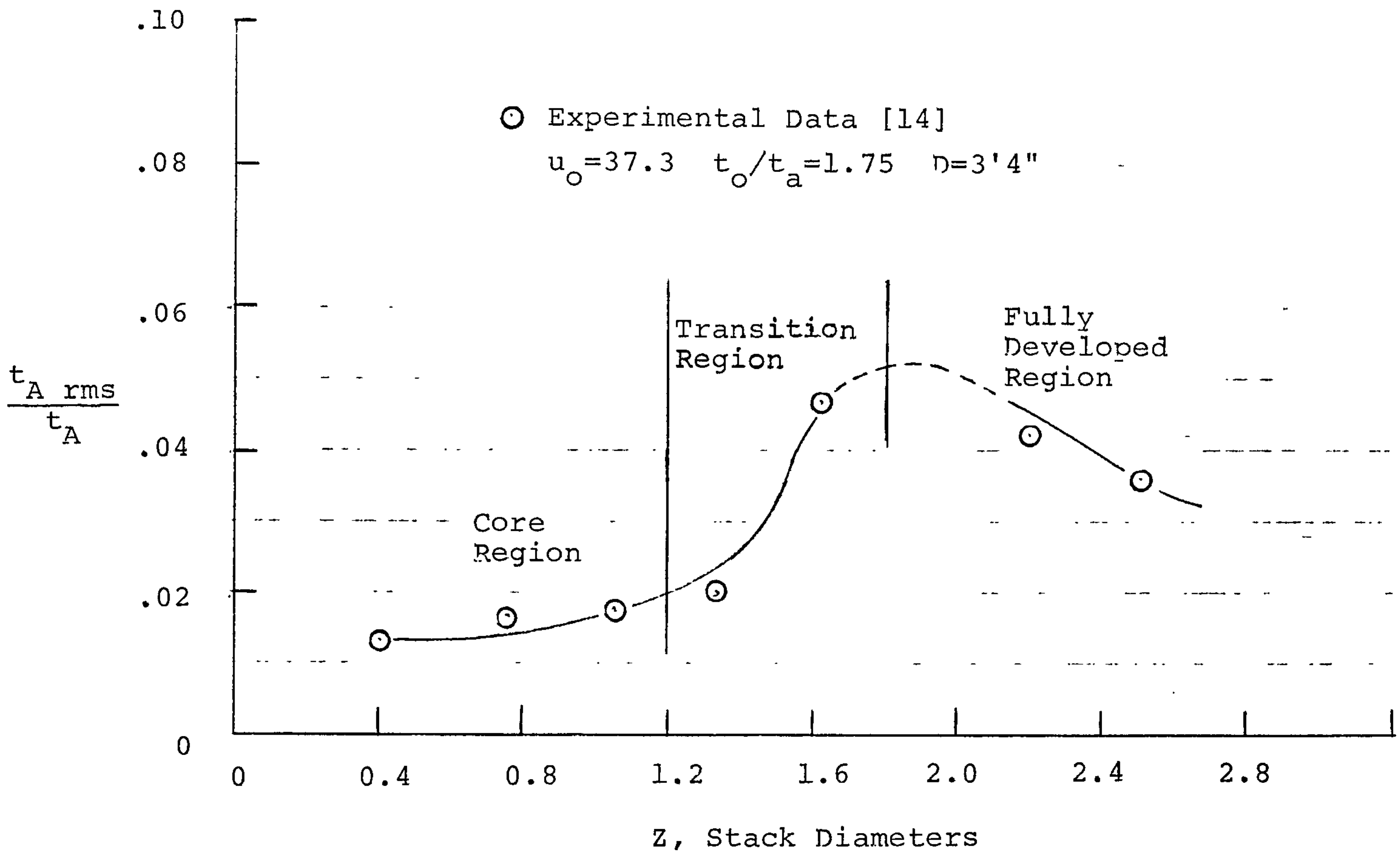

Figure 3-7. Axial Profile of the Relative Intensity of Area Integrated Temperature Fluctuations [14]

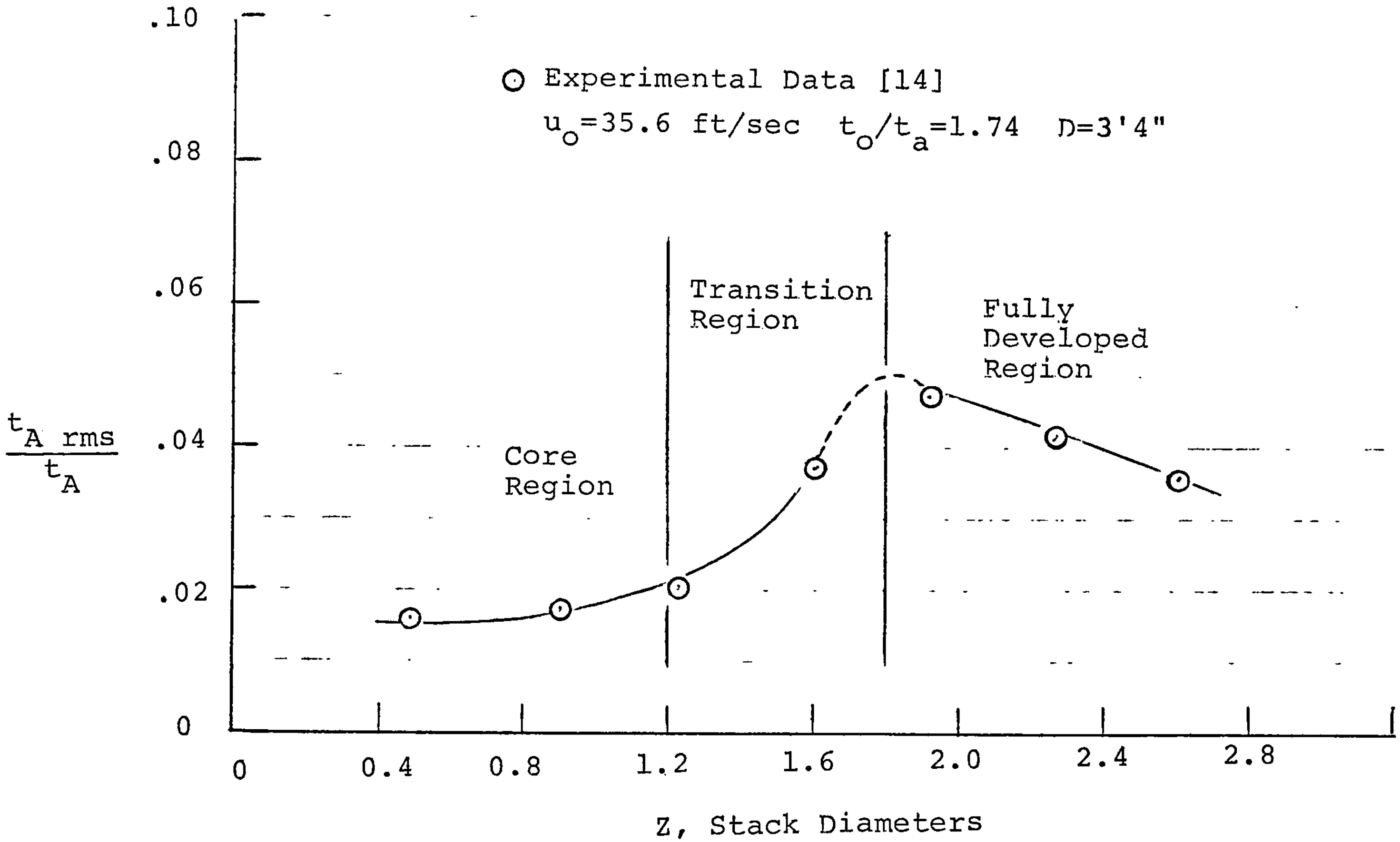

Figure 3-8. Axial Profile of the Relative Intensity of Area Integrated Temperature Fluctuations [14]

Table 3-1 Values of Z_{ct}, Z_{cv}, and F(M)

u_{zo} ft/sec	$\frac{t_o}{t_a}$	M	Tomich & Weger's Correlation			Present Work			
			Z_{ct}	Z_{cv}	F(M)	Z_{ct}	Z_{cv}	Z_{ct}/Z_{cv}	F(M)
822.	2.68	0.755	2.10	2.89	0.00575	3.8	5.0	1.32	0.00575
687.	2.72	0.631	2.08	2.87	0.00617	3.5	4.2	1.20	0.00617
78.0	2.02	0.070	2.42	3.33	0.00921	3.0	3.9	1.30	0.00921
78.0	1.05	0.070	3.35	4.61	0.00921	4.2	5.4	1.29	0.00921
37.3	1.75	0.0343	2.59	3.58	0.00947	1.4	1.8	1.28*	0.0120
35.6	1.74	0.0327	2.60	3.59	0.00948	1.3	1.7	1.28*	0.0125

*This is the average value of Z_{ct}/Z_{cv} for the first four set of data

The average absolute deviation is 5.36×10^{-4} and the average percent deviation is 5.03%.

For the correlations of Z_{ct} and Z_{cv}, linear regressions in the forms of

$$Z_{ct} = A + B \left(\frac{t_o}{t_a}\right) + CM \tag{3-2}$$

$$Z_{ct} = A \left(\frac{t_o}{t_a}\right)^B (M)^C \tag{3-3}$$

were tested. The latter form gives a smaller percent of deviation, and the results are as follows:

$$Z_{ct} = 14.4 \left(\frac{t_o}{t_a}\right)^{-1.16} M^{0.455} \tag{3-4}$$

Avg. % deviation = 10.7%

$$Z_{cv} = 17.5 \left(\frac{t_o}{t_a}\right)^{-1.13} M^{0.430} \tag{3-5}$$

Avg. % of deviation = 10.4%

The values of Z_{ct} and Z_{cv} are small compared with the total length of axial temperature and velocity decay, so a 10 percent error should be acceptable.

B. Generalized Equations

As discussed previously, almost all the analytical solutions derived for the plume temperature and velocity decay are based on the similarity hypothesis and the Gaussian distribution of radial temperature and velocity. From the profiles of the experimental axial temperature and velocity decay, these analytical solutions agree well in the fully developed flow region; however, no account has been taken of the core region. A new model is proposed assuming that: 1) the core regions (Z_{ct} and Z_{cv}) exist where the exit temperature and velocity along the center line remain unchanged; and 2) in the fully developed region, the behavior follows that of Priestly's widely accepted model. In the latter model the most significant parameter, the spreading coefficient, α, was correlated using the experimental data.

The value of Z_{ct} and Z_{cv} are given by the correlations derived previously. The analytical solution for the fully developed region is derived from the equations of conservation of mass, momentum and energy. They are the same equations as (2-1), (2-2) and (2-3), except in the energy equation, the viscous energy dissipation term, $\rho \varepsilon_v \left(\frac{\partial u_z}{\partial r}\right)^2$ is neglected, and the shear stress term $\rho \varepsilon_v \frac{\partial u_z}{\partial r}$ ~~is replaced by τ to simplify the mathematics. The equations~~ then were integrated from $r=0$ to $r=\infty$ using the following boundary conditions, at $r = 0$,

$$\frac{\partial u_z}{\partial r} = 0$$

$$\frac{\partial t}{\partial r} = 0 \qquad \text{for all } z$$

$$u_r = 0$$

at $r \to \infty$,

$$u_z = 0$$

$$t = t_a$$

$$u_r = 0$$

$$\frac{\partial t}{\partial r} = 0 \qquad \text{for all } z$$

$$\frac{\partial u_z}{\partial r} = 0$$

$$\frac{\partial u_r}{\partial r} = 0$$

which imply that at a sufficient radial distance there will be no momentum transfer and heat flow. The equations become,

$$\frac{d}{dz} \int_0^\infty r u_z^2 \rho dr = \int_0^\infty r \frac{\Delta t}{t_a} \rho g \, dr \tag{3-6}$$

$$\frac{d}{dz} \int_0^\infty \frac{1}{2} r u_z^3 \rho dr = \int_0^\infty r u_z \frac{\Delta t}{t_a} \rho g \, dr - \int_0^\infty r\tau \frac{\partial u_z}{\partial r} dr \tag{3-7}$$

$$\frac{d}{dz} \int_0^\infty r u_z \, \Delta t \, \rho dr = -\int_0^\infty r u_z \rho \frac{\partial t_a}{\partial z} dr \tag{3-8}$$

It is assumed that the atmospheric condition is isothermal, i.e., $\frac{\partial t_a}{\partial z} = 0$, the shearing stress is a quadratic function of the relative velocity, i.e.,

$$\tau = \frac{1}{2} \rho u_{zm}^2 \, j \left(\frac{r}{R}\right) \tag{3-9}$$

and the similarity hypothesis is good for the radial profiles of Δt and u_z. Following the argument of Sutton [26] that the profiles are Gaussian and the measures of dispersion are approximately at least the same for Δt and u_z, for which experimental confirmation in the laboratory had been provided by Rouse et al. [22] and by Railston [20], Δt and u_z are taking as

$$\Delta t = \Delta t_m \exp\left(-\frac{r^2}{2R_m^{\,2}}\right) \tag{3-10}$$

$$u_z = u_{zm} \exp\left(-\frac{r^2}{2R_m^{\,2}}\right) \tag{3-11}$$

Substituting Equations (3-9), (3-10) and (3-11) into (3-6), (3-7) and (3-8), and then integrating gives,

$$\frac{d}{dz}\left(R_m^{\,2} u_{zm}^{\,2}\right) = R_m^{\,2} \frac{\Delta t_m}{t_a} g \tag{3-12}$$

$$\frac{d}{dz}\left(R_m^{\,2} u_{zm}^{\,3}\right) = 3R_m^{\,2} u_{zm} \frac{\Delta t_m}{t_a} g - \alpha R_m u_{zm}^{\,3} \tag{3-13}$$

$$\frac{d}{dz}\left(R_m^{\,2} u_{zm} \Delta t_m\right) = 0 \tag{3-14}$$

U_{zm}, Δt_m and R_m are then obtained by an integrating factor method. The final solutions are as follows:

$$R_m = \alpha z' \tag{3-15}$$

$$\Delta t_m = \frac{A_1}{\alpha^2 z'^2}\left(\frac{3}{2}\,\frac{A_1\, g}{t_a \alpha^2 z'} + \frac{A_2}{z'^3}\right)^{-1/3} \tag{3-16}$$

$$u_{zm} = \left(\frac{3}{2}\,\frac{A_1 g}{t_a \alpha^2 z'} + \frac{A_2}{z'^3}\right)^{1/3} \tag{3-17}$$

where

$$z_o = D/2\alpha \tag{3-18}$$

$$z' = z + z_o - z_{ct} \qquad \text{for } \Delta t_m \tag{3-19}$$

$$z' = z + z_o - z_{cv} \qquad \text{for } u_{zm} \tag{3-20}$$

$$A_1 = \alpha^2 \, z_o^{\,2} \, u_o \, \Delta t_o \tag{3-21}$$

$$A_2 = z_o^{\,3} \left[u_o^{\,3} - \frac{3A_1 g}{2t_a \alpha^2 z_o} \right] \tag{3-22}$$

A more detail description for the development of the analytical solution for Δt_m, u_{zm} and R_m is shown in Appendix C.

The linear spreading of the plume is derived as a necessary property of the solution and α is regarded as a spreading coefficient. The origin for z' is taken as the point of concurrence obtained by extending the plume outline below the level of the fully developed region, z_{ct} or z_{cv}. A_1 and A_2 are the constants of integration determined from the initial or exit conditions of the plume.

Substituting Equation (3-18), $z_o = D/2\alpha$ into Equations (3-19) to (3-22), we have

$$z' = \frac{(z - z_{ct})\alpha + D/2}{\alpha} \qquad \text{for } t_m \tag{3-23}$$

$$z' = \frac{(z-z_{cv})\alpha + D/2}{\alpha} \qquad \text{for } u_m \tag{3-24}$$

$$A_1 = \frac{D^2}{4} u_o \; \Delta t_o \tag{3-25}$$

$$A_2 = \frac{D^3}{8\alpha^3} \left[u_o^{\,3} - \frac{3Du_o t_o g}{4t_a \alpha} \right] \tag{3-26}$$

Substituting Equations (3-23) to (3-26) into (3-16) and (3-17), t_m and u_{zm} can be expressed as a function of α and z, the vertical distance from the real source. After some arrangement the following form is obtained

$$\frac{M_1^{\,3}}{\Delta t_m^{\,3}} = \frac{M_2[D/2 + (z-z_{ct})\alpha]^5}{\alpha} + M_3 M_4 \left[\frac{D}{2} + (z-z_{ct})\alpha \right]^3$$

$$- \frac{M_3 M_5 [\frac{D}{2} + (z-z_{ct})\alpha]^3}{\alpha} \tag{3-27}$$

$$u_{zm}^{\,3} = \frac{M_2}{\alpha[(z-z_{cv})\alpha + \frac{D}{2}]} + \frac{M_3}{[(z-z_{cv})\alpha + \frac{D}{2}]^3}$$

$$\times \left(M_4 - \frac{M_5}{\alpha}\right) \tag{3-28a}$$

where

$$M_1 = \frac{D^2}{4} u_o \, \Delta t_o$$

$$M_2 = \frac{3D^2 u_o \Delta t_o g}{8t_a}$$

$$M_3 = \frac{D^3}{8}$$

$$M_4 = u_o^{\;3}$$

$$M_5 = \frac{3Du_o \Delta t_o g}{4t_a}$$

Equations (3-27) and (3-28) are now in the form

$$Y = f(z,\alpha) \tag{3-29}$$

and Scarborough's [30] non-linear least squares method can be used to obtain the best value of α from a given set of values of z and Y. Following Scarborough, the residuals can be written as

$$D_1 = \alpha' \left(\frac{\partial f_i}{\partial \alpha}\right)_o + Y'_1 - Y_1 \tag{3-30}$$

$$D_n = \alpha' \left(\frac{\partial f_n}{\partial \alpha}\right)_o + Y'_n - Y_n$$

Y_i is the experimental data point at z_i and Y'_i is the calculated value of Y obtained from Equation (3-27) or (3-28) using z_i and an estimate of α denoted by α_o. The partial derivatives are valued at $\alpha = \alpha_o$, and the corrected value of α is given by

$$\alpha = \alpha_o + \alpha' \tag{3-31}$$

from the condition for least squares,

$$\sum D_i^2 = \min$$

or

$$\frac{\partial}{\partial \alpha'} \sum_i^n D_i^2 = 0$$

which gives

$$2 \sum_i D_i \frac{\partial D_i}{\partial \alpha'} = 0 \tag{3-32}$$

Equations (3-29) to (3-32) are used to obtain the following solution for α:

$$\alpha = \alpha_o + \frac{\sum_i (Y_i' - Y_i) \left(\frac{\partial f_i}{\partial \alpha}\right)_o}{\sum_i \left[\left(\frac{\partial f_i}{\partial \alpha}\right)_o\right]^2} \tag{3-33}$$

A computer program was set up to solve α for Δt_m and u_{zm} using the experimental data given in Tables 2-1, 2-3, and 2-5. An iterative procedure was used until the absolute difference of the new α and the old α is less than 5% of the new α. The computer program and the results are given in Appendix D.

Since both temperature and velocity data were used for two different equations, and a few assumptions have been made on the radial temperature and velocity profiles as discussed, different values of α for temperature and velocity should be expected and they are denoted by α_t and α_v, respectively. The values of α_t and α_v calculated from the computer program are summarized in Table 3-2, and the values of $\Delta t_m/\Delta t_o$ are u_{zm}/u_{zo} versus vertical distance are shown in Figures 3-1 to 3-6. Fairly good agreement is observed.

In order to predict the axial decay of temperature and velocity, correlations of α_t and α_v as a function of t_o/t_a and M were made by linear programming. The results are as follows:

$$\alpha_t = 0.0422 \left(\frac{t_o}{t_a}\right)^{0.405} (M)^{-0.273}$$

Avg. % deviation = 5.6%

Table 3-2 Values of α from Scarborough's Non-Linear Least Square Method

u_{zo} ft/sec	$\frac{t_o}{t_a}$	M	Z_{ct}	α_t	Avg. % Deviation	Z_{cv}	α_v	Avg.% Deviation
822.	2.68	0.755	3.8	0.070	5.2	5.0	0.082	5.5
687.	2.72	0.631	3.5	0.073	4.8	4.2	0.085	5.7
78.0	2.02	0.070	3.0	0.097	4.9	3.9	0.105	6.5
78.0	1.05	0.070	4.2	0.088	3.2	5.4	0.092	4.8
37.3	1.75	0.0343	1.4	0.141	5.4	1.8	0.145	4.5
35.5	1.74	0.0343	1.3	0.147	4.4	1.8	0.150	4.3

$$\alpha_v = 0.0486 \left(\frac{t_o}{t_a}\right)^{0.435} (M)^{-0.236}$$

Avg. % deviation = 7.3%

The final form of the generalized equations for temperature and velocity decay are as follows:

$$\Delta t_m = \Delta t_o \qquad \text{for } z \leq z_{ct}$$

$$\Delta t_m = \frac{A_1}{\alpha_t^2 z'^2} \left(\frac{3}{2} \frac{A_1 g}{t_a \alpha_t^2 z'} + \frac{A_2}{z'^3}\right)^{-1/3} \qquad \text{for } z > z_{ct}$$

$$u_{zm} = u_{zo} \qquad \text{for } z \leq z_{cv}$$

$$u_{zm} = \left(\frac{3}{2} \frac{A_1 g}{t_a \alpha_v^2 z'} + \frac{A_2}{z'^3}\right)^{1/3} \qquad \text{for } z > z_{ct}$$

$$z_{ct} = 14.4 \left(\frac{t_o}{t_a}\right)^{-1.16} (M)^{0.455} D$$

$$z_{cv} = 17.5 \left(\frac{t_o}{t_a}\right)^{-1.13} (M)^{0.430} D$$

$$\alpha_t = 0.0422 \left(\frac{t_o}{t_a}\right)^{0.405} (M)^{-0.273}$$

$$\alpha_v = .0486 \left(\frac{t_o}{t_a}\right)^{0.435} (M)^{-0.236}$$

$$z_{ot} = D/2\alpha_t$$

$$z_{ov} = D/2\alpha_v$$

$$z' = z + z_{ot} - z_{ct} \qquad \text{for } \Delta t_m$$

$$z' = z + z_{ov} - z_{cv} \qquad \text{for } u_{zm}$$

$$A_1 = \frac{D^2}{4} u_{zo} \Delta t_o$$

$$A_2 = z_{ot}^3 \left(u_{zo}^3 - \frac{3A_1 g}{2t_a \alpha^2{}_t z_{ot}} \right) \qquad \text{for } \Delta t_m$$

$$A_2 = z_{ov}^3 \left(u_{zo}^3 - \frac{3A_1 g}{2t_a \alpha_v{}^2 z_{ov}} \right) \qquad \text{for } u_{zm}$$

CHAPTER IV

RADIAL TEMPERATURE AND VELOCITY DISTRIBUTION

A. Radial Distribution of Temperature and Vertical Velocity

The radial profiles of temperature and vertical velocity calculated by the finite difference program agrees well with Corrsin and Uberoi [9] data as shown in Figure 4-1 and 4-2, but do not agree so well with Tomich and Weger's data, as shown in Figure 4-3 and 4-4.

The radial profiles of temperature and velocity at short distances from the stack exit are shown in Figure 4-5. The radial profiles change gradually from a flat profile to the Gaussian shape of profiles. The edges of the profile are smoothing out in the Gaussian shape.

A comparison of the experimental radial average temperature of the field of view with that calculated from finite difference method is shown in Figure 4-6. The points near the center gives better agreement than the two points near the edges.

An attempt was made to correlate the radial profiles of temperature and velocity obtained from the literature and from the finite difference method using the similarity hypothesis as proposed by many pioneers [20,22,11,24]; i.e.,

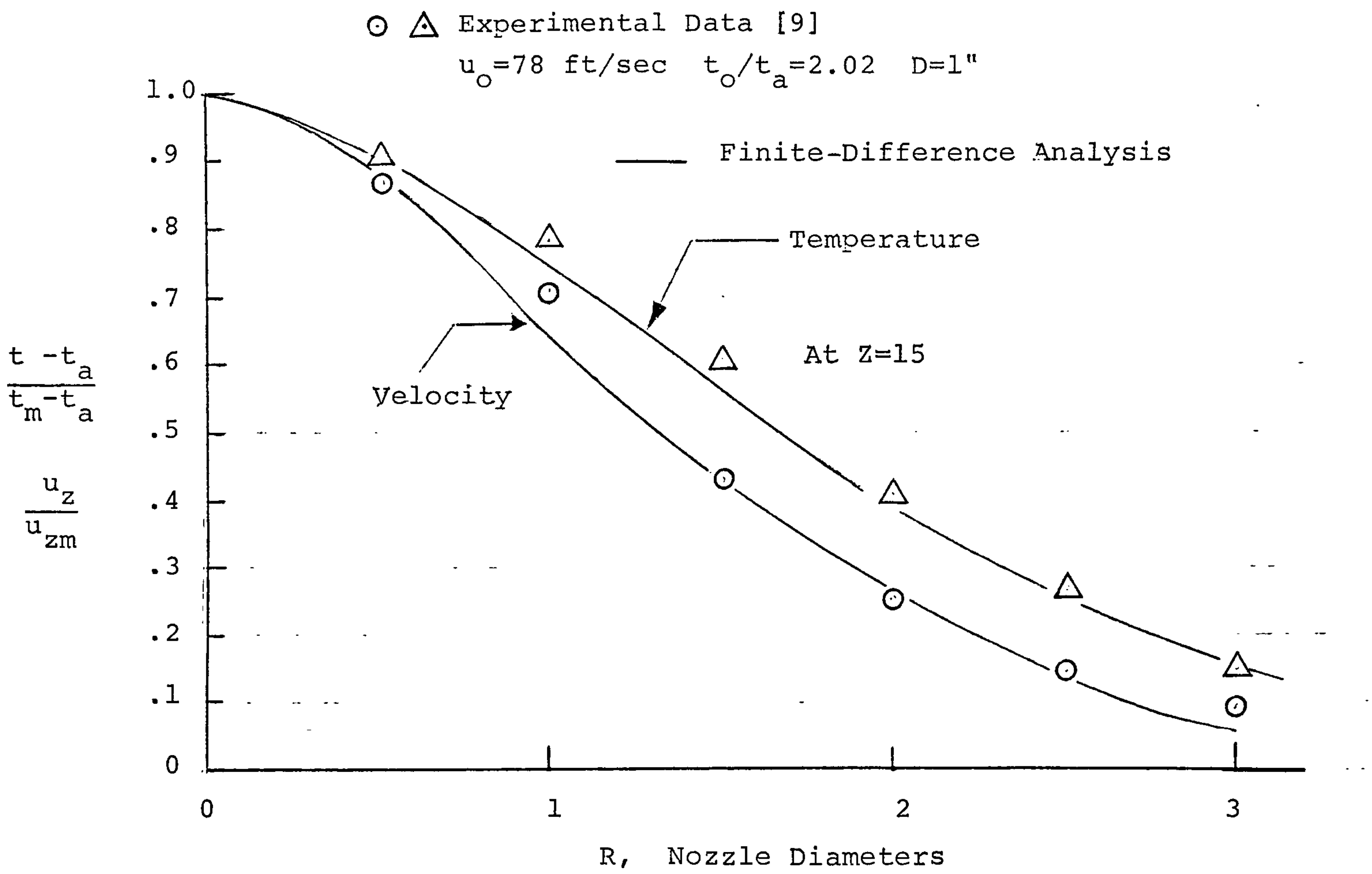

Figure 4-1. Comparision of the Experimental Data [9] with the Analysis for the Radial Distribution of Temperature and Velocity

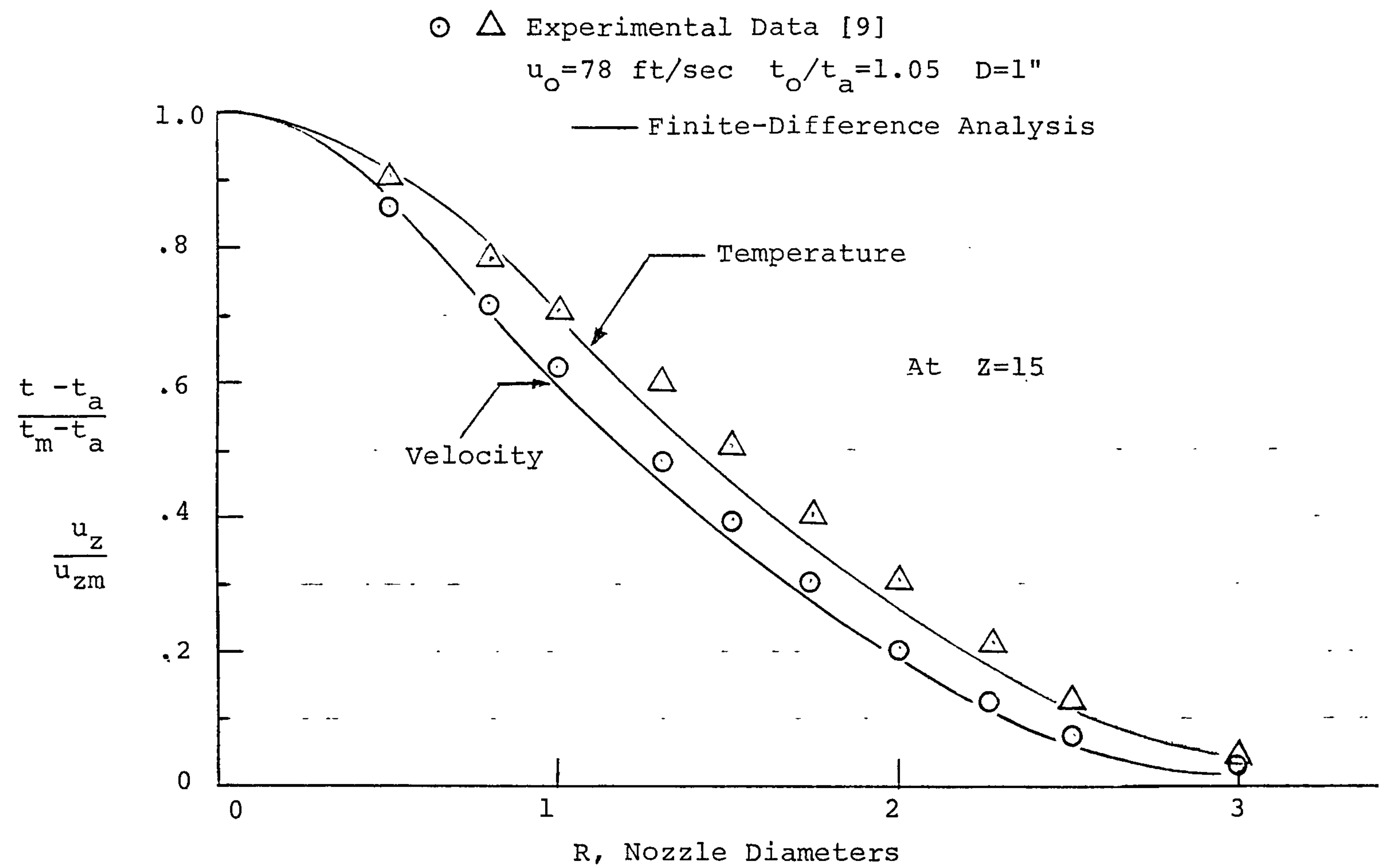

Figure 4-2. Comparision of the Experimental Data [9] with the Analysis for the Radial Distribution of Temperature and Velocity

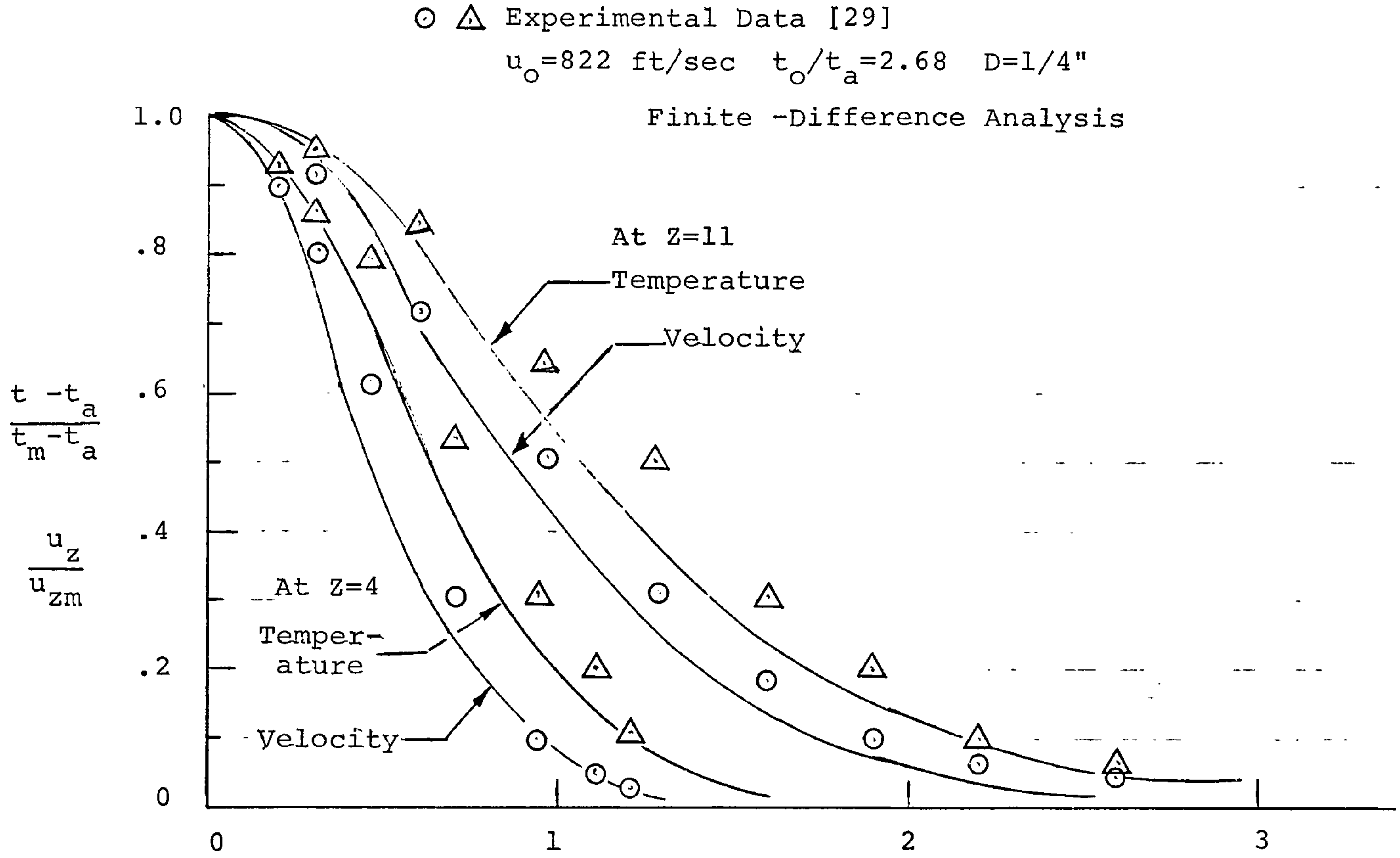

Figure 4-3. Comparision of the Experimental Data [29] with the Analysis for the Radial Distribution of Temperature and Velocity

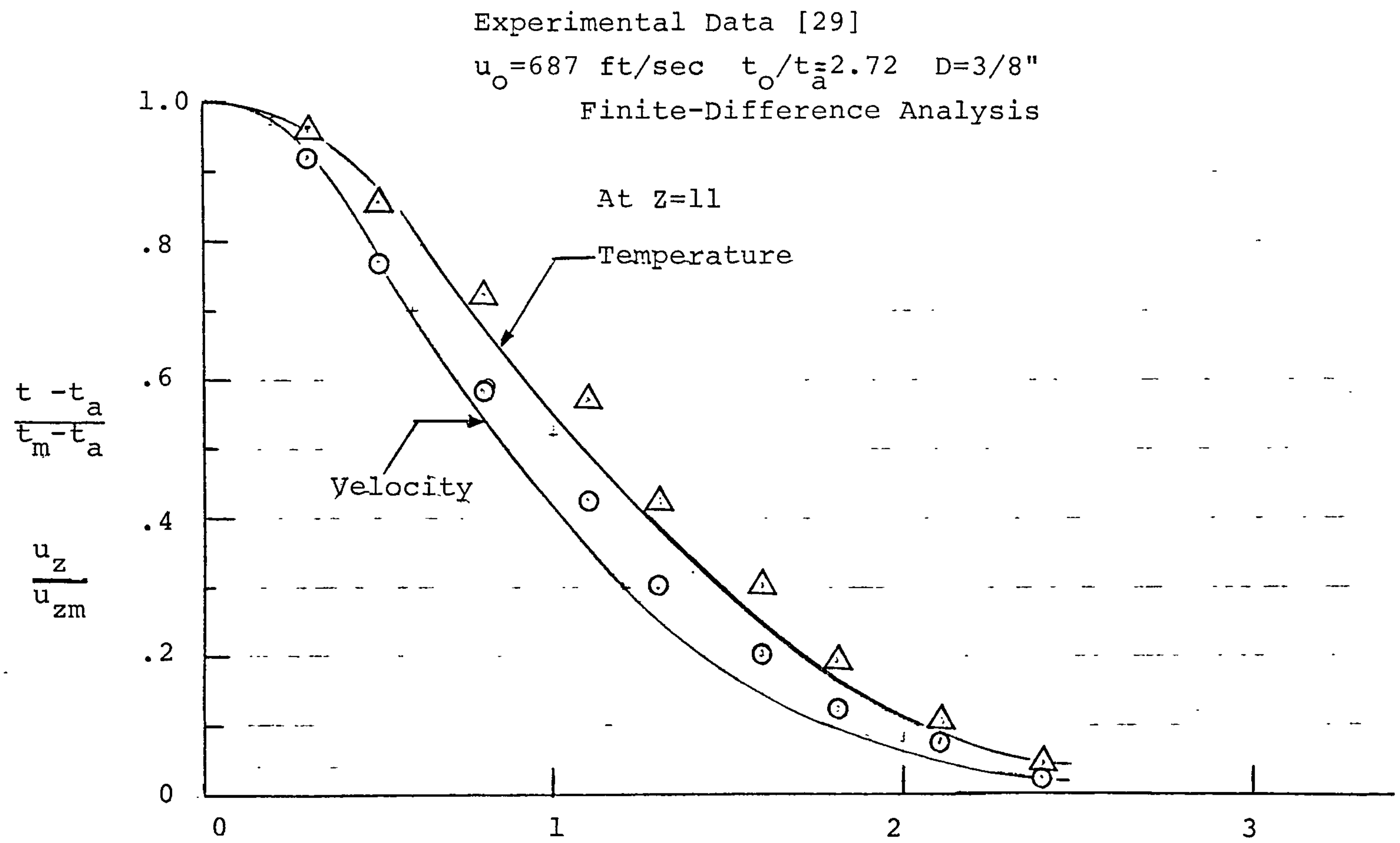

Figure 4-4. Comparision of the Experimental Data [29] with the Analysis for the Radial Distribution of Temperature and Velocity.

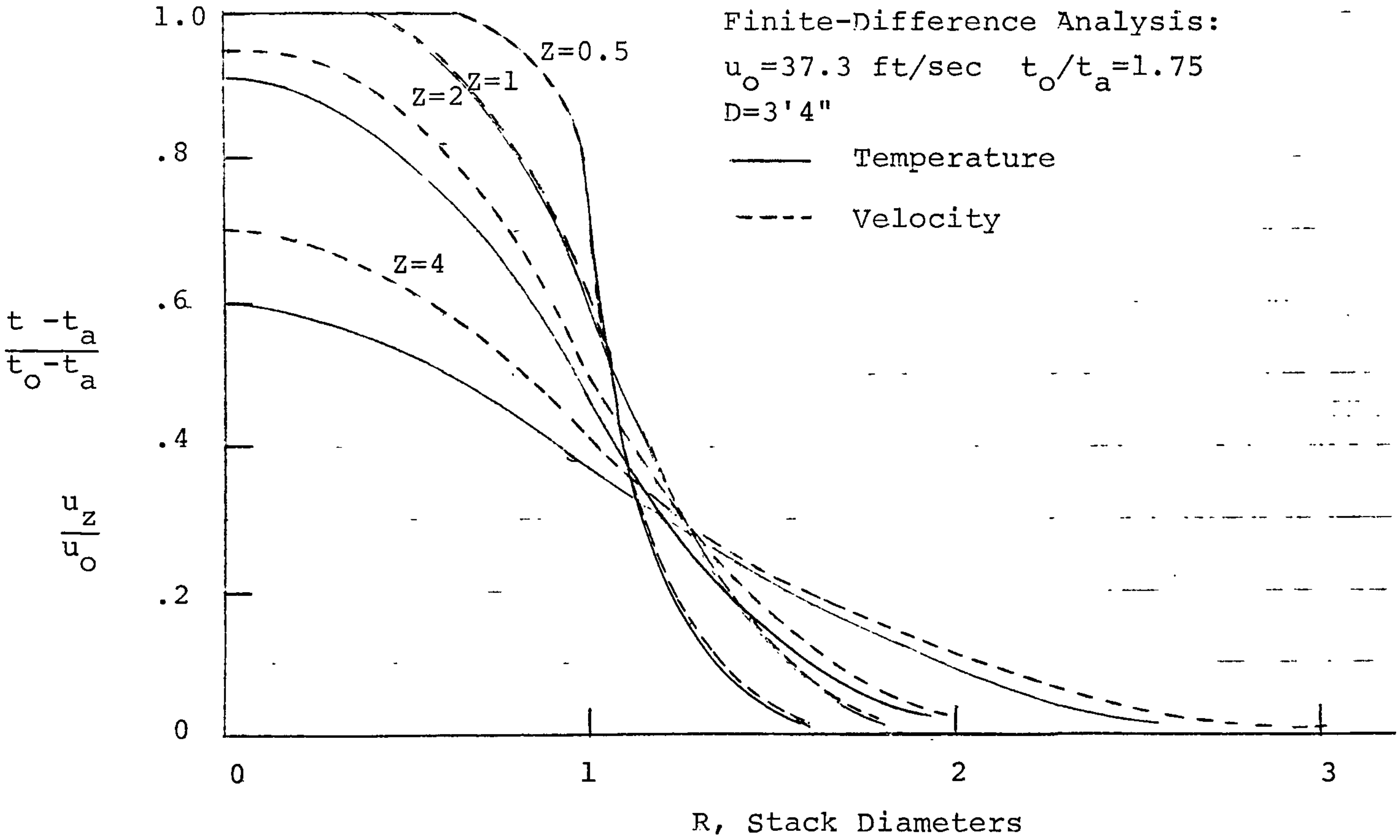

Figure 4-5. Radial Temperature and Velocity Distribution at Short Distance From Finite Difference Analysis.

Temperature Data of Field of View [14]

u_o=29 ft/sec t_o/t_a=1.68 D=3'4"

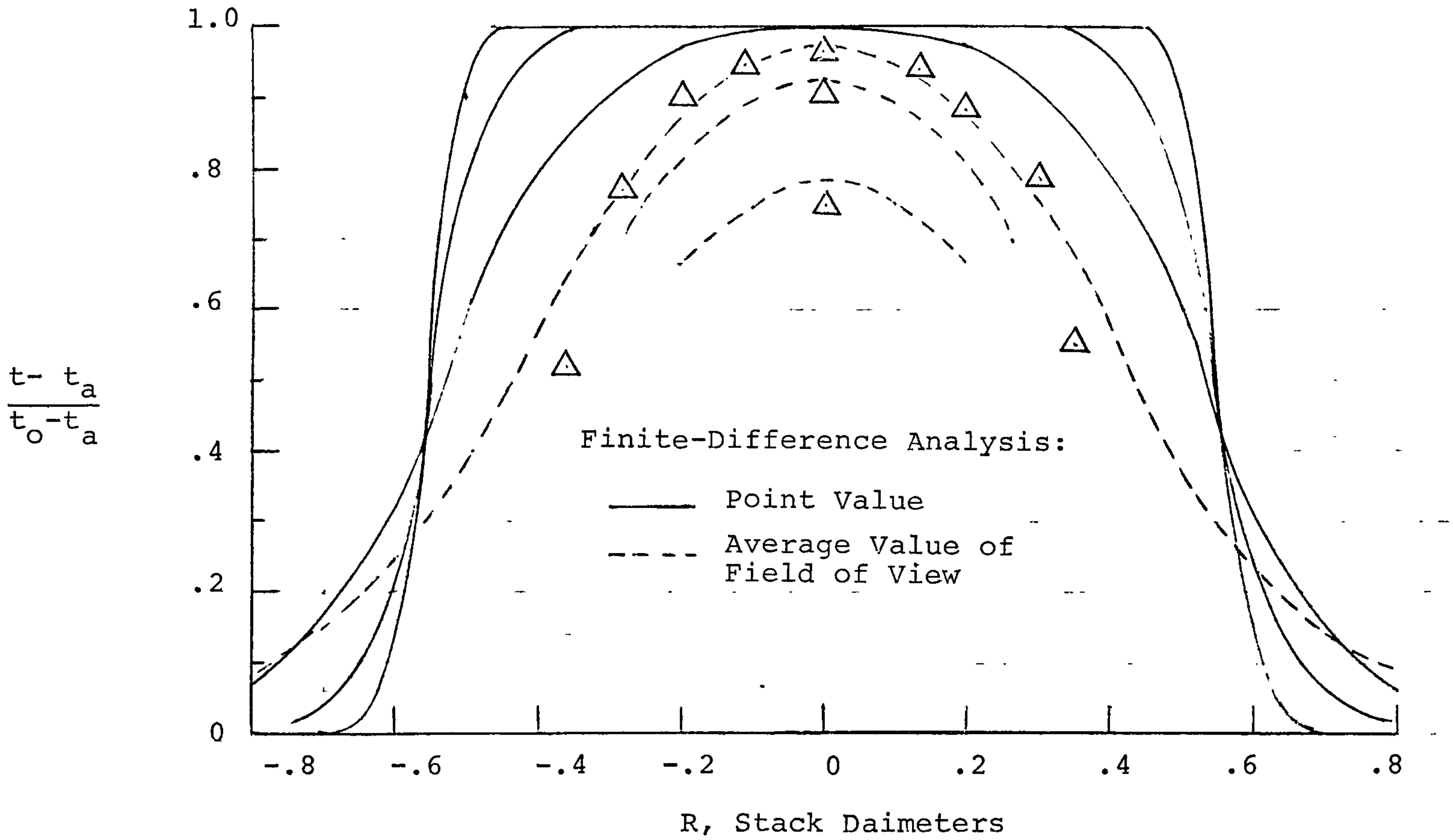

Figure 4-6. Comparision of the Experimental Data [14] with the Analysis for the Radial Distribution of Temperature

$$\frac{\Delta t}{\Delta t_m} = \exp\left(-\beta \frac{r^2}{z^2}\right) \qquad (4-1)$$

$$\frac{u_z}{u_{zm}} = \exp\left(-\eta \frac{r^2}{z^2}\right) \qquad (4-2)$$

where β and η are constants. However, β and η were found to be approximately constant only when z is constant, and β and η increase as z increases. That is to say the radial distribution of temperature and velocity are Gaussian shape, however, the similarity hypothesis for the radial distributions doesnot hold for compressible free jet. The average values of β and η, and their average percent deviations at various values of z, calculated from the literature data and the simulated value from the finite difference method, are given in Table 4-1. The values of β and η are then correlated with the dimensionless variables t_o/t_a, M (Mack number) and Z by the linear regression method; the results are as follows:

$$\beta = 23.14\, Z^{0.680}\, M^{0.229} \left(\frac{t_o}{t_a}\right)^{-0.491} \qquad (4-3)$$

Avg. % deviation = 7.15

$$\eta = 15.33\, Z^{0.688}\, M^{0.0857} \left(\frac{t_o}{t_a}\right)^{-0,329} \qquad (4-4)$$

Avg. % deviation = 6.89

Table 4-1 Variation of β and η with u_{zo}, t_a/t_o, and z

u_{zo} ft/sec	$\frac{t_o}{t_a}$	z/D	η	Avg. % deviation	β	Avg. % deviation	$\frac{\eta}{\beta}$
37.3	1.73	4	28.9	7.1	32.9	5.0	1.14
37.3	1.73	11	45.0	5.5	48.4	4.9	1.08
37.3	1.73	15	56.2	4.7	60.0	4.2	1.07
78.0	2.02	15	52.5	3.8	82.5	7.6	1.57
78.0	1.05	15	74.0	6.5	103.7	6.3	1.39
687.	2.72	11	64.8	7.8	89.4	7.4	1.37
822.	2.68	4	22.0	7.1	38.0	5.0	1.72
822.	2.68	11	57.0	8.6	102.0	7.9	1.77

It is obvious from Equations (4-3) and (4-4) that the values of β and η increases as initial velocity increases and as the temperature ratio $\frac{t_o}{t_a}$ decreases.

Also it is noticed that the ratio of η/β is greater than 1, that is to say the characteristic radius describing the temperature distribution in a heated free jet is greater than that for the velocity distribution. Rouse et al. and Railston [22,20] have reported the value of $\frac{\eta}{\beta} \simeq 1$; Reichart's [19] experimental value for $\frac{\eta}{\beta} = 2$, while our calculated value is between 1 and 2. The value of η/β increases as the exit velocity increases as observed from Table 4-1.

B. Distribution of Radial Velocity

One advantage of the present calculational method is that the calculated results for the radial distribution of the radial velocity component can also be obtained.

A radial distribution of the calculated radial velocity at various vertical position is shown in Figure 4-7. The positive radial velocity near the jet axis is thought to be caused by the spread of the jet as it moves downstream, while the negative (inward) radial velocity at larger radial distance is thought to be caused by the entrainment of ambient air. The magnitude of the inward radial velocity is decreasing as z increases, that is to say the entrainment rate decreases as z increases, or as vertical velocity decreases.

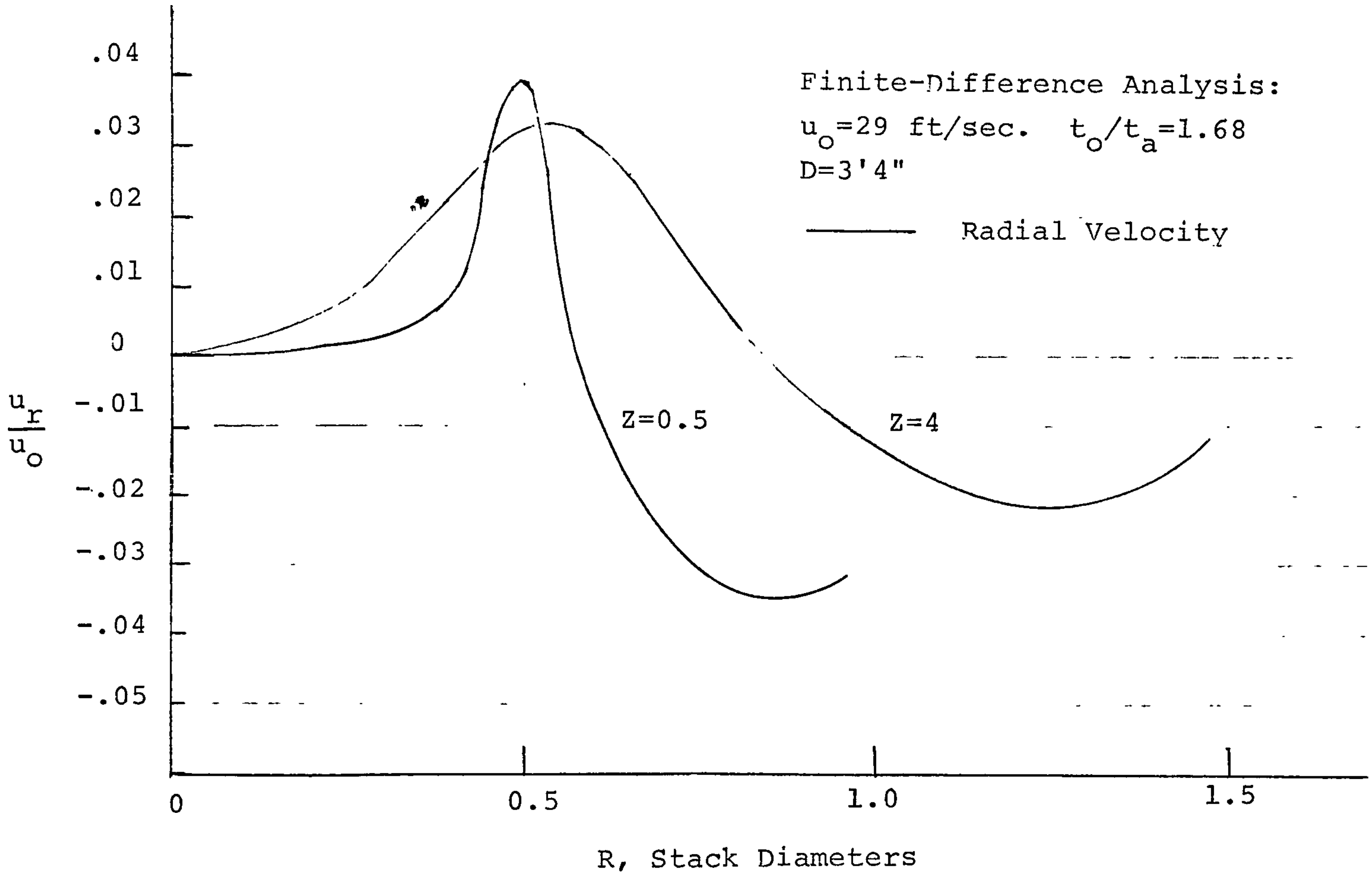

Figure 4-7. Radial Distribution of Radial Velocity from Finite-Difference Analysis

C. Bibliography for Chapters I, II, III and IV

1. Abbott, M.R., Computer J., 7, 47 (1946).

2. Abramovich, G.N., Turbulent Jets Theory, 278-316, ASITA, Translation AD283858 (1962).

3. Batchelor, G.K., Quart. J. Roy. Meterol. Soc., 80, 339 (1954).

4. Becker, H.A., Rosenweig, R.E., and Gwozdg, J.R., AIChE J., 12, 964 (1966).

5. Briggs, G.A., Plume Rise, U.S.A.E.C., Division of Technical Information (1969).

6. Bringfelt, B., Atmospheric Environment, 2, 575-598 (1968).

7. Carnahan, B., Luther, H.A., and Wilkes, J.O., Applied Numerical Methods, 440-442, John Wiley & Sons, New York (1969).

8. Cohen, N.S. Rept. TM 1, 3RO, Aerojet-General Corp., Sacramento, Calif. (1964).

9. Corrsin, S. and Uberoi, M.S., N.A.C.A., Rep. No. 998 (1950).

10. Davis, O.D., Smith, G., and Klauber, G., Science, 186, 732 (1974).

11. Hinze, J.O., and B.G. van der Hegge Zignen, Applied Science Research 1A, 435 (1949).

12. Kleinstein, G., J. Spacecraft Rockets, 1, 403 (1964).

13. Lapidus, Leon, Digital Computation for Chemical Engineers, 254-255, McGraw-Hill, New York (1962).

14. Mahagaokar, M., Ph.D. Dissertation, Chemical Engr. Dept., Uni. of Houston, Houston, Texas.

15. Morton, B.R., Taylor, G.E. and Turner, J.S., Proc. Roy. Soc., London, Ser. A., 234, 1 (1956).

16. Pai, S.I., Quart. Appl. Math., 10, 141 (1952).

17. Prengle, H.W., J., Morgan, C.A., Fang, C.S., Huang, L.K., Campani, P., and Wu, W.W., Environ. Sci. Tech 7, 417 (1973).

18. Priestly, C.H.B. and Ball, F.K., Quart. J. Roy. Meteorol. Soc., 81, 144 (1955).

19. Reichardt, H., Gesetzmakigkeiten der freien Turbulenz. VDI-Forschungsheft, 414, (1942); 2nd ed. 1951.

20. Railston, W., Proc. Phys. Soc., B., 67, 42 (1954).

21. Rosenweig, R.E., Hottel, H.C., and William, G.C., Chem. Engr. Sci. 15, 111 (1961).

22. Rouse, H., Yih, C.S., and Humphreys, H.W., Tellus, 4, 201 (1952).

23. Scarborough, J.B., Numerical Mathematical Analysis, Johns Hopkins Press (1962).

24. Schlichting, H., Boundary Layer Theory, 483-506, McGraw-Hill, New York (1955).

25. Schmidt, W., Z. Angew, Math. Mech. 21, 265 (1941).

26. Sutton, O.G., Micrometeorology, 10-12, McGraw-Hill, New York (1953).

27. Szablewski, W., Intern. J. Heat Mass Transfer, 6, 739 (1963).

28. Tennessee Valley Authority, Full Scale Study of Plume Rise at Large Electric Generating Stations, Muscle Shoals, Alabama.

29. Tomich, J.F., and Weger, E., AIChE J. 30, 948 (1967).

30. Tollmun, W., Z. Agnew, Math. U. Mech., 6, 468 (1926).

31. Warren, N.R., Ph.D. Thesis, Princeton Uni., N.J. (1957).

32. Wegstein, J.G., Commun. Assoc. Computing Mach., 1, 9 (1958).

CHAPTER V

DISCUSSIONS, CONCLUSIONS, AND RECOMMENDATIONS

A. Discussions and Conclusions

1. Finite-Difference Analysis: Starting with pipe flow conditions as intial conditions for the jet, ab initio velocity and temperature calculations were made axially and radially using a finite-difference technique (similar to Tomich and Weger), which included the modified transfer coefficient given in the literature. These calculations agree well with the experimental data for axial decay and radial distribution of temperature and velocity, and indicate the existence of a core region in which the center line properties remain unchanged; and a fully developed region in which radial and axial properties decay. The technique has eliminated the need for some of the simplifying assumptions that were required in previous investigations in order to obtain a solution. Also the finite-difference technique can be set up so that a different form of initial profiles and more complex forms of eddy transfer coefficient can be inserted when the accuracy of the available data is justified. Another advantage of this calculational method is that the distributions of the radial component of velocity are also obtained.

Conclusion : The finite-difference calculational technique has made possible a very general solution of the conservation equations for a compressible turbulent, axially symmetric free jet.

2. The Radial Distribution of Temperature and Velocity:

The experimental results from laboratory free jets and from our infrared remote sensing measurements, and the analytical results from the finite-difference calculations show that the radial distribution of temperature and velocity is approximately Gaussian in the fully developed region . The finite-difference calculations show that the radial profiles change gradually from an initial flat to Gaussian shape. The characteristic radius describing the temperature distribution in a hot free jet is greater than that for the velocity distribution, and both increase as the exit velocity increases; therefore similarity does not hold for hot compressible free jets.

Conclusion : The radial distribution of temperature and velocity in a hot free jet or emerging plume is approximately Gaussian in the fully developed region. And from the difference in the characteristic radius of the temperature and velocity distributions, the mechanisms for heat and momentum transfer are not the same.

3. The Plume Model: An analytical model is proposed which includes, i) core region, and ii) fully developed region solutions for the axial decay of temperature and velocity. The model contains a correlated quantity, α the spreading coefficient, whcih is a function of the plume Mach number and temperature ratio, t_o/t_a, the two most important parameters.

The model agrees well with experimental data; the largest deviation occuring in the very short transition region. Deviations can be reduced to smooth the curve in this region. The axial temperature and velovity were found to decay in a shorter distance as the temperature ratio is increased and the velocity decreased.

Coefficients for the radial distribution of temperature and velocity were correlated as function of Mach number, temperature ratio, t_o/t_a, and the dimensionless axial distance z/D.

Conclusion: It is possible to construct a plume model which provides better agreement with data for the axial decay of temperature and velocity than previous models.

B. Recommendations

1. The correlation coefficients obtained in this work are based on a relatively few set of experimental data. More data at velocities between 20-40 ft/sec should be obtained to justify and improve the correlations.

2. In particular to the remote sensing of temperature measurement by infrared emission interferometry-spectroscopy technique, a more sensitive detector, e.g., the mercury cadmium telluride (Hg Cd Te) photodetector should be used, the field of view can then be reduced, more accurate axial and radial temperature measurements can then be made. This improvement also provides better concentration fata.

3. So far no mass dispersion have been discussed, a turbulent transfer coefficient for concentration may be

introduced to develop a new model for mass dispersion. However, this requires experimental data to justify the theoretical model.

4. No attempt has been made to modify the finite-difference program to fit the cross wind situation. Certain boundary conditions, the eddy transfer coefficients and the schematic structure of the plume should be changed to accompany for the cross wind situations.

5. The finite-difference technique, although it is a powerful technique in solving differential equations, but may not be the best available as far as computer time is concerned, "collocation" method should be faster than the finite-difference method, and collocation may have better convergence or more stable system because it requires a smaller matrix. Collocation method should be considered in future use.

CHAPTER VI

EMISSIONS AS A FUCTION OF EXCESS AIR

As industrial boilers and process heaters are operated at lower excess air levels in order to improve combustion efficiency, the concentration of of pollutants in stack gases will change with flame temperature and combustion rate. The purpose of this chapter is a)- to present data from the literature on gas, oil, and coal fired furnaces indicating the levels of pollutant concentrations, b)- to discuss emissions as a function of excess air, and c)- discuss recent equipment improvements which permit operation at lower excess air levels.

A. Combustion of Gas, Oil and Coal

Natural Gas Combustion

Natural gas is used as fuel extensively in power plants, industrial heating, and for domestic and commercial space heating. The primary component is methane, but with smaller quantities of other hydrocarbon, nitrogen and carbon dioxide. Even though natural gas is considered to relatively clean, some emissions do occur from the combustion reaction. When insufficient air is supplied, large amounts of carbon monoxide may be produced.

Emissions factors for natural gas combustion are presented in Table 6.1 [1].

Fuel Oil Combustion

Fuel oil is classified into two major types, residual and distllate. istillate fuel oil is primarily for domestic use, but is used in some commercial and industrial applications where a high quantity oil is required. Fuel oils are classified by grades: No. 1 to No. 6 from high sulfur content.

Emissions from oil combustion are dependent on type and size of equipment, method of firing, and maintenance. Table 6.2[1] presents emission factors for

Table 6.1 - Emission Factors for Natural Gas Combustion[1]

Pollutant	Type of Unit		
	Power Plant	Industrial Process Boiler	Domestic and Commercial Heating
	$lb/10^6 ft^3$	$lb/10^6 ft^3$	$lb/10^6 ft^3$
Particulates	15	18	19
Sulfur-oxides (SO_2)	0.6	0.6	0.6
Carbon Monoxide (CO)	17	17	20
Hydrocarbons (CH_4)	1	3	8
Nitrogen Oxides (NO_2)	600	(120 to 130)	(80 to 120)

Table 6.2 - Emission Factors for Fuel Oil Combustion[1]

Pollutant	Type of Unit	Industrial and Commercial		
	Power Plant	Residual	Distillate	Domestic
	$lb/10^3 gal$	$lb/10^3 gal$	$lb/10^3 gal$	$lb/10^3 gal$
Particulate	8	23	15	10
Sulfur dioxide	157	157	142	142
Sulfur trioxide	2	2	2	2
Carbon monoxide	3	4	4	5
Hydrocarbons	2	3	3	3
Nitrogen oxides (NO_2)	105	(40 to 80)	(40 to 80)	12
Aldehydes (HCHO)	1	1	2	2

fuel oil combustion. Note that the industrial and commercial category is split into residual and distillate because there is a significant difference in particulate emissions from the same equipment. It should also be noted that power plants emit less particulate matter per quantity of oil consumed, reportedly because of better design and more precise operation of equipment.

Coal Combustion.

Coal, the most abundant fossil fuel in the USA is burned in a wide variety of furnaces to produce steam and process heat; some large pulverized coal-fired units burn 300-400 tons/hr.

Although predominantly carbon, coal contains many compounds in varying amounts. The exact nature and quantity of these compounds are determined by the location of the mine producing the coal and will usually affect the final use of the coal.

Emission from coal is dependent upon the contents of coal, the type of burner, the property and control of the burning process. The emission factors for bituminous coal and anthracite coal combustion are presented in Tables 6.3 and 6.4.

EPA Standard

In late 1971[2] EPA established the following limits on fossil fuel boilers having a heat input greater than 250×10^6 Btu/hr.

Emission	Fuel	$Lb/10^6$Btu Input	Approx.ppm (volumetric dry)
Particulates	All	0.1	0.06 grans/scf)
SO_2	Liquid	0.8	550
	Solid	1.2	520
NO_x	Gaseous	0.2	165
	Liquid	0.3	227
	Solid	0.7	525

For carbon monoxide CO, E.P.A. set the ambient air quality standard at a maximum of $10^{mg}/m^3$ (9 ppm) for 8-hour averaging period, and 40 mg/m^3 (35 ppm) for a 1-hour averaging period.[3]

Table 6.3 - Emission Factors for Bituminous Coal Combustion without control Equipment[1]

Furnace size 10^6 Btu/hr heat input	Particulates lb/ton coal burned	Sulfur oxides lb/ton coal burned	Carbon monoxide lb/ton coal burned	Hydro-carbons lb/ton coal burned	Nitrogen oxides lb/ton coal burned	Aldehydes lb/ton coal burned
Greater than 100						
Pulverized						
General	16	38	1	0.3	18	0.005
Wet bottom	13	38	1	0.3	30	0.005
Dry bottom	17	38	1	0.3	18	0.005
Cyclone	2	38	1	0.3	55	0.005
10 to 100						
Spreader stoker	13	38	2	1	15	0.005
Less than 10						
Spreader stoker	2	38	10	3	6	0.005
Hand-fired units	20	38	90	20	3	0.005

Table 6.4 - Emissions from Anthracite Coal Combustion Without Control Equipment(1)

Type of furnace	Particulate lb/ton	Sulfur dioxide lb/ton	Sulfur trioxide lb/ton	Hydrocarbons lb/ton	Carbon monoxide lb/ton	Nitrogen oxides lb/ton
Pulverized (dry bottom), no fly-ash reinjection	17	38	0.5	0.03	1	18
Overfeed stokers, no fly-ash reinjection	2	38	0.5	0.2	(2 to 10)	(6 to 15)
Hand-fired units	10	36	0.8	2.5	90	3

B. Variations with Excess Air

Particulates are defined as dispersed solid and liquid particles larger than single molecules (~$2x10^{-4}$ microns in diameter) but smaller than 500 microns.

For natural gas particulate emissions are not important, and not much specific data are available in the literature, but it has been shown that increasing the mount of excess air decreases the particulate loading since more complete combustion results.[1]

For fuel oil the normal range of particulate loading is between 0.025 and 0.060 gr./scf.[4] The most commonly reported values are between 0.030 and 0.035 gr/scf.[4] In a series of four tests, it was found that, as the oxygen concentration in the stack gas increased from 2 to 4 percent, the particulate loading decreased from 0.140 to 0.020 gr/scf.[5]

For coal particulates consist primarily of carbon, silica, alumina and iron oxide in fly ash. The quantity is mainly a function of 1) the ash content, 2) the heating value of the fuel, 3) the method by which the coal is burned, and (4) the rate of burning. No specific data relates the particulates concentration as a function of excess air is available in the literature. However, the particulates emission decreases as excess air increases because of more complete combustion. The effect of excess air on the amount of unburned combustibles is shown in Figure 6.1.[6]

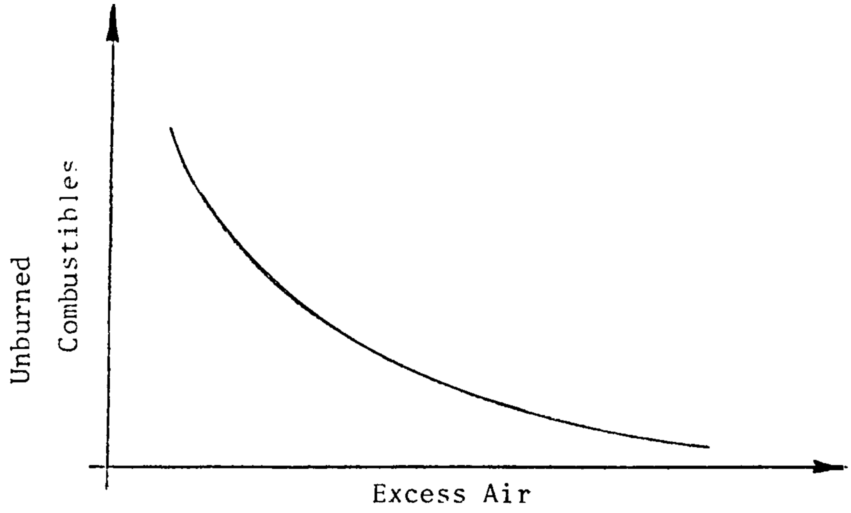

Figure 6.1 - Effect of Excess Air on Unburned Combustibles[6]

Carbon Monoxide and unburned fuel

Insufficient supply of air, poor mixing of air and fuel, low furnace temperature, and insufficient combustion time produce large amounts of carbon monoxide and hydrocarbon. Smoke formation is the characteristic feature of incomplete combustion. There are very little literature data discussed extensively on the effect of excess of oxygen on carbon monoxide and unburned fuel.

However, carbon monoxide and unburned fuel concentrations drop rapidly as excess air is increased from 0%,[1][4][6][7][8] at about 3% to 4% excess oxygen, combustion approaches 100% completion. A number of test runs[7] on a power house burning sulfur free natural gas showed that CO dropped from 540 to less than 10 ppm. CH_4 from 750 to less than 60 ppm, HCHO from 260 to less than 130 ppm, for an increase of excess oxygen from 0% to 4%. The effect of excess oxygen on the concentration of the pollutants is shown in Figure 6.2.

Another set of data obtained from a steam generating coal-pulverized unit[8] is shown in Figure 6.3; for CO, hydrocarbons, and formaldehyde for excess oxygen from 2% to 4.5%.

Oxides of Sulfur

The amount of sulfur oxide is mainly dependent on the sulfur content of the fuel; effect of excess air on sulfur oxide emission is minimal. Emission can be lowered by reducing the sulfur content or installing an SO_2 clean up system--a wet scrubbing or a dry system.[9]

Oxides of Nitrogen, NO_x

The amount of NO_x formed is a function of several variables including, nitrogen content of the fuel, flame temperature, and oxygen availablility.

A substantial portion of the NO_x formed in combustion comes from the nitrogen in the combustion air--called thermal NO_x; which is especially temperature sensitive. Figure 6.4[4] shows this effect which occurs when some of the N_2 in the air forms atomic nitrogen and combines with oxygen to form NO and some NO_2.

Emission of NO_x from combustion of natural gas is indicated to increase linearly as a function of excess air, as shown in Figure 6.2,6.5,6.6, and 6.7 for burning natural gas and propane.[10] It is estimated that as excess O_2 increased 1%, the NO_x concentration increased 15%. Above 5% excess O_2, NO_x concentration increases very slowly or remains constant.

For fuel oil the amount of excess air used in large modern plant is about 16% to 20% or 4 to 5% excess oxygen. This concentration varies with fuel and

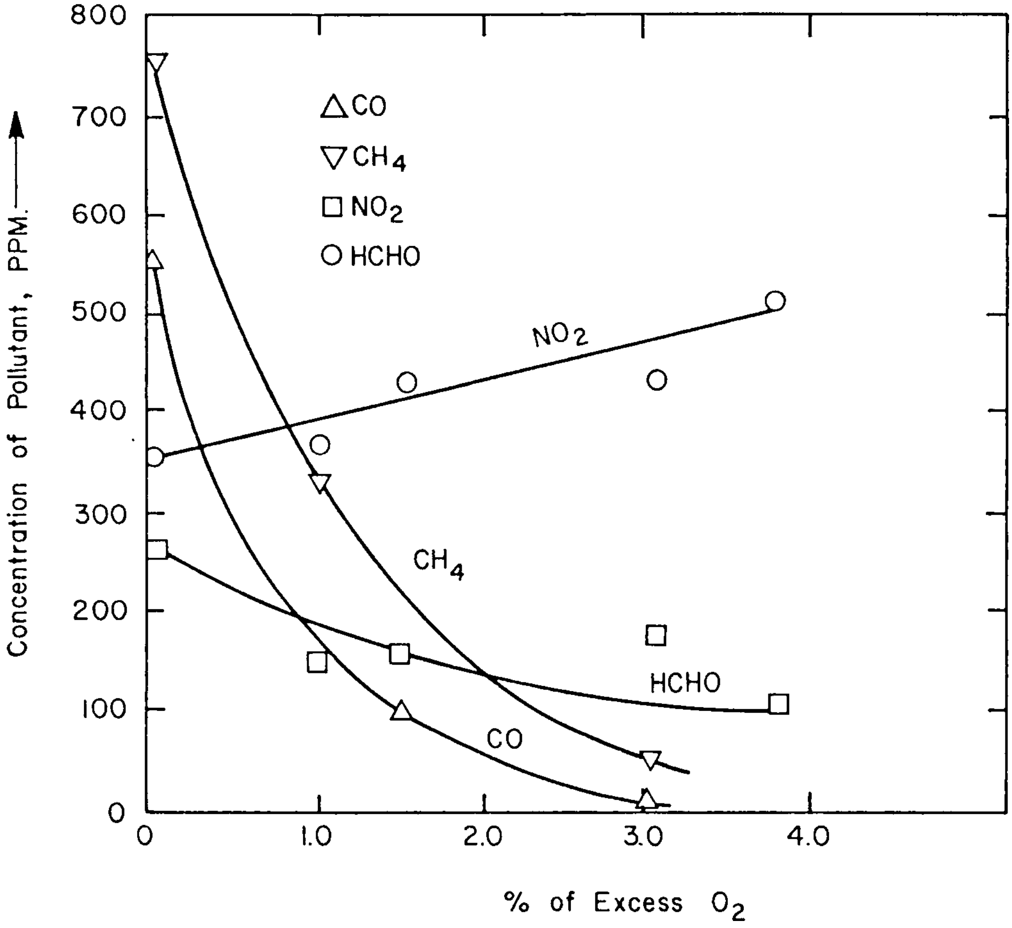

FIGURE 6.2 EFFECT OF EXCESS AIR ON POLLUTANT EMISSION FROM COMBUSTION OF NATURAL GAS[7]

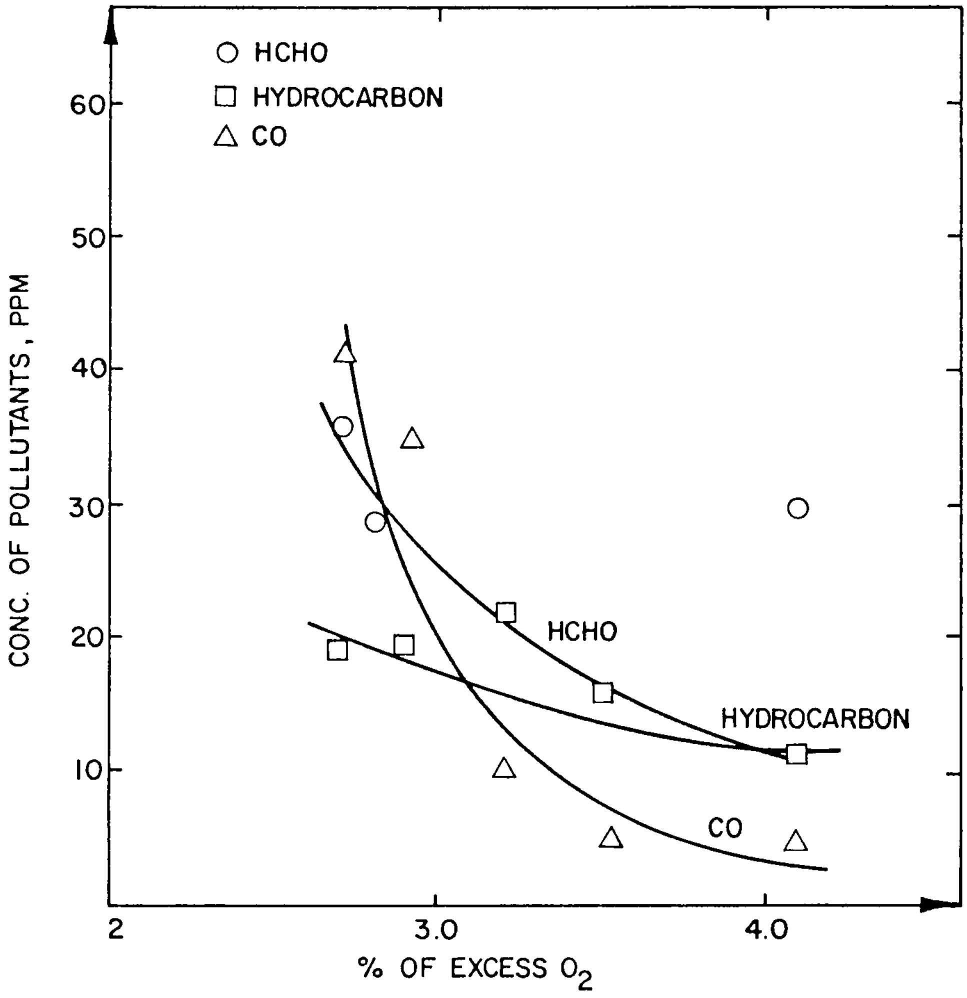

FIGURE 6.3 EFFECT OF EXCESS AIR ON POLLUTANT EMISSIONS FROM A PULVERIZED COAL UNIT[8]

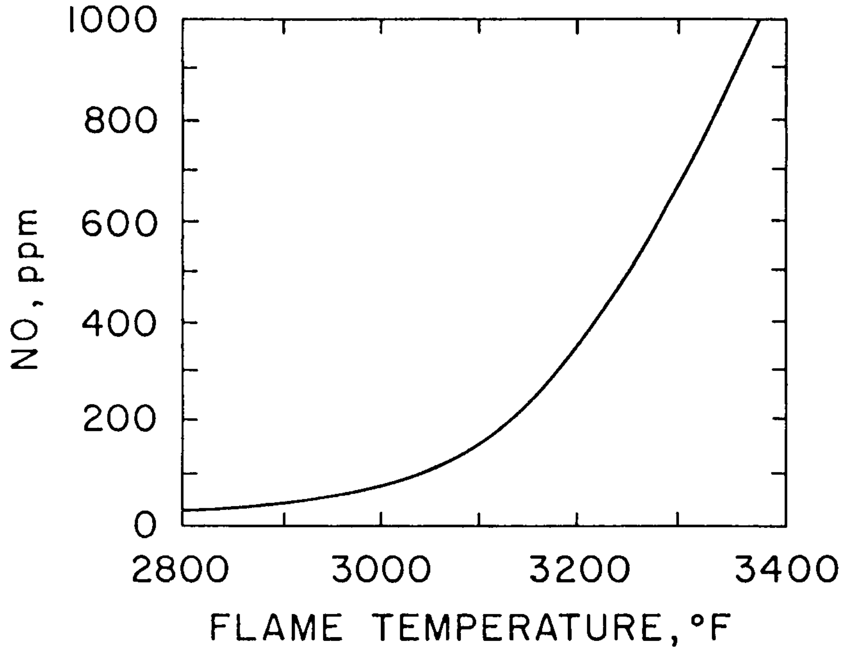

FIGURE 6.4 - THEORETICAL NO vs. FLAME TEMPERATURE, °F[4].

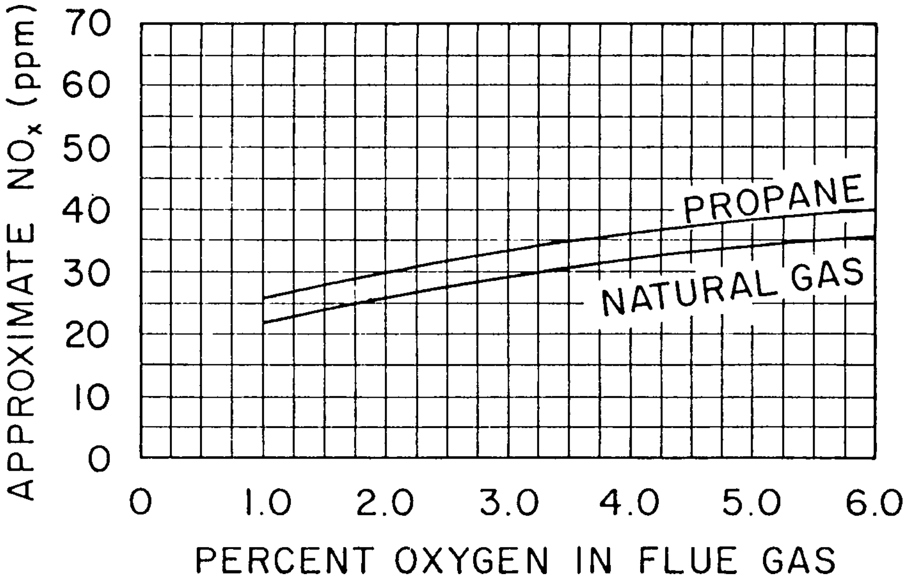

FIGURE 6.5 NO_x vs. PERCENT OXYGEN IN FLUE GAS[10]

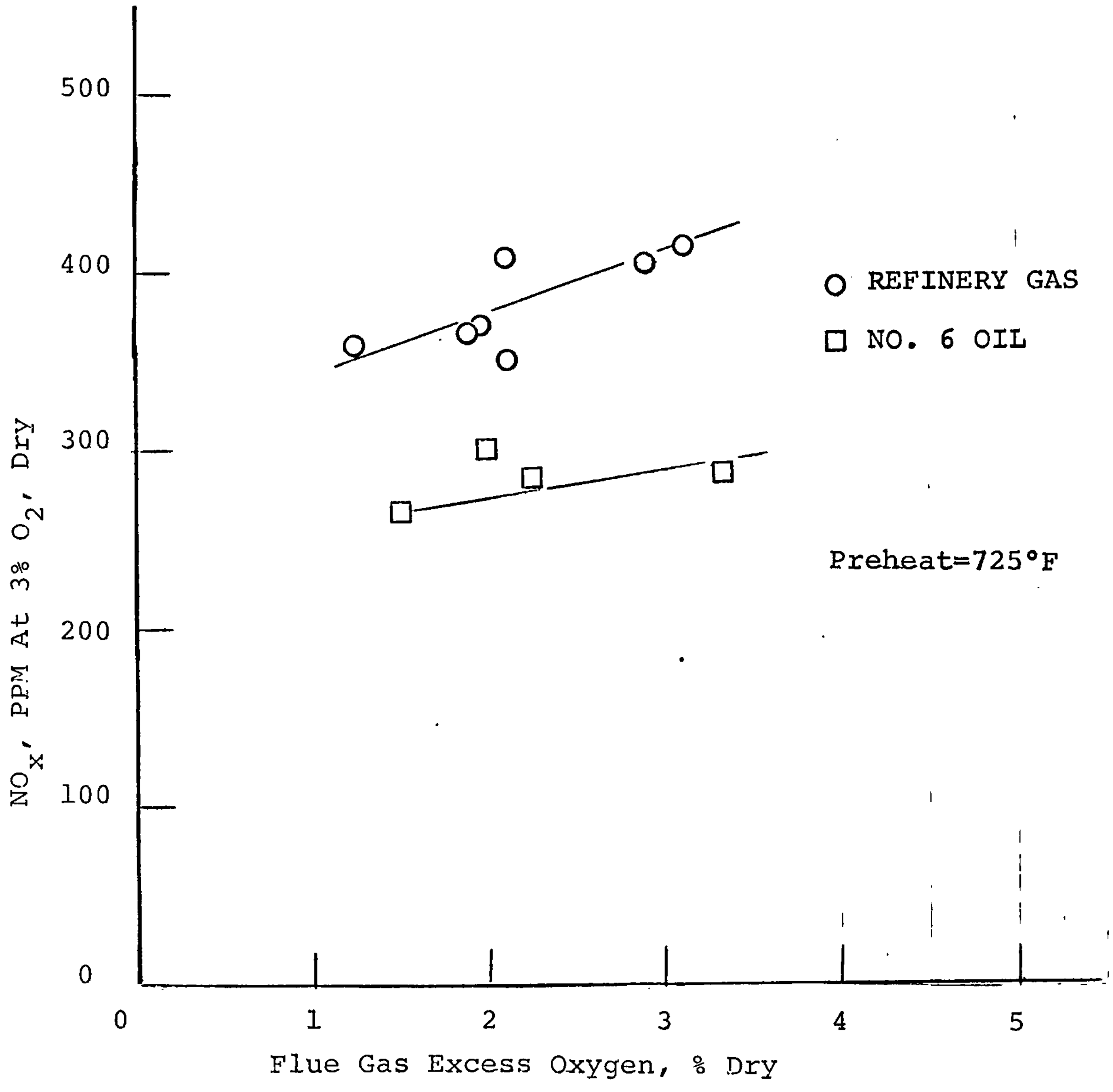

Figure 6-6. NO_x Versus Excess O_2 For A Balanced Draft Heater With Combustion Air Pre-Heat [16].

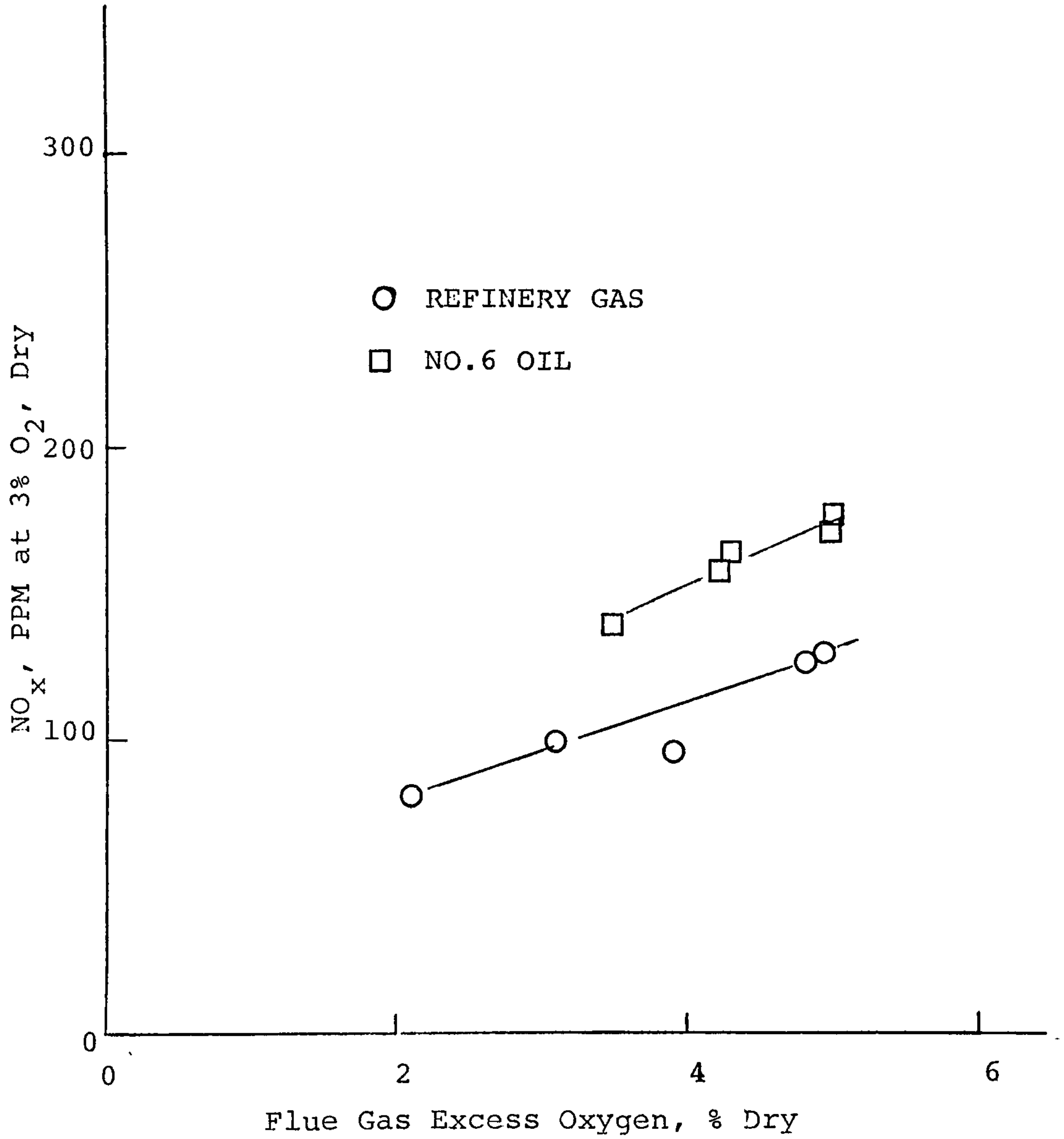

Figure 6.7 NO_x Versus Excess O_2 For A Forced Draft Heater [16]

burner design. A linear relationship has beenestablished indicating that as excess 0_2 decreased by 1%, the NO_x concentration is reduced by 15% for tangentially fired units, and 29% for a horizontally fired unit [11]. Figure 6.6, 6.7, and 6.8 shows the effect of excess air on NO_x emissions from two draft heaters and a large unit.

For coal, emissions of NO_x is mainly dependent on the nitrogen content and the combustion process. The overall conversion oc coal nitrogen to NO_x in a gasification/combustion process was found to be significantly lower than for direct burning of pulverised coal [12]. In Figure 6.9 [12] NO_x emissions from a diffusion flame are nomalized with respect to furnace heat input and oresented as function of furnace oxygen and measured amounts of NH_3 in the fuel gas. The conversion of NH_3 to NO_x contributed between 60 to 180 ppm to the total emission level. Emission of NO_x from different coal combustion for five front wall fired burners using the B & W coal spreader and for 4 tangentially fired burners are shown in Figure 6.10 and 6.11 [17]. For front wall-fired units, the average increase of NO_x emission is 16 ppm for 1% increase of excess air, and for tangentially fired unit is 13 ppm.

C. Equipment Developments

Burners: New 'high efficiency' burners have been designed by manufac turers to operate at low excess air levels, by improving fuel and air distribution, and shorter flame design to minimize loss of sensible heat and unburned fuel concentration. The LoNox burner, [10] a combustion oil and gas and radiant wall burner, utilizes both a tertiary air inlet in the primary tile and a special automatic recirculation oil tile. This special oil tile recirculates combustibles and combustion products back into flame region, lowering NO_x production.

The HB and HEVD burners [13] have been designed to inspirate and mix a large percentage of the total combustion air. Controls are provided for both primary and secondary air adjustments.

Register burners [14] utilize the principle of admitting and controlling the swirl of combustion air through adjustable louvers; which are arranged so that all combustion air is divided into two concentric oppsitely rotating air streams. This provides violent mixing, and as the two air streams cancel rotational velocity, the result is a short, narrow flame. Register burners can also be insulated for preheated air, where used on a pressurized furnace;

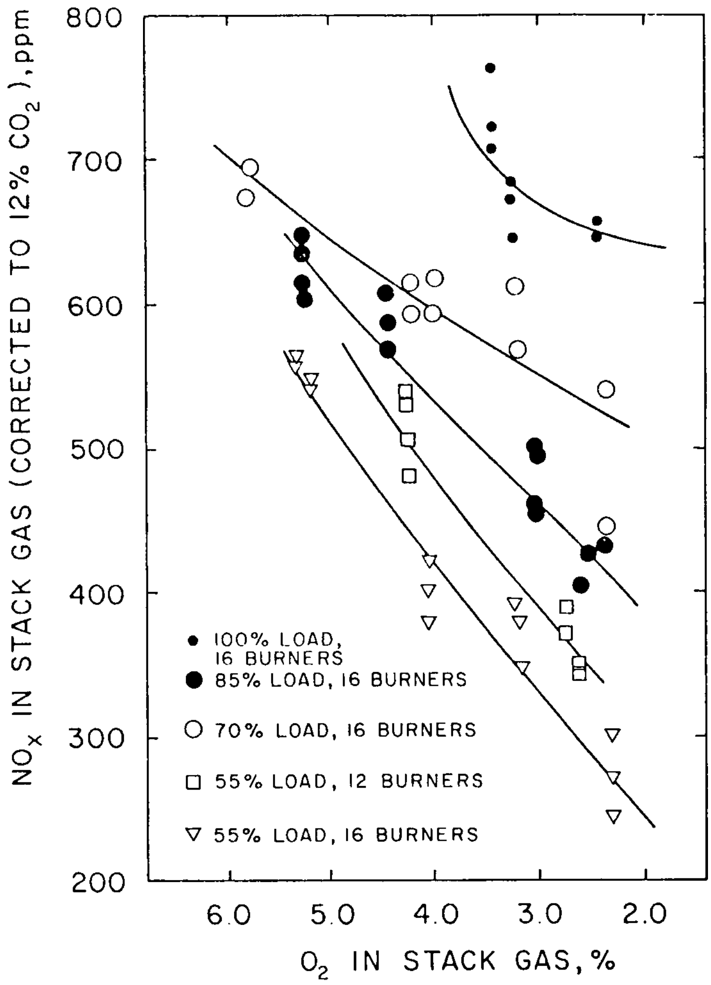

FIGURE 6.8- NO_x EMISSIONS vs. EXCESS OXYGEN(11)
(OIL FIRED UNIT)

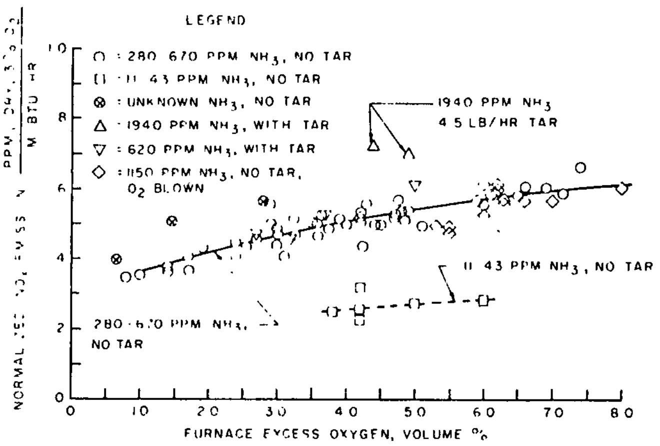

FIGURE 6.9-NO_x EMISSION vs. EXCESS OXYGEN(12)
(FOR DIFFUSION FLAMES COAL FIRED UNIT)

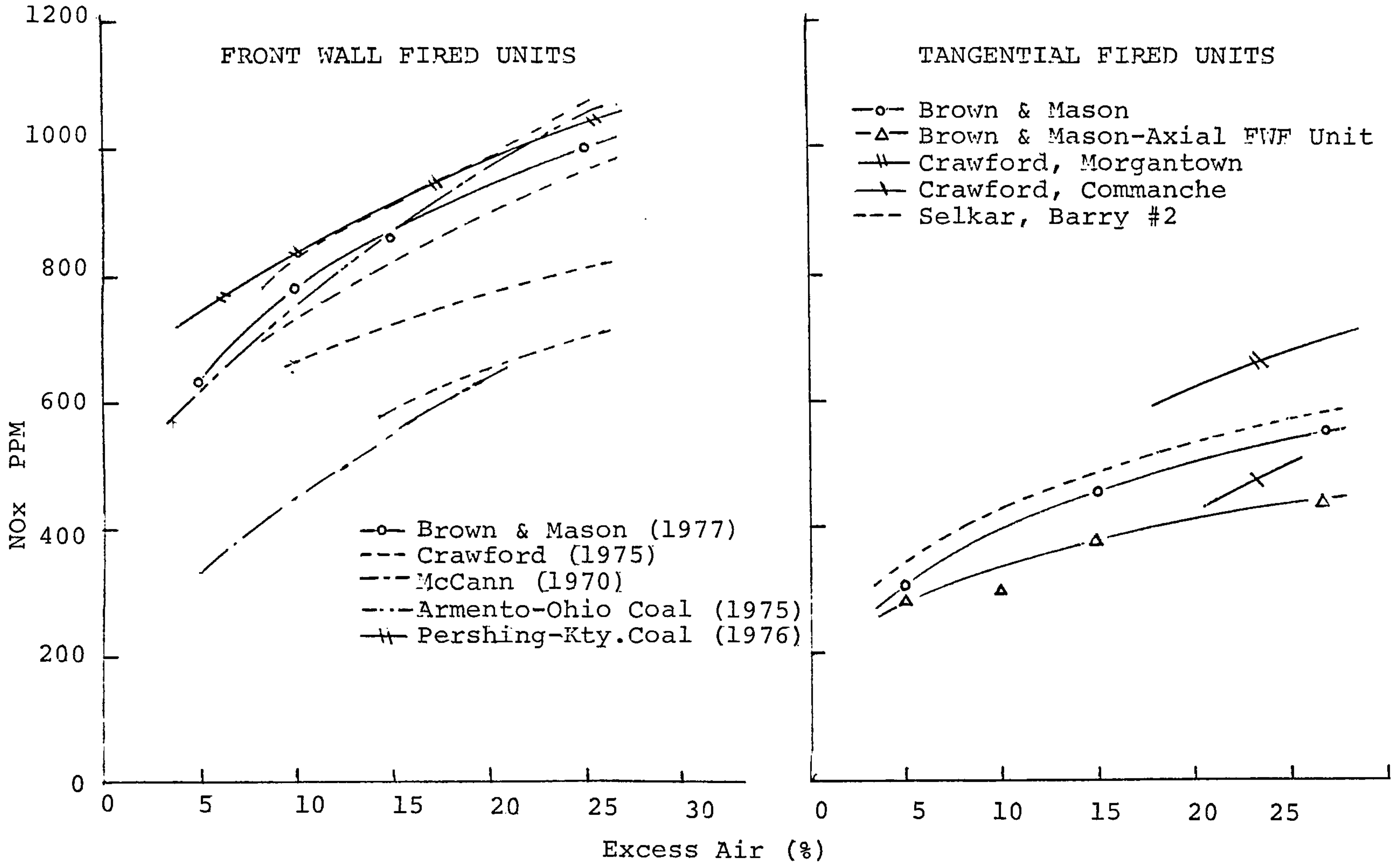

Figure 6-10 NO_x Emission Vs. Excess Air [17]
(Front Wall and Tangentially Coal Fired Units)

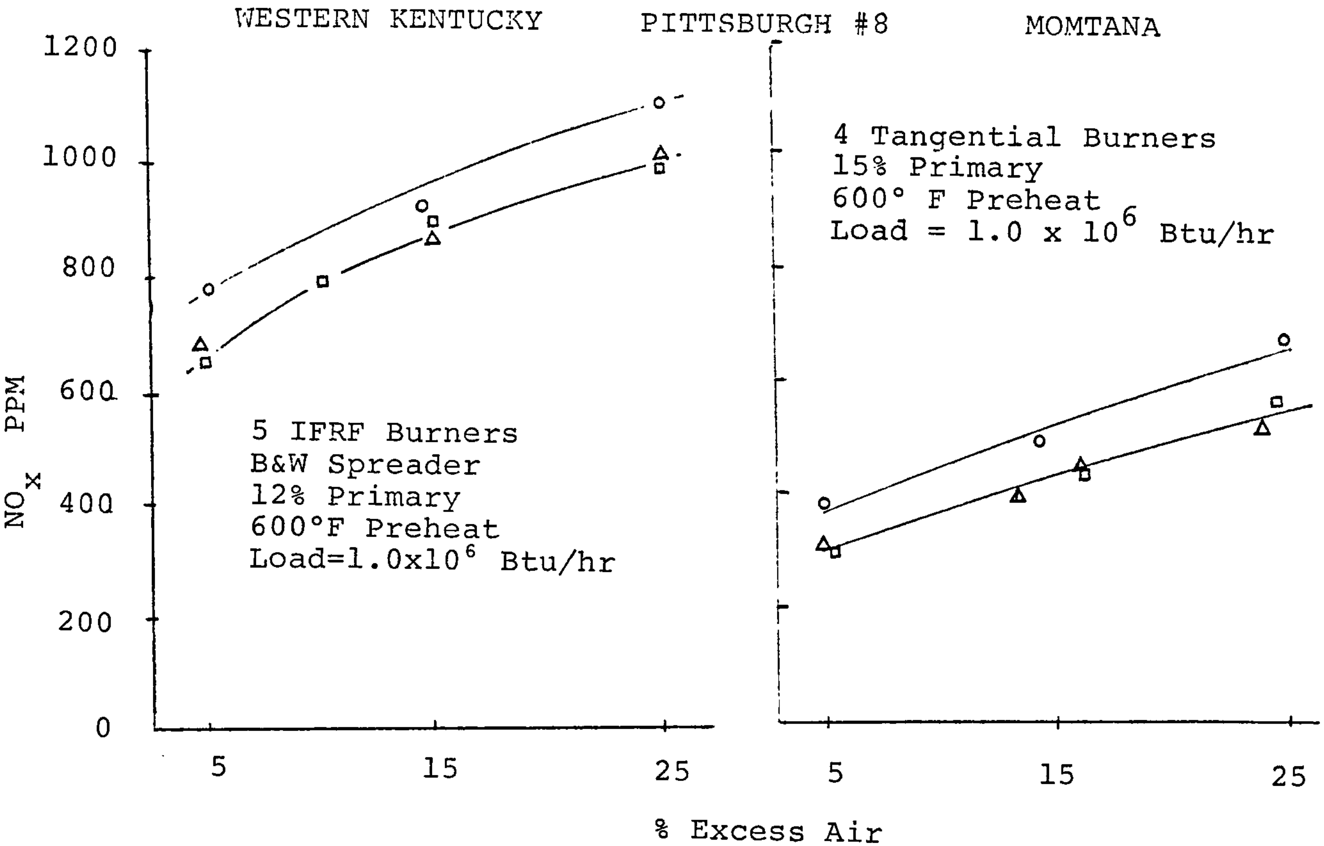

Figure 6-11 NO_x Emissions Vs. Excess Air For Different Coal Composition special peepholes, torch loop and other equipment are available to protect the operator blasts.

Furnaces and Boilers - Large furnaces and boilers are being designed by manufacturers to satisfy the demand for lower cost power. As units were extrapolated to larger sizes certain parameters were held constant: the velocity of the combustion gases in the furnace, the temperature of the flue gas entering the convection surface, and the time required to completely burn the fuel. As the surface to volume ratio in the active combustion zone decreased the peak and average flame temperature increased, and increased NO_x formation. In addition, burners that are designed for high turbulence and rapid burning rates to assure complete and stable utilization of the fuel over the widest load range possible result in high NO_x generation. Two stage combustion and flue gas recirculation, as illustrated by Figure 6.12 has been found to be an effective method to reduce NO_x. Figures 6.13 and 6.14 indicate how NO_x is reduced by these methods, for gas and oil fuels.

D. Conclusions.

The material presented in this report indicates that excess air (oxygen) plays an important role in energy savings and emission of certain pollutants.

To achieve high combustion efficiency and comply with current enviromental standards, equipment manufacturers have started to improve the design of burners furnaces and boilers. Sucessful combustion devices have been developed for less than 6% excess air, and some burners can operate down to 1% excess oxygen. More research and development work is needed to produce hgih efficiency combustion devices which will meet enviromental standards and operate at 0-1% excess oxygen levels.

Advanced instrumentation and monitoring devices are needed to achieve optimum operating conditions and thereby higher efficiencies.

E. Literature Cited

(1) U.S. Enviromental Protection Agency: "Compilation of Air Pollutant Emission Factors," PHS No. 999-AP-42 (1973)

(2) Wolfe, W.C., "Control of Atmospheric Emissions from Industrial Boilers," Technical Paper, Babcock & Wilcox, BR-961-PGTP-72-29 (1972).

(3) Prengle, H.W., Jr., "Process Plant Econdynamics," p.10, Lecture 3, preliminary ed. (1974)

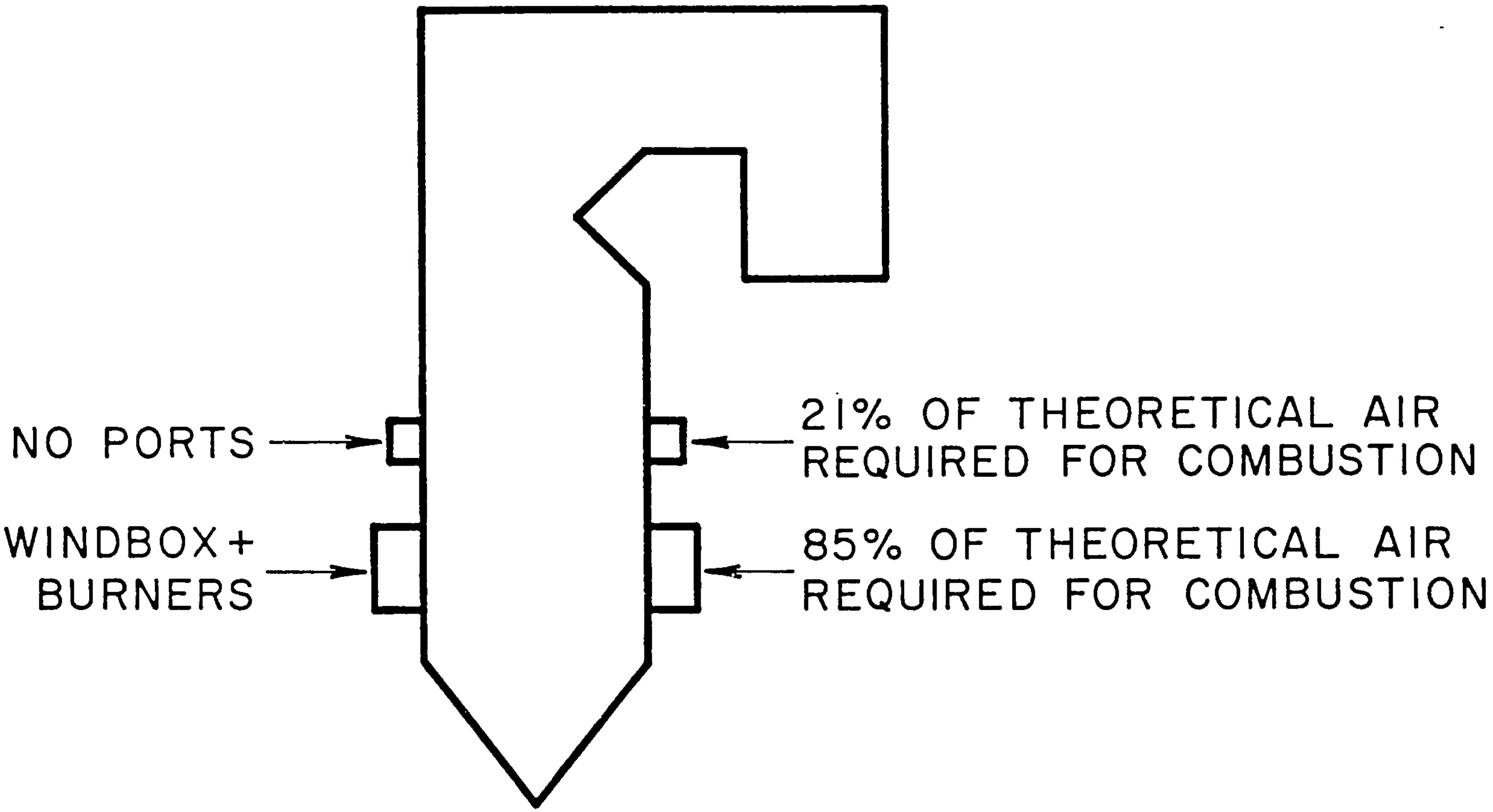

FIGURE 6-12 - SCHEMATIC SHOWING METHOD OF AIR ADMISSION FOR TWO STAGE COMBUSTION PROCESS [15].

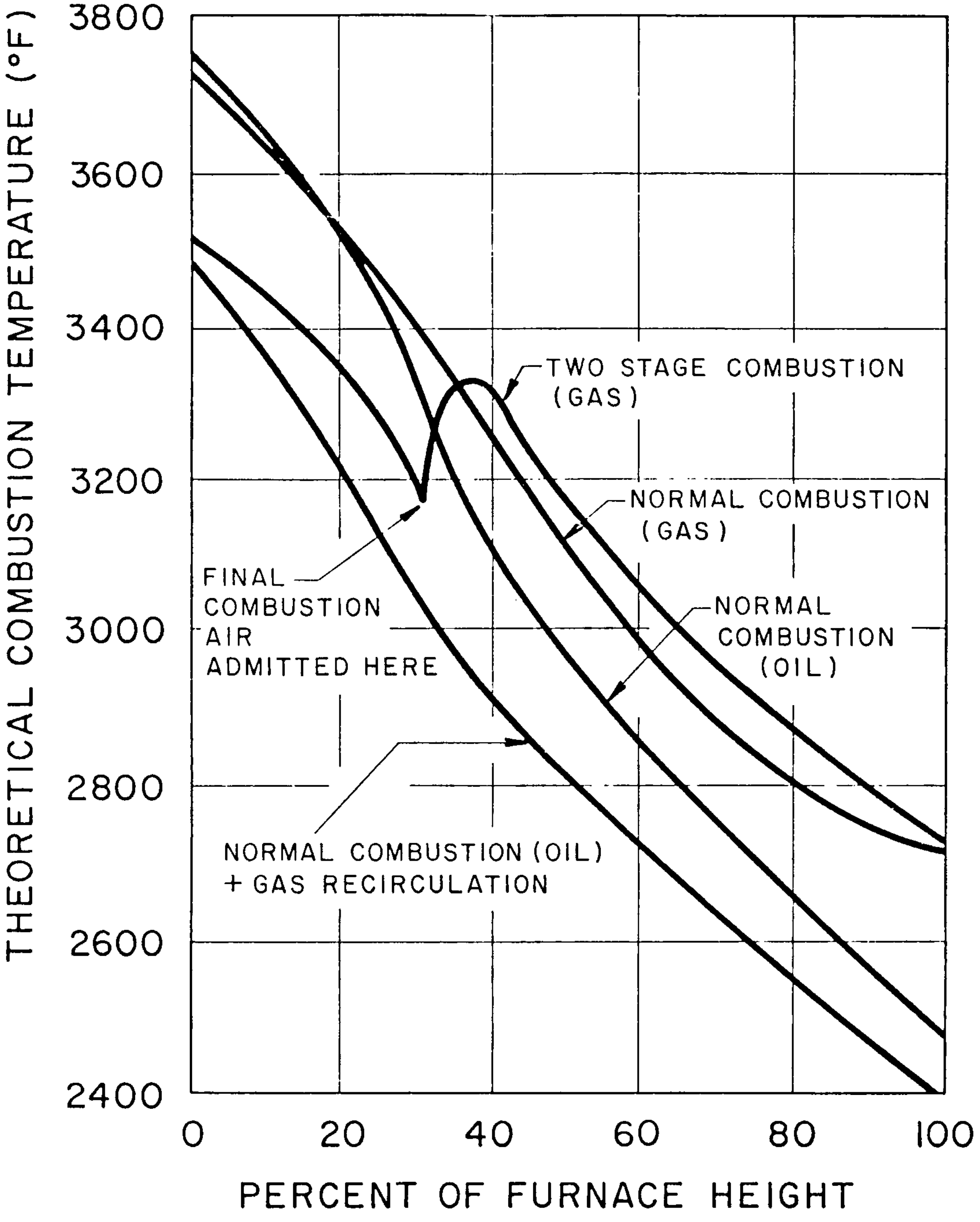

FIGURE 6.13 - EFFECT OF GAS RECIRCULATION AND TWO STAGE COMBUSTION ON COMBUSTION TEMPERATURE[15].

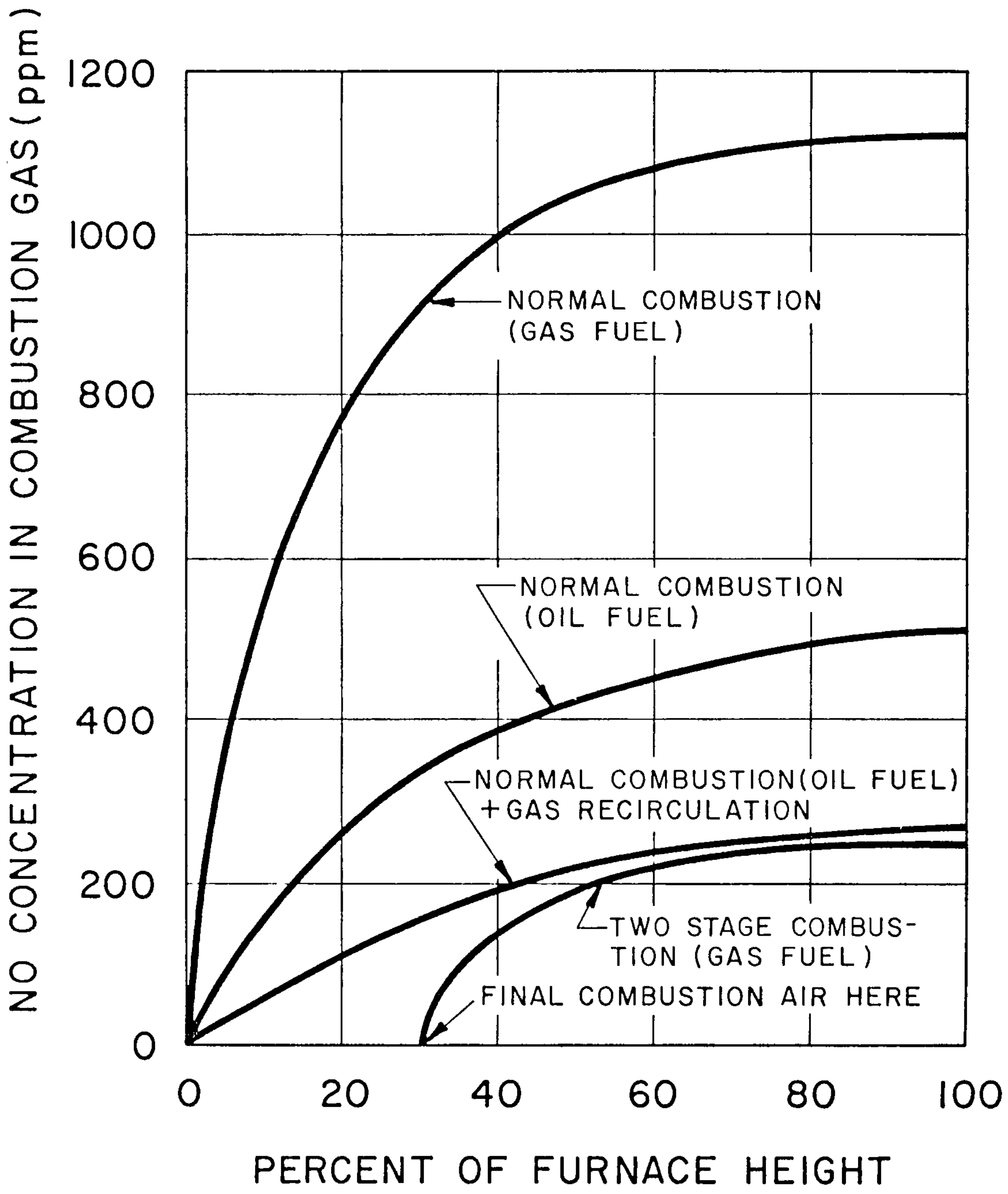

FIGURE 6.14 - EFFECT OF GAS RECIRCULATION AND TWO STAGE COMBUSTION OF NO FORMATION[15].

(4) Smith, W.S., "Atmospheric Emission from Fuel Oil Combustion," An Inventory Guide. U.S. P.H.S. 999-AP-2 (1962).

(5) Jefferis, G.C. and Sensenbaugh, J.D., 'Effect of Operating Variables on the Stack Emission from a Modern Power Station Boiler.' ASME (Oct.22,1959).

(6) Smith, W.S. and Gruba, C.W., "Atmospheric Emission from Coal Combustion," An Inventory Guide. P.H.S. 999-AP-24 (1966).

(7) Mahagaokar, U., Remote Sensing of Temperature and Composition of Gas Plumes by IR Emission Interferometry-Spectroscopy, Ph.D. Dissertation, University of Houston (1976).

(8) Cuffe, S.T., Gerstle, R.W., Orwing, A.A., Schwartz, C.H., "Air Pollutant Emissions from Coal Fired Power Plants," Report No.1, JAPCA 14: 353-362 (Sept. 1964).

(9) Weidman, G.H., Utterback, P.M., "Liquid Fuel Analysis--their effect on Combustion and Emissions," Technical Paper BR-1061, Babcock and Wilcox, (April 1976).

(10) John Zink Company, Brochure: "LoNox Burner" (current).

(11) Mills, J.L., Leudtke, R.D., Woolrich, P.F., and Perry, L.B., "Emissions of oxides of nitrogen from stationary sources in Los Angeles"; Report 3: L.A. County Air Pollution Control District, (July 1961).

(12) Lisanskas, R.A., Johnson, S.A., "NO_x Formation during Gas Combustion," Chem. Eng. Prog. 72, 76 (Aug 1976).

(13) John Zink Company, Brochures: Series HB Burner, Series HEVD Burner (current).

(14) Coen Company, Brochure: Coen Register Burners, Burlingame, California (current).

(15) James, D.E., "A Boiler Manufacturers View on Nitric Acid Formation," presented at 5th Technical Meeting, West Coast Section, APCA, Tech. Paper BR-922, TPO-74, Babcock and Wilcox (October 1970).

(16) Hunter S.C. and Carter W.A., "Application of Combustion Technology for NO_x Emissions Reduction on Petroleum Process Heaters," AIChE Paper No. 64C P-186, March, 1977.

(17) Brown R.A., Mason H.B., Pershing D.W. and Wendt J.O.L., "Investigation of First and Second Stage Variables On Control of NO_x Emissions In A Pulverised Coal Furnace", presented at 83rd National Meeting, AIChE March 24, 1977, Houston, Texas.

CHAPTER VII

IMPROVED IRRS SIGNAL PROCESS METHOD

A. Introduction

The application of remote sensing techniques combining infrared radiometry and spectroscopy, to measure pollutant emissions quantitatively was started in 1968 by Prengle et al. [3]. Briefly, the interferometer spectrometer method consists of receiving, by a telescope, infrared emission signals characteristic of each pollutant species in a hot gas plume. The basic optical element is the Michaelson interferometer with one fixed and one movable mirror which scans the entire infrared region (2.0μ to 25μ) and produces an electrical signal from the detector called an interferogram. With adequate digital Fourier transformation of the interferogram a spectrogram of the source is obtained, intensity vs. frequency. Figures 7-1a and 7-1b show the infrared emission spectrum (0-3600 cm^{-1}) from a furnace burning natural gas operated with zero excess air. The components studied include CO, NO, NO_2, CH_4, C_2H_4, SO_2, H_2S, HCHO, CH_3CHO and C_2H_6. In 1976, Mahagaokar [1] developed process spectral data obtained by remote sensing, to identify different species, and to determine the temperature and composition of the remote gas plume.

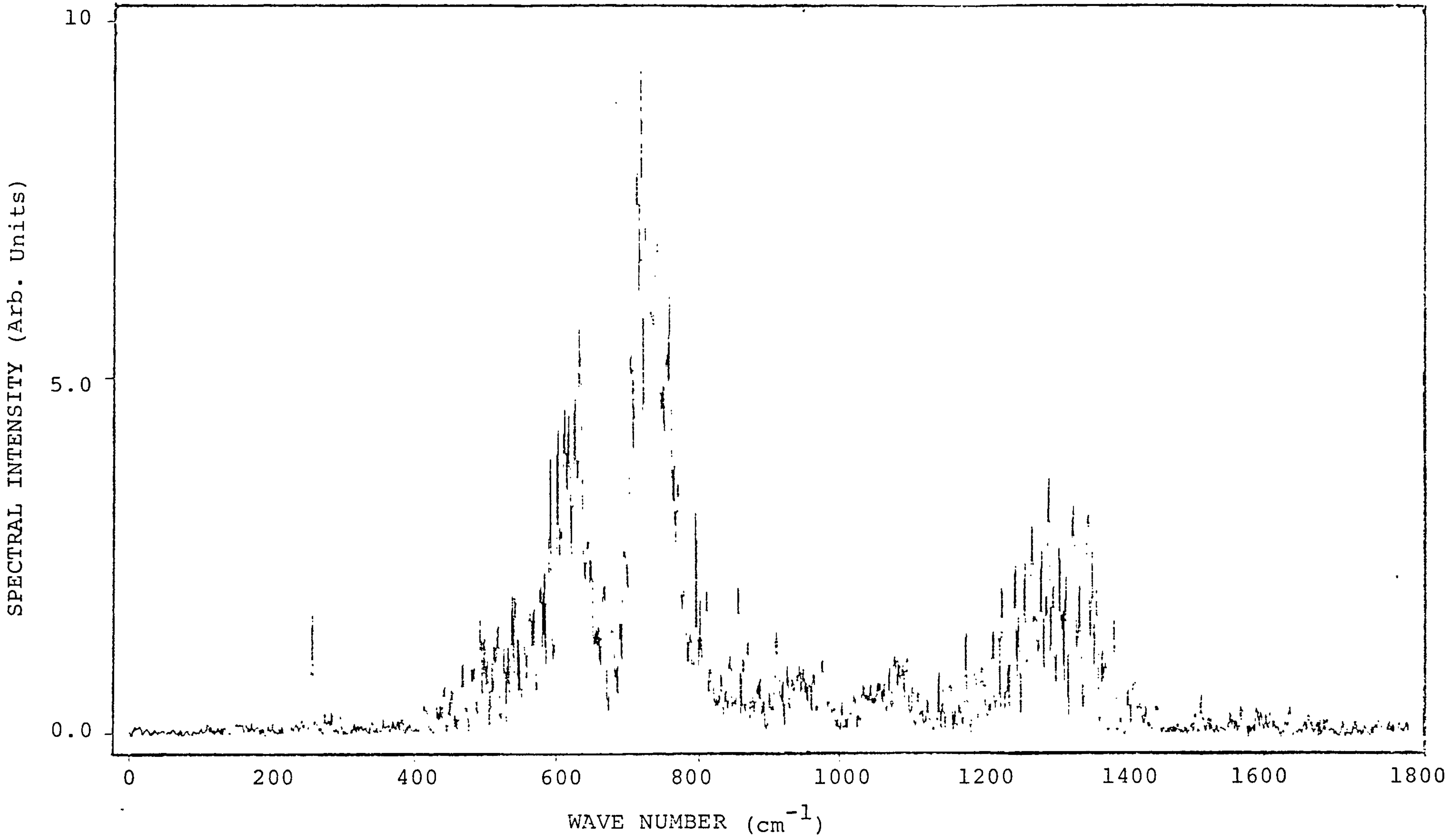

Figure 7-1a Infrared Emission Spectrum ($0-1800^{-1}$) of Plume from Furnace Operated with Zero Excess Air [1]

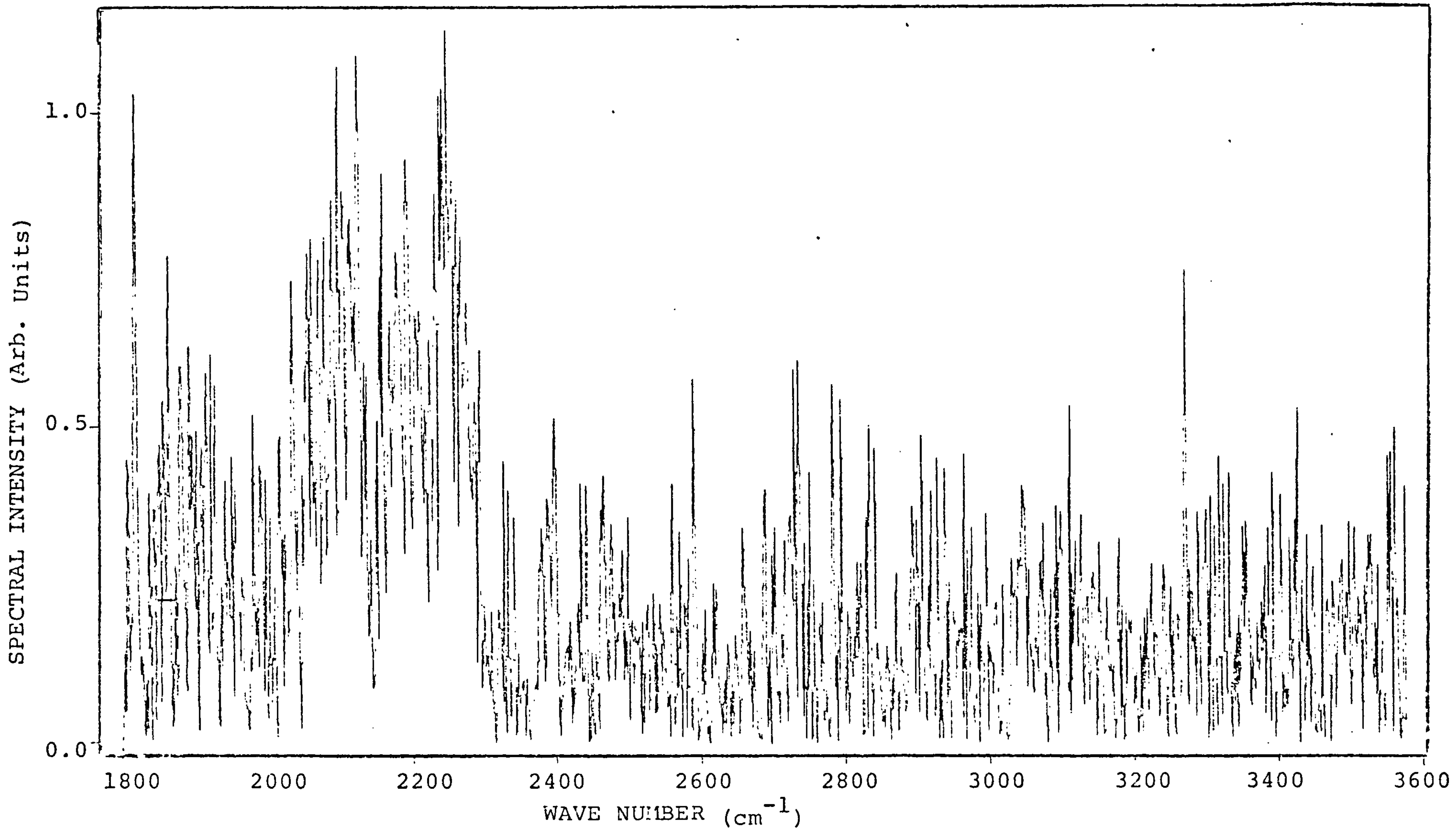

Figure 7-1b. Infrared Emission Spectrum (1800 cm^{-1} - 3600 cm^{-1}) of Plume from Furnace Operated with Zero Excess Air [1]

Special attention has been focused on the CO centration because at the characteristic frequency location there is no interference from CO_2 and H_2O, and the well known P-R structure spectrogram should be observed. It is the purpose of the present study 1) to reevaluate the model for calculating the concentration of CO, 2) to develop a new data processing model for CO, and 3) to serve as a general method to improve the data processing of other components.

B. The IR Spectrum of CO

CO is a diatomic molecule which in the gas phase undergoes vibration and rotation about its center of gravity and acts like a "vibrating-rotator ". Figure 7-2 [4] shows the vibrational-rotational spectrum of CO under high resolution. The band is centered at $\bar{\nu}_o = 2143\ cm^{-1}$, and those rotational lines with $\bar{\nu} < \bar{\nu}_o$ are the P branch while those with $\bar{\nu} > \bar{\nu}_o$ are the R branch, which gives CO the well know P-R structure.

The intensity of the rotational (P and R) wings is proportional to the number of molecules undergoing transitions from a particular rotational level, J, which the population can be obtained from the Boltzman distribution [5]

$$\frac{N_J}{N} = g_J e^{-BJ(J+1)hc/kT} \tag{2-1}$$

The value of J for which equation (7-1) is a maximum, which would be the J at peak of the P and R branches is given by,

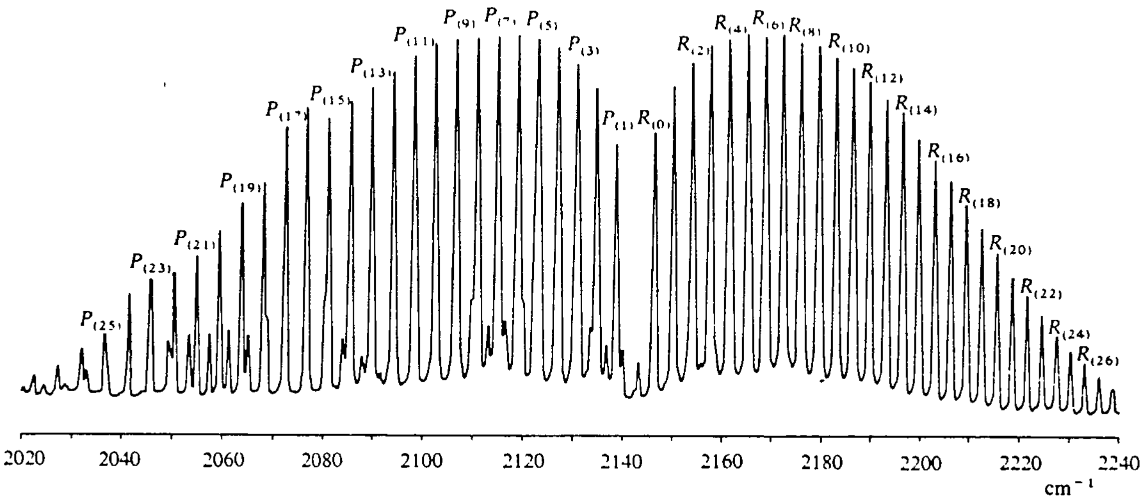

Figure 7-2. The Vibration-Rotation Spectrum of Carbon Monoxide under High Resolution [4]

$$J = \left(\frac{kT}{2Bhc}\right)^{1/2} - \frac{1}{2} \tag{7-2}$$

The separation between the two maxima is given by,

$$\Delta\bar{\nu}_{max} = \left(\frac{8kTB}{hc}\right)^{1/2} + 2B \tag{7-3}$$

A computer program was set up based on Equation (7-1) to simulate the spectrogram of CO, and an example generated from the simulation at a T = 500° K is shown in Figure 7-3. The line separation, obtained from [4], is 2B = 3.94. The maximum intensity of the line occurs at J = 9. The half width of the spectral lines, $\Delta\bar{\nu}_{o_{1/2}}$ is given by,

$$\Delta\bar{\nu}_{o_{1/2}} = \frac{4\sigma^2\bar{u}_o n_o}{c} \tag{7-4}$$

where

σ = collision diameter (cm)

= 3.590 x 10^{-8} cm (from [6])

$\bar{u}_o$ = average kinetic velocity (cm/sec)

$= \frac{8RT}{M}$

n_o = number of molecules/cm^3

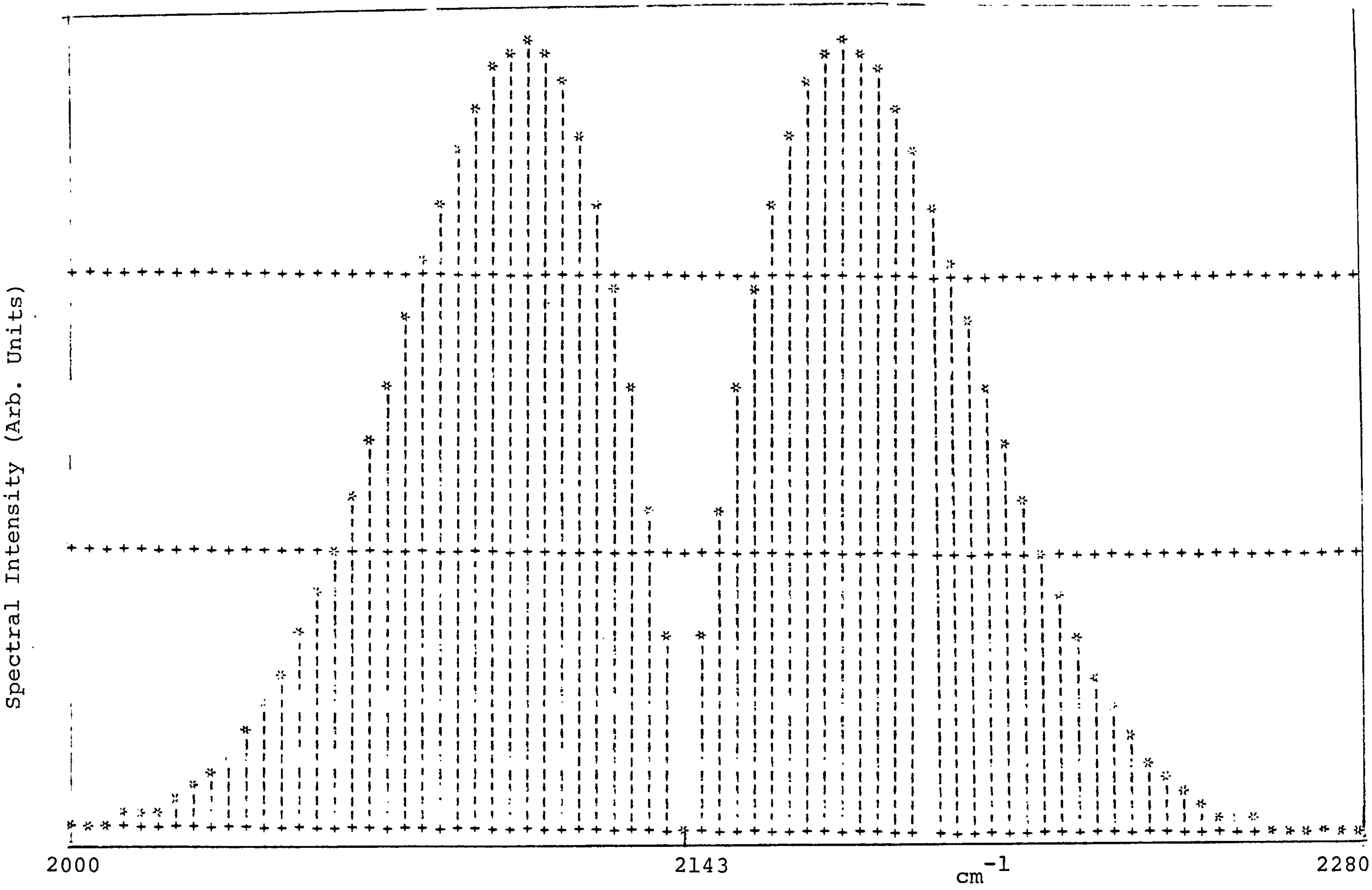

Figure 7-3 Simulated Spectrogram of CO

The value of $\Delta\bar{\nu}_{o1/2}$ calculated at 500^{o} K

$$\Delta\bar{\nu}_{o1/2} = 0.227 \text{ cm}^{-}$$

C. Equipment Characteristics

Resolution: The maximum retardation A of the interferometer, the greatest optical path difference between the transmitting and reflecting beam of the Michelson interferometer, determines the resolution of the spectrogram, and is given by [7],

$$\text{Resolution} = \frac{1}{A} \tag{7-5}$$

The maximum retardation operating in the experiment is 0.25 cm; therefore, the resolution is 4.0 cm^{-1}, which means that two lines cannot be resolved when computed from the above interferogram if their line difference is less than 4.0 cm^{-1}.

Sampling Interval in the Interferogram: Woodward states [8] that any waveform that is a sinusoidal function of time or distance can be digitized unambiguously using a sample frequency equal to twice the band width of the system; the interferogram may then be completely reconstructed without any loss of information or signal-to-noise ratio.

In order to completely reconstruct the interferogram, the sampling interval δ should be [9],

$$\delta \leq \frac{1}{2(\bar{\nu}_{max} - \bar{\nu}_{min})} \tag{7-6a}$$

$$\bar{\nu}_{max} = \frac{10^4}{2.8\mu} \text{ cm}^{-1} = 3571 \text{ cm}^{-1}$$

$$\bar{\nu}_{min} = \frac{10^4}{25\mu} \text{ cm}^{-1} = 400 \text{ cm}^{-1}$$

Therefore, $\delta \leq 1.576 \times 10^{-4}$ cm (7-6b)

It is a characteristic of the equipment to sample at multiples of 6328Å; the laser is a HeNe unit which produces a line at 6328Å; therefore, the maximum δ is,

$$\delta = 2 \times 6328\text{Å} = 1.2656 \times 10^{-4} \text{ cm}$$

which satisfies Equation (7-6b). Therefore the total sampling points in the interferogram is,

$$\text{Sampling Points} = \frac{A}{\delta}$$

$$= \frac{0.25 \text{ cm}}{1.2656 \times 10^{-4} \text{ cm}}$$

$$= 1975 \text{ pts.}$$

Information Intervals in the Spectrogram: The spectrogram is obtained by a Fourier transformation of the interferogram, and the Cooley-Tukey algorithm is used for the transformation. It is a characteristic of the Cooley-Tukey algorithm that the number of data points is $N = 2^n$, when n is a positive integer. Therefore the minimum number of points should be N > 1975 to avoid loss of information; therefore, N = 2048 pts (n=11). The intensity of the spectrogram is then stored at an Information Interval =

$$\frac{1}{(2x\delta)\cdot N} = 1.929\ cm^{-1}$$

D. CO Concentration from IRRS

The concentration model [1] for a pollutant, C_i is given by,

$$C_i(ppm) = \frac{(S_{\Delta\bar{\nu}_i}) \times 10^6}{(R_{\bar{\nu}} GA_m)(T_{ai}\beta_{\bar{\nu}})(X^2 \bar{W}_{Bi} L_e k_{\bar{\nu}_i} \Delta\bar{\nu}_i)} \tag{7-7}$$

where $S_{\Delta\bar{\nu}_i}$ is the integrated area of the spectrogram of the pollutant i at the assigned wave number range, $\Delta\bar{\nu}_i$, or

$$S_{\Delta\bar{\nu}_i} = \int_{\Delta\bar{\nu}_i} S_{\bar{\nu}} d\bar{\nu}$$

and $S_{\bar{\nu}}$ is the spectral intensity at $\bar{\nu}$. $k_{\bar{\nu}_i}$ is the average absorption coefficient of the pollutant i at $\bar{\nu}_i$. It is important to point out that because of a lack of literature data, Rock's [2] absorption coefficient measurements and correlations were used,

$$\left(\frac{1}{k_{\bar{\nu},m}}\right)^2 = \left(\frac{1}{k_{\bar{\nu}_o}}\right)^2 = \frac{M'X^n}{k_{\bar{\nu}_o} A'} + \frac{X^n}{A'} \tag{7-9}$$

where $k_{\bar{\nu},m}$ is the maximum absorption coefficient at low resolution instead of the average value. Also the other parameters in Equation (7-7) relate to the system characteristics, and the surrounding conditions, in particular are not related to the spectral structure of CO.

A simulated spectrogram of CO, $S_{\bar{\nu}}$ vs. $\bar{\nu}$ is generated, which resembles that obtainable from equipment, i.e., the spectral lines of CO were simulated for a resolution of $4 cm^{-1}$, and the resulting intensity $S_{\bar{\nu}}$ was stored and printed out at an interval of $1.929\ cm^{-1}$. The spectrogram was generated in the following way. Consider any two spectral lines in Figure 7-4, at wave number X(J) and X(J+1). The intensity of the lines f(J) and f(J+1) have been stored when the true spectrogram of CO was generated as given by Equation (7-1) or Figure 7-3. The base width of the spectral lines X_1 to X_2 is $0.454\ cm^{-1}$, twice the calculated half-width of the spectral lines. The sampling point XX(N) starts at around $1993.\ cm^{-1}$ and samples at an interval of $1.929\ cm^{-1}$. The intensity $S_{\bar{\nu}}$ is equal to the sum of the area (arbitrary units) of the spectral lines (triangles)

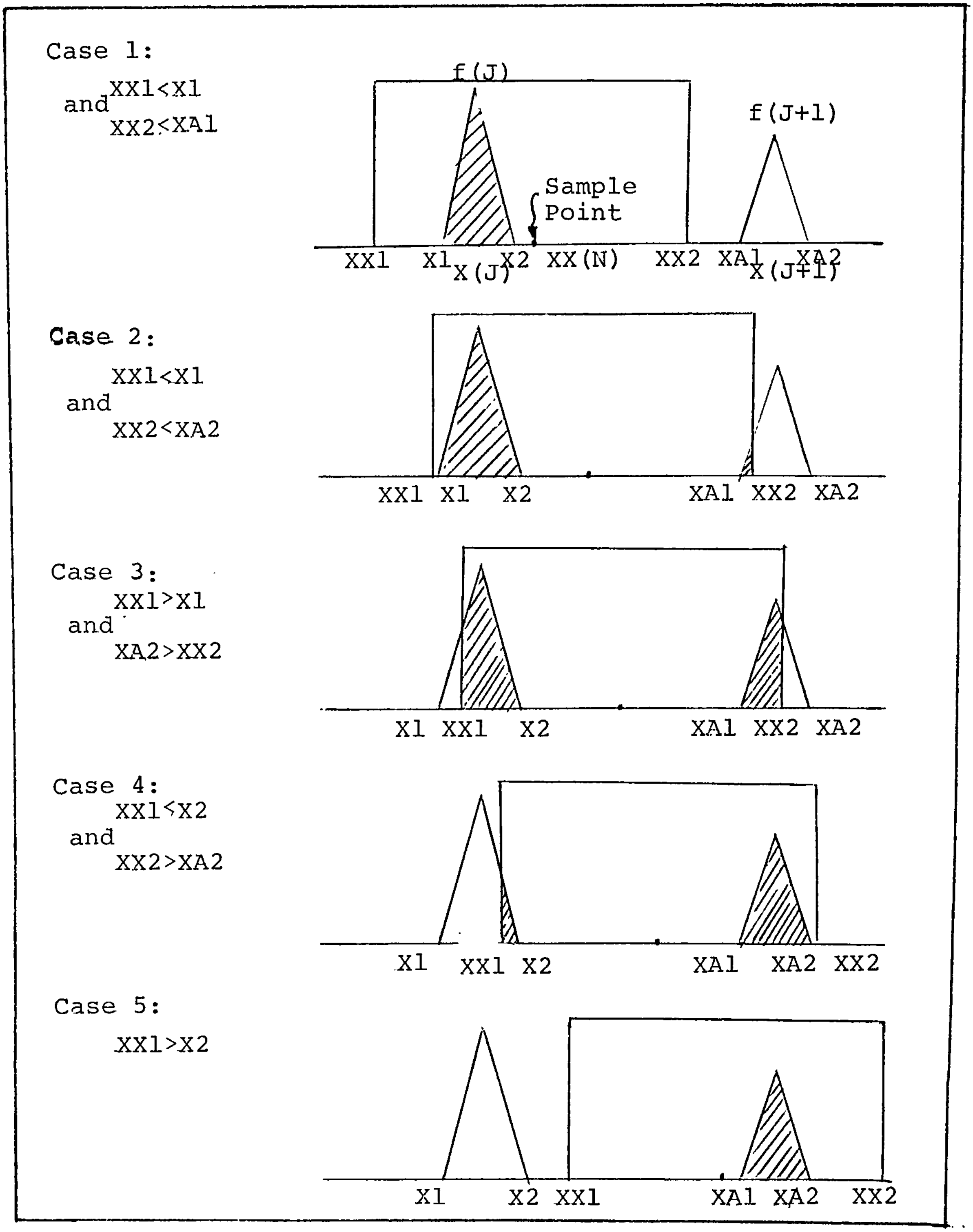

Figure 7-4 Simulation of Spectrogram

covered by the rectangle of width (XX_1 to XX_2) equal to $4cm^{-1}$, which is equivalent to a resolution of $4cm^{-1}$. Figure 7-4 shows the five different situations for calculating $S_{\bar{\nu}}$. A computer program with an algorithm base on these five situations was set up to generate the spectrogram $S_{\bar{\nu}}$ vs. $\bar{\nu}$. Two generated spectrograms with resolution of $4cm^{-1}$ and print out interval of 1.929 cm^{-1} at two different starting points 1993.12 cm^{-1} and 1993.32 cm^{-1}, are shown in Figure 7-5a and 7-5b, respectively. By comparison to an actual spectrogram, Figure 7-6, obtained from a run of the experimental equipment, the P-R structure can be visualized, and the ups and downs can be understood because of the equipment resolution and information interval. Also as observed from experimental spectrograms, consistent interferences appeared short of 2090 cm^{-1} and beyond 2205 cm^{-1}. Figure 7-6 also shows this effect, which is probably due to the interference of some unburned hydrocarbons in the plume. A new wave number range 2090 cm^{-1} to 2205 cm^{-1} is recommended to replace the old range 2060 to 2220 cm^{-1}.

Also, it is observed that the value of the generated $S_{\bar{\nu}}$ is greater than the true $S_{\bar{\nu}}$ because of the system resolution; $S_{\Delta\bar{\nu}}$ is used in calculating the concentration of the pollutants. The true and the generated $S_{\Delta\bar{\nu}}$ values are calculated and compared; the values, i.e, the area of

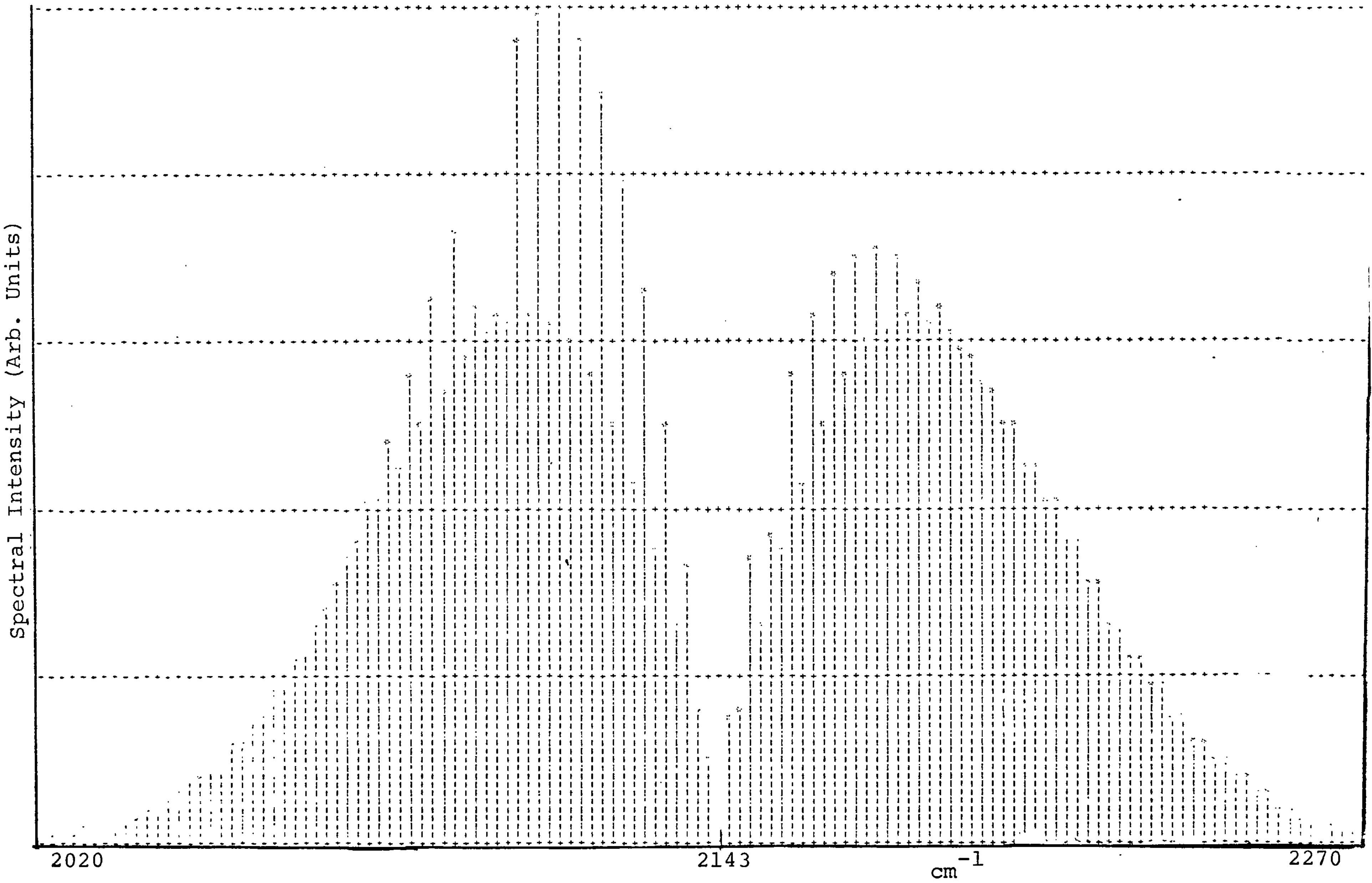

Figure 7-5a Simulated Spectrogram of CO Resembling Experimental Condition with Starting Sampled Point at $1993.12 cm^{-1}$

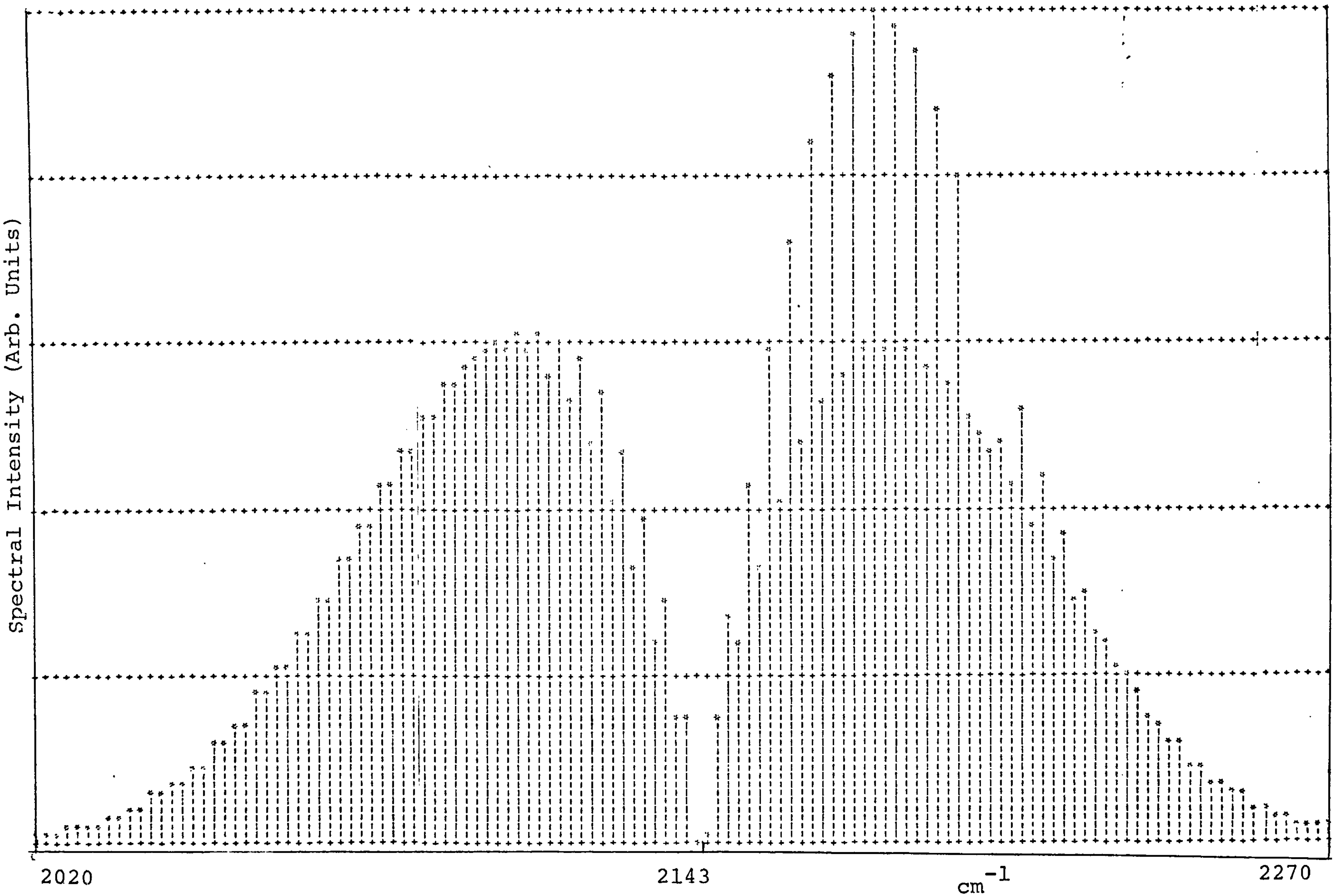

Figure 7-5b Simulated Spectrogram of CO Resembling Experimental Condition with Starting Sampled Point at 1993.32cm-1

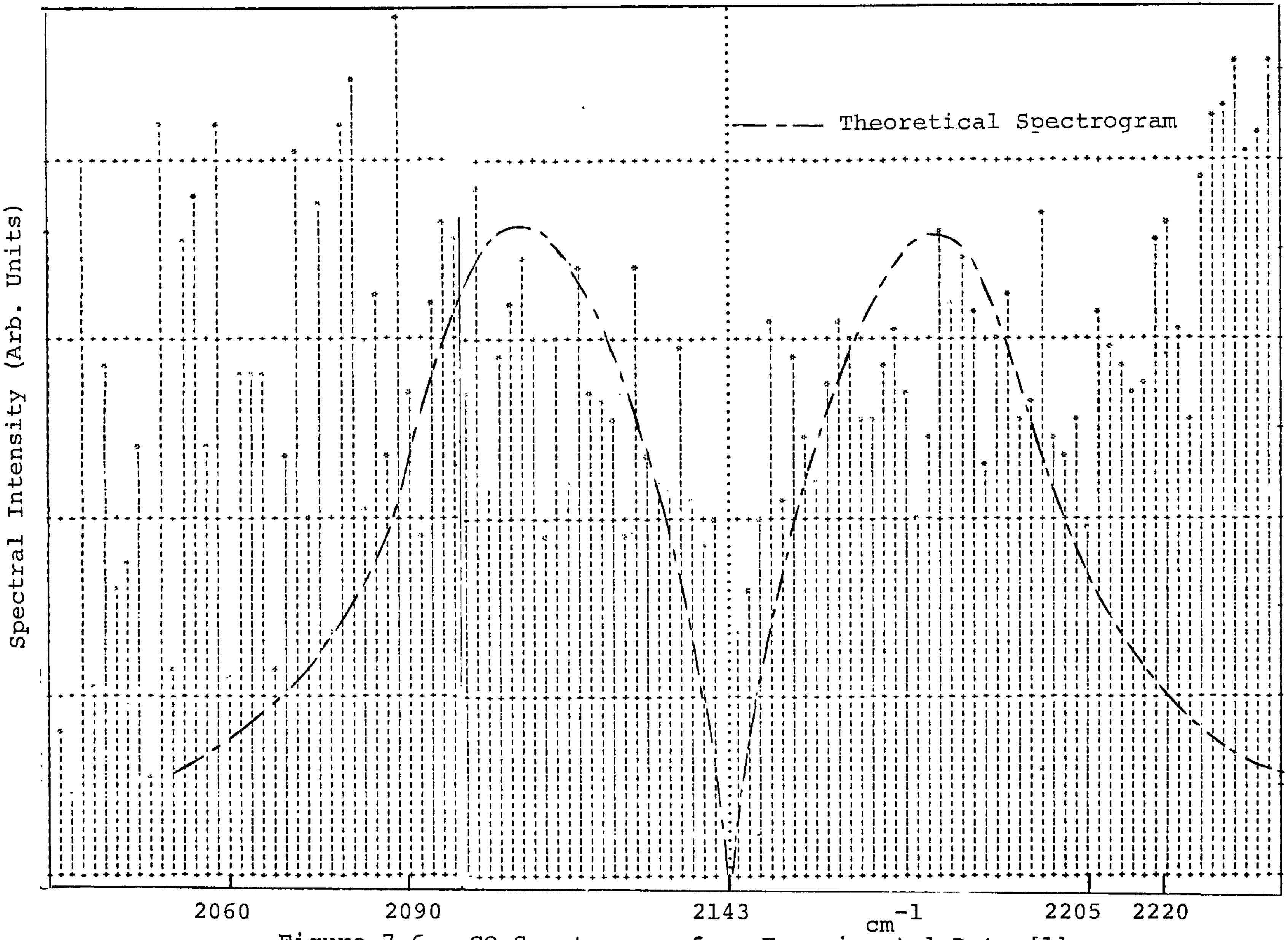

Figure 7-6. CO Spectrogram from Experimental Data [1]

the spectrograms in Figure 7-3 and 7-5, are obtained simply by the summation of small rectangles method. For the complete CO spectrogram,

$$\frac{\text{Generated } S_{\Delta\bar{\nu}}}{\text{True } S_{\Delta\bar{\nu}}} = 1.11$$

and for the range 2090 $\leftrightarrow$ 2205 cm^{-1}

$$\frac{\text{Generated } S_{\Delta\bar{\nu}}}{\text{True } S_{\Delta\bar{\nu}}} = 1.10$$

The generated $S_{\Delta\bar{\nu}}$ used above is the average of 10 generated $S_{\Delta\bar{\nu}}$ from 10 different starting points. In order to account for this error, the value of $S_{\Delta\bar{\nu}}$ calculated from experimental data should use a factor of 1/1.10 = 0.909.

It was pointed out previously that the value of $k_{\bar{\nu}_i}$ used, from Rock's correlation, is the maximum value instead of the average value. The value of $S_{\bar{\nu}}$ at the maximum, i.e., at P_9 or R_9, is 1.166 (arbitrary units), the average value of $S_{\bar{\nu}}$ from 2090 to 2205 cm^{-1} (i.e., P_1 to P_{14} and R_0 to R_{16}) is 0.915. As an approximation, the value of $k_{\bar{\nu}_i}$ obtained from Rock's correlation should be multiplied by a factor of 0.915/1.116 = 0.820, for this particular wave number range in order to obtain a more correct result.

As an example, let's consider Run #312, the spectrogram of CO is Figure 7-6 and the previously calculated concentration is 915 ppm. The value of:

$$S_{\Delta\bar{\nu}}\ (2060 - 2220\ \text{cm}^{-1}) = 142.72\ \text{(arbitrary)}$$

$$\Delta\bar{\nu} = 160\ \text{cm}^{-1}$$

and,

$$S_{\Delta\bar{\nu}}\ (2090 - 2205\ \text{cm}^{-1}) = 100.53\ \text{(arbitrary)}$$

$$\Delta\bar{\nu} = 115\ \text{cm}^{-1}$$

Assuming all parameters except $S_{\Delta\bar{\nu}_i}$, $k_{\bar{\nu}_i}$ and $\Delta\bar{\nu}_i$, do not change in Equation 7-7 with the new wave number range, the corrected concentration of CO is given by,

$$C(CO) = 915\ \text{ppm} \times \frac{100.33 \times 0.090}{14272} \times \frac{160\ \text{cm}^{-1}}{115\ \text{cm}^{-1}} \times \frac{k_{\bar{\nu}_i}}{0.820 k_{\bar{\nu}_i}}$$

$$= 992\ \text{ppm}$$

Therefore, the following conclusions are made:

1. For a resolution of 4 cm^{-1}, the integrated area of the concentration signal, $S_{\Delta\bar{\nu}}$, due to overlapping, is about 1.1 times higher than the true value.

2. Judging and comparing the theoretical to experimental spectrograms, consistant interferences from other compounds,

most likely unburnt hydrocarbon, appear on the edges of the assigned wave number range. A new range is proposed to minimize this effect.

3. The absorption coefficient used had been the maximum value. An average value is obtained as a function of the maximum value based on the theoretical spectral intensity of the spectral lines.

Finally, in the future $S_{\Delta\bar{\nu}}$ and $k_{\bar{\nu}}$ for CO should be calculated

$$S_{\Delta\bar{\nu}} = 0.909\ S_{\Delta\bar{\nu}}\ \text{(observed)}$$

$$k_{\bar{\nu}} = 0.820\ k_{\bar{\nu}_i}\ \text{(Rock's value)}$$

E. Recommendations

1. Since the integrated area of the concentration signal is related to the resolution and the spectral structure of the molecule, the effect on other components should be studied.

2. Besides interferences from the expecting components, other unpredicted interferences may also exist, the spectrogram of the components should be reviewed to minimize the error.

3. The absorption coefficients of the components should be reevaluated.

F. Symbols & Nomenclature

Upper Case

A	maximum retardation (cm)
A_m	area of the receiving mirror of the telescope, cm^2
B	average rotational line seperation (cm^{-})
C_i	concentration of component i, ppm
G	system gain
J	rotational level
L_e	equivalent path length (cm)
N	total number of molecules
N_J	number of molecules in the J-th rotational state
$R_{\bar{\nu}}$	average spectral responsivity at $^{-}$
$S_{\Delta\bar{\nu}_i}$	integrated area of the spectrogram of pollutant i
S_ν	spectral concentration signal
T	absolute temperature
T_{ai}	average atmospheric transmittance of component i
$\bar{W}_{\beta i}$	average emissive power for the location of component i
X	dimensionless radius of the plume relative to the distance

Lower Case

c	speed of light
g_J	degeneracy
h	Planck's constant
k	Boltzmann's constant
$k_{\bar{\nu}_i}$	spectral absorption coefficient for component i

η_o	number of molecules/unit volume
$\bar{u}_o$	average kinetic velocity

Geek Letters

$\beta_{\bar{\nu}}$	spectral background radiation factor
δ	sampling interval
$\bar{\nu}, \Delta\bar{\nu}$	spectral frequency and bandwidth in wave numbers (cm^{-1}), respectively
$\bar{\nu}_o$	band centre location (cm^{-1}) of the CO spectrogram
$\Delta\bar{\nu}_{max}$	the seperation between two maximum intensity spectral lines (cm^{-1})
$\Delta\bar{\nu}_{o1/2}$	half-width of band cm^{-1}
σ	collision diameter

G. Literature Cited

1. Mahagaokar, U., Ph.D Dissertation, Chem. Engr. Dept., Uni. of Houston., Texas, (1976).

2. Rock, K.L., M.S. Thesis, Chem. Engr. Dept., Uni. of Houston, Texas, (1975)

3. Prengle, H.W. Jr., Morgan, C.A., Fang, C.S., Huang, L.K., Campani, P., and Wu,W.W., Enviro. Sci, Technol., 7, 417 (1973).

4. Banwell,C.N., Fundamentals of Molecular Spectroscopy, McGraw-Hill, N.Y. (1966).

5. Curtice, S., Ph.D. Dissertation, ChE. Dept., Uni. of Houston, Texas (1974)

6. Hirschfelder J.O., Curtiss,C.F., and Bird, R.B., Molecular Theory of Gases and Liquids, 1110-1112, Wiley, N.Y. (1974).

7. Bell R.J., Introductory Fourier Transform Spectroscopy, Academic Press, N.Y. (1974).

8. Woodward, M., Probability and Information Theory, Pergamon Press, N.Y. (1955).

9. Griffiths P.R., Chemical Infrared Fourier Transform Spectroscopy, Wiley, N.Y., (1975).

APPENDIX A

SOLUTION OF FINITE-DEIFFERENCE EQUATIONS

The finite-difference solution used here is a variation of the fully implicit method of Abbott [25] for constant temperature, axially symetric flow system. The equations that have been developed in Chapter II were further developed here such that the equations are readily solved by the Gaussian method of elimination. Equations (2-18), (2-19) and (2-20) are now written as (A-1), (A-2) and (A-3):

$$U_Z \frac{\partial P}{\partial Z} + P \frac{\partial U_Z}{\partial Z} + U_R \frac{\partial P}{\partial R} + P \frac{\partial U_R}{\partial R} + \frac{P U_R}{R} = 0 \qquad \text{(A-1)}$$

$$P U_Z \frac{\partial U_Z}{\partial Z} + P U_R \frac{\partial U_Z}{\partial R} = A_V \left[\frac{\partial^2 U_Z}{\partial R^2} + \frac{1}{R} \frac{\partial U_Z}{\partial R} \right] + \frac{Dg}{u_0^2} [P_A - P] \qquad \text{(A-2)}$$

$$P U_Z \frac{\partial T}{\partial Z} + P U_R \frac{\partial T}{\partial R} = A_T \left[\frac{\partial^2 T}{\partial R^2} + \frac{1}{R} \frac{\partial T}{\partial R} \right] + N_{Ec} A_V \left(\frac{\partial U_Z}{\partial R} \right)^2 \qquad \text{(A-3)}$$

The following finite-difference approximations for derivatives at $(Z + \Delta Z, R)$ were used:

$$\frac{\partial U_Z}{\partial Z} = \frac{U_Z(Z+\Delta Z, R) - U_Z(Z,R)}{\Delta Z} \qquad \text{(A-4)}$$

$$\frac{\partial U_Z}{\partial R} = \frac{U_Z(Z+\Delta Z, R+\Delta R) - U_Z(Z+\Delta Z, R-\Delta R)}{2\Delta R} \qquad \text{(A-5)}$$

$$\frac{\partial^2 U_Z}{\partial R^2} = \frac{U_Z(Z+\Delta Z, R+\Delta R) - 2U_Z(Z+\Delta Z, R) + U_Z(Z+\Delta Z, R-\Delta R)}{\Delta R^2} \qquad \text{(A-6)}$$

$$\frac{\partial U_R}{\partial R} = \frac{U_R(Z+\Delta Z, R) - U_R(Z+\Delta Z, R-\Delta R)}{\Delta R} \qquad (A-7)$$

$$\frac{\partial P}{\partial Z} = \frac{P(Z+\Delta Z, R) - P(Z, R)}{\Delta Z} \qquad (A-8)$$

$$\frac{\partial P}{\partial R} = \frac{P(Z+\Delta Z, R+\Delta R) - P(Z+\Delta Z, R-\Delta R)}{2\Delta R} \qquad (A-9)$$

$$\frac{\partial T}{\partial Z} = \frac{T(Z+\Delta Z, R) - T(Z, R)}{\Delta Z} \qquad (A-10)$$

$$\frac{\partial T}{\partial R} = \frac{T(Z+\Delta Z, R+\Delta R) - T(Z+\Delta Z, R-\Delta R)}{2\Delta R} \qquad (A-11)$$

$$\frac{\partial^2 T}{\partial R^2} = \frac{T(Z+\Delta Z, R+\Delta R) - 2T(Z+\Delta Z, R) + T(Z+\Delta Z, R-\Delta R)}{\Delta R^2} \qquad (A-12)$$

Substituting Equations (A-4) to (A-12) into Equations (A-1), (A-2), and (A-3), the Equations then are linearlized by taking the coefficients (shown as the underlined coefficients in the equations) of the non-linear terms at their known value on the previous line of the net work or from the iteration. Equations (A-1) to (A-3) become:

$$U_Z(Z,R)\,\frac{P(Z+\Delta Z, R) - P(Z,R)}{\Delta Z} + P(Z,R)\,\frac{U_Z(Z+\Delta Z, R) - U_Z(Z,R)}{\Delta Z}$$

$$+ U_R(Z,R)\,\frac{P(Z+\Delta Z, R+\Delta R) - P(Z+\Delta Z, R-\Delta R)}{2\Delta R}$$

$$+ P(Z,R)\,\frac{U_R(Z+\Delta Z, R),\ U_R(Z+\Delta Z, R-\Delta R)}{\Delta R}$$

$$+ \frac{P(Z,R)\cdot U_R(Z,R)}{R} = 0 \qquad (A-13)$$

$$P(Z,R)\,U_Z(Z,R)\,\frac{U_Z(Z+\Delta Z,R)-U_Z(Z,R)}{\Delta Z}$$

$$+\,P(Z,R)\,U_R(Z,R)\,\frac{U_Z(Z+\Delta Z,R+\Delta R)-U_Z(Z+\Delta Z,R-\Delta R)}{2\Delta R}$$

$$=A_V\left[\frac{U_Z(Z+\Delta Z,R+\Delta R)-2U_Z(Z+\Delta Z,R)+U_Z(Z+\Delta Z,R-\Delta R)}{\Delta R^2}\right.$$

$$\left.+\,\frac{1}{R}\,\frac{U_Z(Z+\Delta Z,R+\Delta R)-U_Z(Z+\Delta Z,R-\Delta R)}{2\Delta R}\right]$$

$$+\,\frac{Dg}{u_o^2}\left[P_A-P(Z,R)\right] \qquad \text{(A-14)}$$

$$P(Z,R)\,U_Z(Z,R)\,\frac{T(Z+\Delta Z,R)-T(Z,R)}{\Delta Z}$$

$$+\,P(Z,R)\,U_R(Z,R)\,\frac{T(Z+\Delta Z,R+\Delta R)-T(Z+\Delta Z,R-\Delta R)}{2\Delta R}$$

$$=A_T\left[\frac{T(Z+\Delta Z,R+\Delta R)-2T(Z+\Delta Z,R)+T(Z+\Delta Z,R-\Delta R)}{\Delta R^2}\right.$$

$$\left.+\,\frac{1}{R}\,\frac{T(Z+\Delta Z,R+\Delta R)-T(Z+\Delta Z,R-\Delta R)}{2\Delta R}\right]$$

$$+\,N_{Ec}A_V\;\frac{U_Z(Z+\Delta Z,R+\Delta R)-U_Z(Z+\Delta Z,R-\Delta R)}{2\Delta R}\cdot$$

$$\frac{U_Z(Z,R+\Delta R)-U_Z(Z,R-\Delta R)}{2\Delta R} \qquad \text{(A-15)}$$

Supposedly, we are going to calculate the values of T, U_Z, U_R, and P of the points from 1 to N on line Z=1, the following procedure is used. First we calculate the T values for the points. Consider point 1, as shown in Figure A-1; from the boundary conditions as given in Chapter II, subsitute the values

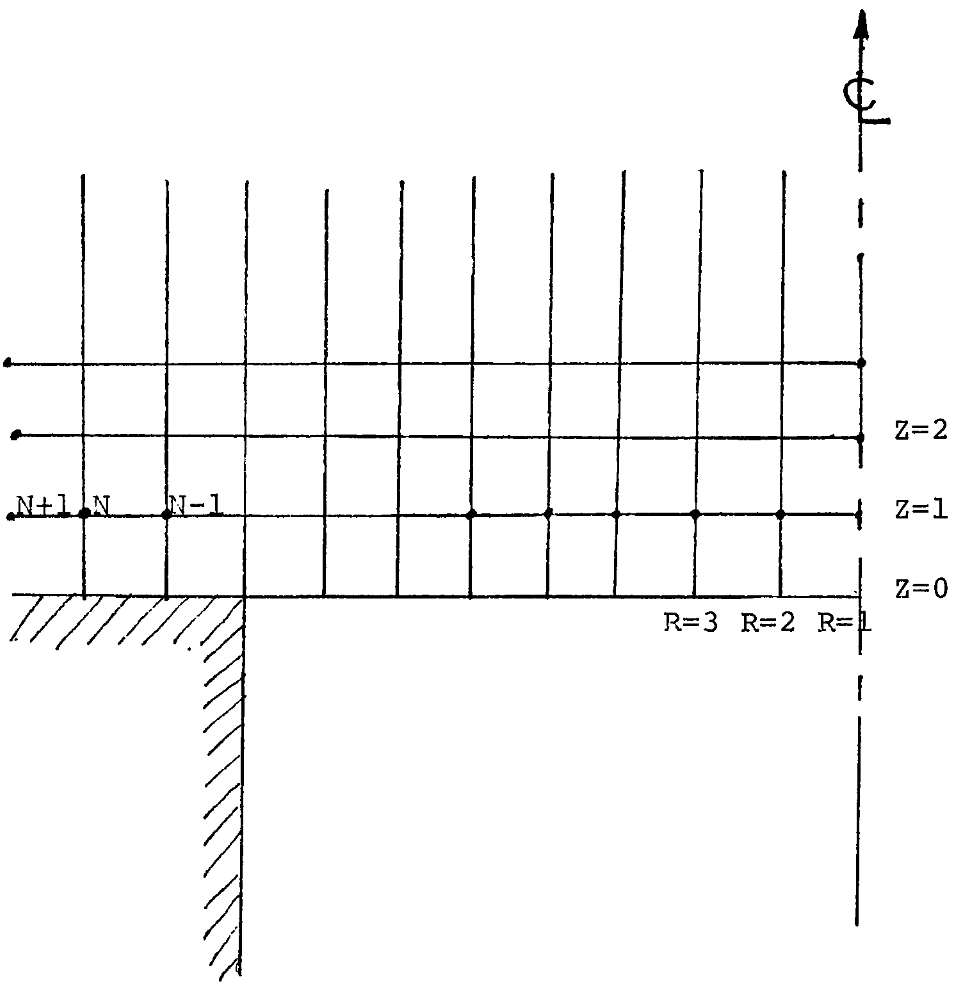

Figure A-1. The Finite-Difference Grid System into Equation (A-15); after some arrangement it become

$$P(0,1)\,U_z(0,1)\ \frac{T(1,1)-T(0,1)}{\Delta Z} = A_T\left[\frac{2T(1,2)-2T(1,1)}{\Delta R^2} + \frac{1}{R}\,\frac{T(1,2)-T(1,1)}{\Delta R}\right] + N_{Ec}A_v\left[\frac{U_z(0,2)-U_z(0,1)}{\Delta R}\right]^2 \qquad (A-16)$$

Futher rearrangement, the Equation can be put into the following form:

$$b_1T(1,1) + c_1T(1,2) = d_1 \qquad (A-17)$$

where
$$b_1 = P(0,1)U_Z(0,1)\Delta R^2R$$
$$c_1 = 2A_T(\Delta ZR + \Delta Z\Delta R)$$
$$d_1 = -N_{Ec}A_V[U_Z(0,2)-U_Z(0,1)]^2R\Delta Z - P(0,1)U_Z(0,1)T(0,1)\Delta R^2R$$

For point 2, Equation (A-15), after substitution and rearrangement becomes

$$a_2T(1,1) + b_2T(1,2) + c_2T(1,3) = d_2 \qquad (A-18)$$

where
$$a_2 = 2A_TR\Delta Z - A_T\Delta Z\Delta R + P(0,2)U_R(0,2)\Delta Z\Delta R$$
$$b_2 = -A_TR\Delta Z - P(0,2)U_Z(0,2)\Delta R^2R$$
$$c_2 = 2A_TR\Delta Z + A_T\Delta R\Delta Z - P(0,2)U_R(0,2)\Delta R\Delta Z$$
$$d_2 = -0.5N_{Ec}A_V[U_Z(0,3)-U_Z(0,1)]^2R\Delta Z - P(0,2)U_Z(0,2)\Delta R^2R$$

The system of Equations for each line can be written in the following form:

$$
\begin{aligned}
&b_1T(1,1) + c_1T(1,2) &&= d_1 \\
&a_2T(1,1) + b_2T(1,2) + c_2T(1,3) &&= d_2 \\
&\qquad a_3T(1,2) + b_3T(1,3) + c_3T(1,4) &&= d_3 \\
&\qquad\quad \cdots\cdot \quad \cdots\cdot \quad \cdots\cdot && \\
&\qquad\quad a_{N-1}T(1,N-2)+b_{N-1}T(1,N-1)+c_NT(1,N) &&= d_{N-1} \\
&\qquad\qquad a_NT(1,N-1) + b_NT(1,N) &&= d_N
\end{aligned} \tag{A-19}
$$

The a,b,c, and d values are known scalers. The matrix of coefficients a,b, and c alone is called a tridiagonal matrix. The system is readily solved by the Gaussian elimination method [32]. The alogarithm for the solution of the system is

$$
\begin{aligned}
&\beta_1 = b_1, && \gamma_1 = d_1/\beta_1 \\
&\beta_i = \frac{b_i - a_i c_{i-1}}{\beta_{i-1}} && i=2,3, \ldots,N \\
&\gamma_i = \frac{d_i - a_i \gamma_{i-1}}{\beta_i} && i=2,3, \ldots,N
\end{aligned} \tag{A-20}
$$

$$T(1,N) = \gamma_N$$

$$T(1,i) = \gamma_i - c_iT(1,i+1)$$

After solving T, the values of P is calculated

$$P(1,i) = \frac{1}{T(1,i)\ (1.0 - t_a/t_o) + t_a/t_o} \tag{A-21}$$

The values of U_Z and U_R were then solved similarly to T using Equations (A-14) and (A-13) respectively. The computational accuracy was then improved with an iterative procedure until the deviations of the assumed and the newly cal-was less than 5% on U_Z and T, and the solution is carried downstream to $Z+2\Delta Z$, etc. A procedure developed by Wegstein [27] :

$$\bar{T}(\text{New}) = 0.33T(\text{Old}) + 0.67T(\text{New}) \qquad \text{(A-22)}$$

was used to accelerate the iterative process.

APPENDIX B

FINITE-DIFFERENCE PROGRAM AND RESULT

The finite- difference program was set up to calculate the thermal and momentum structure of gas plume (or free jet) exhausting into quiesent air. The input data required for the system are the exit velocity, exit temperature, the ambient temperature, and the stack diameter (or the nozzle diameter). Other input data required for calculation purpose are described in the comment statements. The initial profiles of temperature and velocity are step functions. Also initial profiles of arbitary shape can be input into the program by changing the read format of the initial profiles. The computer program and the result print out are included in this APPENDIX.

```
$$WATFIV TIME=300,LINES=5000
C       THIS PROGRAM SOLVES THE FREE JET PROBLEM BY USING
C       AN ABBOTT-TYPE FINITE DIFFERENCE SOLUTION OF THE
C       CONSERVATIONS.
C       INPUT DATA
C       INPUT DATA
C       TO-JET EXIT TEMPERATURE,DEG. R
C       TA-AMBIENT TEMPERATURE,DEG. R
C       UO-JET EXIT VELOCITY,FT./SEC.
C       DELZ1-FIRST Z-DIRECTION FINITE DIFFERENCE STEP SIZE
C       DELZ2-SECOND Z-DIRECTION FINITE DIFFERENCE STEP SIZE
C       DELZ3-THIRD Z-DIRECTION FINITE DIFFERENCE STEP SIZE
C       DELR1-FIRST R-DIRECTION FINITE DIFFERENCE STEP SIZE
C       DELR2-SECOND R- DIRECTION FINITE DIFFERENCE STEP SIZE
C       DELR3-THIRD R-DIRECTION FINITE DIFFERENCE STEP SIZE
C       PRNO-TURBULENT PRANDTL NUMBER
C       TOL-TOLERENCE FOR ITERATIVE CONVERGENCE
C       II -NUMBER OF LINES OF THE FIRST Z-DIRECTION STEP SIZE
C       IS - FOR THE SECOND S
C       IS - FOR THE SECOND Z STEP
C       IT-I FOR THE THIRD STEP
C       JI, JS, JT FOR, THE R- STEP SIZE
C       KNOZ-Z-DIRECTION  LINE NUMBER OF NOZZLE
C       LIMIT-LIMITING NUMBER OF ITERATIONS
        DIMENSION OLDVZ(501),OLDVR(501),OLDRO(501),VZ(501),VR(501),
       XT(501),RO(501),A(501),B(501),C(501),D(501),TEST(501),OLDT(501)
 1002  READ (5,100) TO,TA,UO,DELZ1,DELZ2,DELZ3,DELR1,DELR2,
       XDELR3,PRNO,TOL
  100  FORMAT (8F10.0)
       WRITE (6,111) TO,TA,UO,DELZ1,DELZ2,DELZ3,DELR1,DELR2,
       XDELR3,PRNO,TOL
  111  FORMAT (11(2X,F8.3))
       READ (5,200) II,IS,IT,JI,JS,JT,KNOZ,LIMIT
       WRITE (6,200) II,IS,IT,JI,JS,JT,KNOZ,LIMIT
  200  FORMAT (8I5)
       READ (5,300) CONST, CPC, DIA
  300  FORMAT (3F10.0)
       WRITE (6,369)  CONST, CPC
  369  FORMAT(2(5X,F10.5))
       WRITE (6, 7679)  UO,TO,TA,DIA
 7679  FORMAT (1H1,/////,30X, 'FINITE DIFFERENCE PROGRAM',/,
      120X,'CALCULATION THE THERMAL AND MOMENTUM STRUCTURE OF GAS ',
      2'PLUME',
      3//, 30X, 'EXIT VELOCITY, FT/SEC=',F10.5,/,
      430X,'EXIT PLUME TEMPERATURE, DEG. R =',F10.5,/,
      530X,'AMBIENT TEMPERATURE, DEG. R=',F10.5,/,
      630X,'DIAMETER OF THE STACK, FT =',F10.5,/)
       PAR=0.333
       J=JI
       KAPPA=DELR2/DELR1
       NU=DELR3/DELR2
       PKAP=DELZ2/DELZ1
       OMEGA=DELZ3/DELZ1
       KNOZ1=KNOZ-1
C      INITIAL PROFILE VALUES
       DO 1 N=1,KNOZ1
       OLDVZ(N)=1.0
       OLDT(N)=1.0
       OLDVR(N)=0.0
     1 OLDRO(N)=1.0
       DO 2 N=KNOZ,J
       OLDVZ(N)=0.0
       OLDT(N)=0.0
       OLDVR(N)=0.0
     2 OLDRO(N)=TO/TA
       DO 8 N=1,J
       VZ(N)=OLDVZ(N)
       T(N)=OLDT(N)
       VR(N)=OLDVR(N)
     8 RO(N)=OLDRO(N)
       POS=1.0
       M=2
```

```
2001  IF (II-M) 1003,2003,3003
1003  IF (IS-M) 4003,5003,6003
4003  IF (IT-M) 2000,2000,7003
3003  ZP1=M-1
      Z=ZP1*DELZ1
      DELZ=DELZ1
      DELR=DELR1
      J=JI
      POS=POS+1.0
      SET=1.0/DELZ1 +1.0
      GO TO 1001
2003  DO 13 N=1,JI,KAPPA
      NEW=(N-1)/KAPPA+1
      OLDVZ(NEW)=OLDVZ(N)
      OLDT(NEW)=OLDT(N)
      OLDVR(NEW)=OLDVR(N)
   13 OLDRO(NEW)=OLDRO(N)
      DO 14 N=NEW,JS
      OLDVZ(N)=0.0
      OLDT(N)=0.0
      NM=N-1
      RP=N
      RPM=N-1
      OLDVR(N)=OLDVR(NM)*RPM/RP
   14 OLDRO(N)=TO/TA
      DO 48 N=1,JS
      VZ(N)=OLDVZ(N)
      T(N)=OLDT(N)
      VR(N)=OLDVR(N)
   48 RO(N)=OLDRO(N)
6003  ZP1=(II-2)
      ZP2=M-II+1
      Z=ZP1*DELZ1+ZP2*DELZ2
      DELZ=DELZ2
      DELR=DELR2
      J=JS
      POS=POS+PKAP
      GO TO 1001
5003  DO 15 N=1,JS,NU
      NEW=(N-1)/NU+1
      OLDVZ(NEW)=OLDVZ(N)
      OLDT(NEW)=OLDT(N)
      OLDVR(NEW)=OLDVR(N)
   15 OLDRO(NEW)=OLDRO(N)
      DO 16 N=NEW,JT
      OLDVZ(N)=0.0
      OLDT(N)=0.0
      NM=N-1
      RP=N
      RPM=N-1
      OLDVR(N)=OLDVR(NM)*RPM/RP
   16 OLDRO(N)=TO/TA
      DO 38 N=1,JT
      VZ(N)=OLDVZ(N)
      T(N)=OLDT(N)
      VR(N)=OLDVR(N)
   38 RO(N)=OLDRO(N)
7003  ZP2=IS-II
      ZP3=M-IS+1
      Z=ZP1*DELZ1+ZP2*DELZ2+ZP3*DELZ3
      DELZ=DELZ3
      DELR=DELR3
      J=JT
      POS=POS+OMEGA
1001  INCR=0.0
      J1=J-1
      J2=J-2
      ZPOTC=4.73/((TO/TA)**0.5)
      ZPOTC=0.8
      IF (Z-ZPOTC) 1004,1004,2004
1004  FVZ=CPC
      GO TO 3004
```

```
200 FVZ=1.0
3001 REYK=CONST*((TO/TA)**0.5)*OLDRO(1)*FVZ
     ZTPC=3.43/((TO/TA)**0.5)
      ZTPC=0.8
     IF (Z-ZTPC)1005,1005,2005
1005 FT=CPC*PRNO
     GO TO 3005
2005 FT=1.0
3005 PRK=(CONST*((TO/TA)**0.5)*OLDRO(1)*FT)/PRNO
     C1=REYK/(DELR*DELR)
     CC1=PRK/(DELR*DELR)
3001 WRITE (6,50)
 50  FORMAT(/////, 8X,'UZ(Z,R)', 8X,'UR(Z,R)', 8X,'T(Z,R)',10X,
    1'RO(Z,R)',11X,'Z',14X,'R')
     VZ(J)=0.0
     T(J)=0.0
     RO(J)=TO/TA
8001 A(1)=RO(1)*VZ(1)/DELZ+4.0*CC1
     B(1)=-4.0*CC1
     D(1)=RO(1)*VZ(1)*(1.0/OLDRO(1)-TA/TO)/((1.0-TA/TO)*DELZ)
     DO 18 N=2,J1
     RP=N-1
     R=RP*DELR
     CC2=PRK/(2.0*R*DELR)
     CC3=RO(N)*VR(N)/(2.0*DELR)
     CC4=RO(N)*VZ(N)/DELZ
     NP=N+1
     NM=N-1
     C(N)=CC2-CC3-CC1
     A(N)=CC4+2.0*CC1
     B(N)=CC3-CC2-CC1
     AT=(1.0/RO(N))*TO
     CP=171.5+0.02696*AT-0.00000396*AT*AT
     THETA = (1.0/OLDRO(N)-TA/TO)/(1.0-TA/TO)
  18 D(N)=CC4*THETA+U0*U0/(32.2*CP*(TO-TA))*REYK*(VZ(NP)*VZ
    X(NP)-2.0*VZ(NP)*VZ(NM)+VZ(NM)*VZ(NM))/(4.0*DELR*DELR)
     DO 22 N=1,J
  22 TEST(N)=T(N)
     D(1)=D(1)/A(1)
     DO 19 N=2,J1
     N1=N-1
     B(N1)=B(N1)/A(N1)
     A(N)=A(N)-C(N)*B(N1)
  19 D(N)=(D(N)-C(N)*D(N1))/A(N)
     T(J1)=D(J1)
     RO(J1)=1.0/(T(J1)*(1.0-TA/TO)+TA/TO)
     DO 20 N=1,J2
     NN=J2-N+1
     NN1=NN+1
  20 T(NN)=D(NN)-B(NN)*T(NN1)
     DO 66 N=1,J
     T(N)=PAR*TEST(N)+ (1.0-PAR)*T(N)
  66 RO(N)=1.0/(T(N)*(1.0-TA/TO)+TA/TO)
     DO 23 N=1,J
     DIFF=ABS (TEST(N)-T(N))
     IF (DIFF-TOL) 23,23,9001
  23 CONTINUE
     ERR1=0.0
     GO TO 24
9001 ERR1=1.0
  24 A(1)=RO(1)*VZ(1)/DELZ+4.0*C1
     B(1)=-4.0*C1
     D(1)=RO(1)*VZ(1)*OLDVZ(1)/DELZ
     DO 3 N=2,J1
     RP=N-1
     R=RP*DELR
     C2=REYK/(2.0*R*DELR)
     C3=RO(N)*VR(N)/(2.0*DELR)
     C4=RO(N)*VZ(N)/DELZ
     C(N)=C2-C3-C1
     A(N)=C4+2.0*C1
     B(N)=C3-C2-C1
   3 D(N)=C4*OLDVZ(N)
     DO 17 N=1,J
  17 TEST(N)=VZ(N)
     D(1)=D(1)/A(1)
```

```
      DO 4 N=2,J1
      N1=N-1
      B(N1)=D(N1)/A(N1)
      A(N)=A(N)-C(N)*B(N1)
    4 D(N)=(D(N)-C(N)*D(N1))/A(N)
      VZ(J1)=D(J1)
      DO 5 N=1,J2
      NN=J2-N+1
      NN1=NN+1
    5 VZ(NN)=D(NN)-B(NN)*VZ(NN1)
      DO 666 N=1,J
  666 VZ(N)=PAR*TEST(N)+(1.0-PAR)*VZ(N)
      DO 6 N=2,J
      N1=N-1
      RP=N1
      R=RP*DELR
      CE1=1.0/((2.0*RO(N))/DELR-RO(N1)/DELR+RO(N)/R)
      CE2=RO(N)*(OLDVZ(N)-VZ(N))/DELZ
      CE3=VZ(N)*(OLDRO(N)-RO(N))/DELZ
      CE4=RO(N)*VR(N1)/DELR
    6 VR(N)=CE1*(CE2+CE3+CE4)
      DO 10 N=1,J1
      ERROR=ABS (TEST(N)-VZ(N))
      IF (ERROR-TOL) 10,10,5001
   10 CONTINUE
      IF (ERR1) 26,26,5001
   26 CONTINUE
      IF (POS- S_T) 3002,3002,2000
 3002 POS=1.0
      DO 7 N=1,J
      RP= N-1
      R=RP*DELR
      RF=R
      IF (M.LE.36.AND.M.GE.27) GO TO 699
      IF (M.LE.3 ) GO TO 69
   67 RF=R*5/3.
      IF (M.LE.44) GO TO 699
  671 RF=R*2.
      GO TO 699
   69 RF=R
      WRITE(6,150) VZ(N),VR(N),T(N),RO(N),Z,RF
      GO TO 7
  699 L=N/2
      LL=L*2 +1
      IF (LL.GT.N) GO TO 7
      WRITE(6,150) VZ(N),VR(N),T(N),RO(N),Z,RF
    7 CONTINUE
  150 FORMAT (4F15.5,2F15.3)
      MM=M/2
      MMM=MM*2
      IF (MMM.LT.M) GO TO 4001
  152 WRITE (6,151)
  151 FORMAT(1H1)
 4001 DO 9 N=1,J
      OLDVZ(N)=VZ(N)
      OLDT(N)=T(N)
      OLDVR(N)=VR(N)
    9 OLDRO(N)=RO(N)
      M=M+1
      GO TO 2001
 5001 INCR=INCR+1
      IF (INCR-LIMIT) 1009,1009,7001
 1009 GO TO 3001
 7001 DO 12 N=1,J
      RP=N-1
      R=RP*DELR
      WRITE (6,250) VZ(N),VR(N),T(N),RO(N),M,N,Z,R
  250 FORMAT (4F20.8,2I5,2F15.8)
      WRITE (6,99) TEST(N)
   99 FORMAT (F20.8)
   12 CONTINUE
 2000 CONTINUE
      STOP
      END
```

FINITE DIFFERENCE PROGRAM
CALCULATION THE THERMAL AND MOMENTUM STRUCTURE OF GAS PLUME

EXIT VELOCITY, FT/SEC= 37.30000
EXIT PLUME TEMPERATURE, DEG. R = 912.00000
AMBIENT TEMPERATURE, DEG. R= 526.00000
DIAMETER OF THE STACK, FT = 3.40000

UZ(Z,R)	UR(Z,R)	T(Z,R)	RO(Z,R)	Z	R
1.00000	0.00000	1.00000	1.00000	0.100	0.000
1.00000	0.00000	1.00000	1.00000	0.100	0.100
1.00000	0.00000	1.00000	1.00000	0.100	0.200
1.00000	0.00000	1.00000	1.00000	0.100	0.300
1.00000	0.00000	1.00000	1.00000	0.100	0.400
0.99990	0.00000	0.99999	1.00000	0.100	0.500
0.99995	0.00003	0.99995	1.00002	0.100	0.600
0.99969	0.00018	0.99969	1.00013	0.100	0.700
0.99789	0.00124	0.99789	1.00089	0.100	0.800
0.98549	0.00869	0.98548	1.00618	0.100	0.900
0.89333	0.06306	0.89333	1.04496	0.100	1.000
0.18730	-0.06991	0.18955	1.52211	0.100	1.100
0.04638	-0.09760	0.04706	1.67597	0.100	1.200
0.01710	-0.10426	0.01737	1.71201	0.100	1.300
0.00957	-0.10563	0.00960	1.72171	0.100	1.400
0.00573	-0.10413	0.00577	1.72653	0.100	1.500
0.00275	-0.10038	0.00275	1.73035	0.100	1.600
0.00000	-0.09462	0.00000	1.73354	0.100	1.700

UZ(Z,R)	UR(Z,R)	T(Z,R)	RO(Z,R)	Z	R
1.00000	0.00000	1.00000	1.00000	0.200	0.000
1.00000	0.00000	1.00000	1.00000	0.200	0.100
1.00000	0.00000	1.00000	1.00000	0.200	0.200
1.00000	0.00000	1.00000	1.00000	0.200	0.300
0.99994	0.00000	0.99999	1.00000	0.200	0.400
0.99996	0.00002	0.99995	1.00002	0.200	0.500
0.99977	0.00010	0.99979	1.00009	0.200	0.600
0.99880	0.00053	0.99850	1.00051	0.200	0.700
0.99339	0.00278	0.99338	1.00251	0.200	0.800
0.96511	0.01314	0.96505	1.01501	0.200	0.900
0.82945	0.04892	0.82722	1.07791	0.200	1.000
0.28388	-0.02259	0.28475	1.43416	0.200	1.100
0.09146	-0.05395	0.09201	1.62417	0.200	1.200
0.03385	-0.05294	0.03388	1.69178	0.200	1.300
0.01557	-0.06349	0.01537	1.71450	0.200	1.400
0.00767	-0.06099	0.00750	1.72435	0.200	1.500
0.00309	-0.05754	0.00301	1.73001	0.200	1.600
0.00000	-0.05423	0.00000	1.73384	0.200	1.700

UZ(Z,R)	UR(Z,R)	T(Z,R)	RO(Z,R)	Z	R
1.00000	0.00000	1.00000	1.00000	0.300	0.000
1.00000	0.00000	1.00000	1.00000	0.300	0.100
1.00000	0.00000	1.00000	1.00000	0.300	0.200
1.00000	0.00000	1.00000	1.00000	0.300	0.300
0.99998	0.00001	0.99998	1.00001	0.300	0.400
0.99991	0.00003	0.99991	1.00004	0.300	0.500
0.99954	0.00015	0.99954	1.00020	0.300	0.600
0.99769	0.00069	0.99768	1.00078	0.300	0.700
0.98892	0.00290	0.98888	1.00473	0.300	0.800
0.95036	0.01025	0.95014	1.02156	0.300	0.900
0.79972	0.02484	0.79898	1.09299	0.300	1.000
0.32889	-0.00878	0.32823	1.39728	0.300	1.100
0.12831	-0.03536	0.12740	1.58560	0.300	1.200
0.05404	-0.04864	0.05335	1.66851	0.300	1.300
0.02446	-0.05253	0.02403	1.70380	0.300	1.400
0.01093	-0.05182	0.01071	1.72032	0.300	1.500
0.00395	-0.04934	0.00386	1.72894	0.300	1.600
0.00000	-0.04647	0.00000	1.73384	0.300	1.700

UZ(Z,R)	UR(Z,R)	T(Z,R)	RO(Z,R)	Z	R
1.00000	0.00000	1.00000	1.00000	0.400	0.000
1.00000	0.00000	1.00000	1.00000	0.400	0.100
1.00000	0.00000	1.00000	1.00000	0.400	0.200
0.99999	0.00000	0.99999	1.00000	0.400	0.300
0.99996	0.00001	0.99996	1.00002	0.400	0.400
0.99982	0.00005	0.99982	1.00008	0.400	0.500
0.99916	0.00023	0.99916	1.00036	0.400	0.600
0.99619	0.00096	0.99617	1.00152	0.400	0.700
0.98365	0.00354	0.98355	1.00701	0.400	0.800
0.93513	0.01108	0.93475	1.02840	0.400	0.900
0.77257	0.01426	0.77146	1.10709	0.400	1.000
0.36396	-0.00268	0.36259	1.36945	0.400	1.100
0.16135	-0.01685	0.15975	1.55191	0.400	1.200
0.07430	-0.04063	0.07316	1.64549	0.400	1.300
0.03527	-0.04660	0.03462	1.69089	0.400	1.400
0.01613	-0.04790	0.01581	1.71306	0.400	1.500
0.00589	-0.04658	0.00576	1.72654	0.400	1.600
0.00000	-0.04382	0.00000	1.73334	0.400	1.700

UZ(Z,R)	UR(Z,R)	T(Z,R)	RO(Z,R)	Z	R
1.00000	0.00000	1.00000	1.00000	0.500	0.000
1.00000	0.00000	1.00000	1.00000	0.500	0.100
0.99999	0.00000	1.00000	1.00000	0.500	0.200
0.99998	0.00000	0.99998	1.00001	0.500	0.300
0.99993	0.00002	0.99993	1.00003	0.500	0.400
0.99968	0.00008	0.99968	1.00013	0.500	0.500
0.99863	0.00033	0.99863	1.00058	0.500	0.600
0.99432	0.00123	0.99429	1.00242	0.500	0.700
0.97775	0.00410	0.97761	1.00957	0.500	0.800
0.92032	0.01137	0.91978	1.03514	0.500	0.900
0.75096	0.02154	0.74963	1.11853	0.500	1.000
0.39037	0.00083	0.38863	1.34909	0.500	1.100
0.18648	-0.01915	0.18653	1.52508	0.500	1.200
0.09207	-0.03143	0.09068	1.62566	0.500	1.300
0.04532	-0.03731	0.04451	1.67900	0.500	1.400
0.02119	-0.03903	0.02079	1.70779	0.500	1.500
0.00785	-0.03823	0.00769	1.72411	0.500	1.600
0.00000	-0.03592	0.00000	1.73334	0.500	1.700

UZ(Z,R)	UR(Z,R)	T(Z,R)	RO(Z,R)	Z	R
1.00000	0.00000	1.00000	1.00000	0.600	0.000
1.00000	0.00000	1.00000	1.00000	0.600	0.100
0.99999	0.00000	0.99999	1.00000	0.600	0.200
0.99997	0.00001	0.99997	1.00001	0.600	0.300
0.99985	0.00003	0.99988	1.00005	0.600	0.400
0.99949	0.00012	0.99947	1.00021	0.600	0.500
0.99795	0.00044	0.99794	1.00087	0.600	0.600
0.99209	0.00150	0.99204	1.00338	0.600	0.700
0.97140	0.00458	0.97119	1.01235	0.600	0.800
0.90609	0.01151	0.90541	1.04170	0.600	0.900
0.73330	0.01954	0.73184	1.12803	0.600	1.000
0.41064	0.00320	0.40874	1.33378	0.600	1.100
0.21225	-0.01450	0.21013	1.50220	0.600	1.200
0.10963	-0.02673	0.10806	1.60645	0.600	1.300
0.05656	-0.03410	0.05563	1.66584	0.600	1.400
0.02762	-0.03717	0.02712	1.70001	0.600	1.500
0.01063	-0.03717	0.01044	1.72066	0.600	1.600
0.00000	-0.03486	0.00000	1.73354	0.600	1.700

UZ(Z,R)	UR(Z,R)	T(Z,R)	RO(Z,R)	Z	R
1.00000	0.00000	1.00000	1.00000	0.700	0.000
0.99999	0.00000	1.00000	1.00000	0.700	0.100
0.99999	0.00000	0.99999	1.00000	0.700	0.200
0.99995	0.00001	0.99995	1.00002	0.700	0.300
0.99980	0.00004	0.99981	1.00008	0.700	0.400
0.99924	0.00016	0.99923	1.00032	0.700	0.500
0.99710	0.00055	0.99709	1.00124	0.700	0.600
0.98952	0.00177	0.98944	1.00449	0.700	0.700
0.96459	0.00500	0.96442	1.01529	0.700	0.800
0.89256	0.01152	0.89177	1.04801	0.700	0.900
0.71678	0.01786	0.71724	1.13594	0.700	1.000
0.42640	0.00477	0.42443	1.32206	0.700	1.100
0.23248	-0.01047	0.23030	1.48318	0.700	1.200
0.12509	-0.02152	0.12343	1.58983	0.700	1.300
0.06648	-0.02788	0.06544	1.65439	0.700	1.400
0.03312	-0.03051	0.03256	1.69338	0.700	1.500
0.01294	-0.03046	0.01272	1.71731	0.700	1.600
0.00000	-0.02852	0.00000	1.73334	0.700	1.700

UZ(Z,R)	UR(Z,R)	T(Z,R)	RO(Z,R)	Z	R
0.99972	0.00000	0.99940	1.00025	0.800	0.000
0.99969	0.00000	0.99928	1.00030	0.800	0.100
0.99944	0.00004	0.99854	1.00049	0.800	0.200
0.99881	0.00020	0.99760	1.00093	0.800	0.300
0.99730	0.00071	0.99550	1.00191	0.800	0.400
0.99364	0.00217	0.99045	1.00476	0.800	0.500
0.98494	0.00596	0.97947	1.00876	0.800	0.600
0.96474	0.01475	0.95597	1.01899	0.800	0.700
0.92001	0.03224	0.90754	1.04073	0.800	0.800
0.82915	0.07651	0.81493	1.08499	0.800	0.900
0.6708[illegible]	0.07537	0.66092	1.16756	0.800	1.000
0.46397	0.04057	0.46443	1.29312	0.800	1.100
0.30103	-0.01133	0.30336	1.41339	0.800	1.200
0.18969	-0.05796	0.19968	1.51225	0.800	1.300
0.11532	-0.09113	0.12489	1.58828	0.800	1.400
0.06440	-0.10940	0.07163	1.64726	0.800	1.500
0.02781	-0.11362	0.03165	1.69449	0.800	1.600
0.00000	-0.10506	0.00000	1.73354	0.800	1.700

UZ(Z,R)	UR(Z,R)	T(Z,R)	RO(Z,R)	Z	R
0.99916	0.00000	0.99807	1.00082	0.900	0.000
0.99901	0.00002	0.99774	1.00096	0.900	0.100
0.99838	0.00010	0.99665	1.00142	0.900	0.200
0.99692	0.00038	0.99427	1.00243	0.900	0.300
0.99376	0.00111	0.98952	1.00445	0.900	0.400
0.98706	0.00286	0.98031	1.00840	0.900	0.500
0.97314	0.00658	0.96279	1.01600	0.900	0.600
0.94517	0.01353	0.93035	1.03037	0.900	0.700
0.89171	0.02457	0.87238	1.05636	0.900	0.800
0.79757	0.03698	0.77303	1.10367	0.900	0.900
0.65283	0.04133	0.63953	1.18003	0.900	1.000
0.47674	0.02676	0.47530	1.28547	0.900	1.100
0.32703	0.00505	0.33439	1.39221	0.900	1.200
0.21485	-0.01445	0.22628	1.48693	0.900	1.300
0.13394	-0.02782	0.14542	1.56665	0.900	1.400
0.07550	-0.03455	0.08441	1.63270	0.900	1.500
0.03251	-0.03572	0.03733	1.68761	0.900	1.600
0.00000	-0.03291	0.00000	1.73334	0.900	1.700

UZ(Z,R)	UR(Z,R)	T(Z,R)	RO(Z,R)	Z	R
0.99816	0.00000	0.99577	1.00179	1.000	0.000
0.99782	0.00005	0.99519	1.00204	1.000	0.100
0.99667	0.00021	0.99324	1.00247	1.000	0.200
0.99413	0.00066	0.98924	1.00458	1.000	0.300
0.98903	0.00171	0.98173	1.00779	1.000	0.400
0.97901	0.00392	0.96528	1.01361	1.000	0.500
0.96005	0.00815	0.94493	1.02391	1.000	0.600
0.92549	0.01532	0.90534	1.04174	1.000	0.700
0.86560	0.02555	0.84195	1.07169	1.000	0.800
0.77026	0.03622	0.74735	1.11974	1.000	0.900
0.63660	0.04017	0.62111	1.19099	1.000	1.000
0.48301	0.03009	0.47941	1.28261	1.000	1.100
0.34723	0.01185	0.35276	1.37730	1.000	1.200
0.23973	-0.00832	0.24969	1.46534	1.000	1.300
0.15737	-0.02622	0.16773	1.54392	1.000	1.400
0.09364	-0.03896	0.10171	1.61341	1.000	1.500
0.04267	-0.04432	0.04694	1.67611	1.000	1.600
0.00000	-0.04058	0.00000	1.73384	1.000	1.700

UZ(Z,R)	UR(Z,R)	T(Z,R)	RO(Z,R)	Z	R
0.99659	0.00000	0.99240	1.00323	1.100	0.000
0.99605	0.00011	0.99150	1.00361	1.100	0.100
0.99423	0.00038	0.98857	1.00436	1.100	0.200
0.99042	0.00102	0.98274	1.00736	1.100	0.300
0.98314	0.00237	0.97241	1.01181	1.100	0.400
0.96983	0.00497	0.95494	1.01944	1.100	0.500
0.94626	0.00951	0.92642	1.03214	1.100	0.600
0.90623	0.01653	0.88164	1.05274	1.100	0.700
0.84221	0.02561	0.81485	1.08503	1.100	0.800
0.74760	0.03411	0.72216	1.13326	1.100	0.900
0.62355	0.03671	0.60604	1.20010	1.100	1.000
0.48603	0.02927	0.47985	1.28230	1.100	1.100
0.36057	0.01584	0.36339	1.36882	1.100	1.200
0.25627	0.00137	0.26388	1.45256	1.100	1.300
0.17222	-0.01070	0.18082	1.53072	1.100	1.400
0.10419	-0.01850	0.11116	1.60307	1.100	1.500
0.04783	-0.02142	0.05173	1.67043	1.100	1.600
0.00000	-0.01956	0.00000	1.73384	1.100	1.700

UZ(Z,R)	UR(Z,R)	T(Z,R)	RO(Z,R)	Z	R
0.99433	0.00000	0.98768	1.00516	1.200	0.000
0.99361	0.00019	0.98664	1.00560	1.200	0.100
0.99104	0.00059	0.98265	1.00740	1.200	0.200
0.98534	0.00143	0.97495	1.01071	1.200	0.300
0.97631	0.00307	0.96186	1.01641	1.200	0.400
0.95977	0.00599	0.94073	1.02573	1.200	0.500
0.93211	0.01070	0.90799	1.04052	1.200	0.600
0.88787	0.01743	0.85936	1.06329	1.200	0.700
0.82115	0.02547	0.79084	1.09712	1.200	0.800
0.72827	0.03238	0.70079	1.14590	1.200	0.900
0.61230	0.03427	0.59293	1.20815	1.200	1.000
0.48688	0.02865	0.47303	1.28357	1.200	1.100
0.36988	0.01911	0.36967	1.36386	1.200	1.200
0.26911	0.00611	0.27385	1.44371	1.200	1.300
0.18480	-0.00467	0.19102	1.52067	1.200	1.400
0.11405	-0.01248	0.11931	1.59426	1.200	1.500
0.05337	-0.01610	0.05632	1.66502	1.200	1.600
0.00000	-0.01466	0.00000	1.73394	1.200	1.700

UZ(Z,R)	UR(Z,R)	T(Z,R)	RO(Z,R)	Z	R
0.99150	0.00000	0.98220	1.00759	1.300	0.000
0.99046	0.00030	0.98060	1.00828	1.300	0.100
0.98707	0.00085	0.97554	1.01046	1.300	0.200
0.98038	0.00190	0.96601	1.01460	1.300	0.300
0.96864	0.00379	0.95031	1.02148	1.300	0.400
0.94908	0.00694	0.92596	1.03235	1.300	0.500
0.91786	0.01171	0.88981	1.04892	1.300	0.600
0.87033	0.01807	0.83848	1.07338	1.300	0.700
0.80209	0.02518	0.76932	1.10820	1.300	0.800
0.71142	0.03090	0.68214	1.15544	1.300	0.900
0.60239	0.03236	0.58102	1.21556	1.300	1.000
0.48615	0.02810	0.47460	1.28597	1.300	1.100
0.37595	0.01990	0.37261	1.36154	1.300	1.200
0.27831	0.01039	0.28000	1.43830	1.300	1.300
0.19404	0.00177	0.19773	1.51414	1.300	1.400
0.12125	-0.00449	0.12473	1.58845	1.300	1.500
0.05732	-0.00752	0.05934	1.66149	1.300	1.600
0.00000	-0.00683	0.00000	1.73384	1.300	1.700

UZ(Z,R)	UP(Z,R)	T(Z,R)	RO(Z,R)	Z	R
0.98790	0.00000	0.97538	1.01053	1.400	0.000
0.98655	0.00043	0.97344	1.01137	1.400	0.100
0.98234	0.00114	0.96732	1.01402	1.400	0.200
0.97415	0.00239	0.95606	1.01895	1.400	0.300
0.96025	0.00450	0.93300	1.02675	1.400	0.400
0.93793	0.00782	0.91039	1.03919	1.400	0.500
0.90369	0.01255	0.87204	1.05726	1.400	0.600
0.85366	0.01853	0.81887	1.08303	1.400	0.700
0.78472	0.02483	0.74979	1.11844	1.400	0.800
0.69640	0.02964	0.66547	1.16494	1.400	0.900
0.59322	0.03085	0.56992	1.22234	1.400	1.000
0.49432	0.02756	0.47011	1.28912	1.400	1.100
0.37977	0.02104	0.37332	1.36009	1.400	1.200
0.28501	0.01327	0.28365	1.43511	1.400	1.300
0.20119	0.00598	0.20227	1.50974	1.400	1.400
0.12706	0.00046	0.12366	1.58426	1.400	1.500
0.06061	-0.00247	0.06165	1.65830	1.400	1.600
0.00000	-0.00225	0.00000	1.73334	1.400	1.700

UZ(Z,R)	UR(Z,R)	T(Z,R)	RO(Z,R)	Z	R
0.98358	0.00000	0.96749	1.01395	1.500	0.000
0.98197	0.00057	0.96521	1.01494	1.500	0.100
0.97687	0.00145	0.95311	1.01805	1.500	0.200
0.96723	0.00290	0.94525	1.02372	1.500	0.300
0.95127	0.00520	0.92510	1.03274	1.500	0.400
0.92646	0.00862	0.89567	1.04620	1.500	0.500
0.88970	0.01327	0.85474	1.06551	1.500	0.600
0.83733	0.01885	0.80041	1.09227	1.500	0.700
0.76875	0.02446	0.73185	1.12802	1.500	0.800
0.68292	0.02858	0.65025	1.17375	1.500	0.900
0.58467	0.02966	0.55935	1.22926	1.500	1.000
0.48157	0.02713	0.46484	1.29233	1.500	1.100
0.38181	0.02193	0.37235	1.36174	1.500	1.200
0.28966	0.01560	0.28533	1.43366	1.500	1.300
0.20645	0.00955	0.20500	1.50711	1.500	1.400
0.13144	0.00484	0.13122	1.58155	1.500	1.500
0.06313	0.00216	0.06320	1.65699	1.500	1.600
0.00000	0.00196	0.00000	1.73384	1.500	1.700

UZ(Z,R)	UR(Z,R)	T(Z,R)	RO(Z,R)	Z	R
0.97853	0.00000	0.95860	1.01733	1.600	0.000
0.97665	0.00073	0.95602	1.01897	1.600	0.100
0.97070	0.00178	0.94801	1.02250	1.600	0.200
0.95963	0.00340	0.93371	1.02847	1.600	0.300
0.94133	0.00586	0.91175	1.03570	1.600	0.400
0.91480	0.00935	0.88042	1.05331	1.600	0.500
0.87595	0.01387	0.83793	1.07355	1.600	0.600
0.82273	0.01907	0.78294	1.10117	1.600	0.700
0.75394	0.02410	0.71518	1.13707	1.600	0.800
0.67046	0.02770	0.63613	1.18204	1.600	0.900
0.57649	0.02871	0.54917	1.23580	1.600	1.000
0.47333	0.02677	0.45902	1.29676	1.600	1.100
0.38251	0.02261	0.37017	1.36346	1.600	1.200
0.29271	0.01741	0.28555	1.43346	1.600	1.300
0.21026	0.01231	0.20638	1.50578	1.600	1.400
0.13475	0.00820	0.13278	1.57990	1.600	1.500
0.06507	0.00569	0.06421	1.65581	1.600	1.600
0.00000	0.00515	0.00000	1.73334	1.600	1.700

UZ(Z,R)	UR(Z,R)	T(Z,R)	RO(Z,R)	Z	R
0.97279	0.00000	0.94881	1.02215	1.700	0.000
0.97064	0.00090	0.94595	1.02341	1.700	0.100
0.96387	0.00212	0.93713	1.02734	1.700	0.200
0.95151	0.00391	0.92157	1.03433	1.700	0.300
0.93193	0.00649	0.89808	1.04508	1.700	0.400
0.90303	0.01000	0.86521	1.06050	1.700	0.500
0.86251	0.01437	0.82159	1.08168	1.700	0.600
0.80844	0.01922	0.76632	1.10976	1.700	0.700
0.74011	0.02377	0.69954	1.14570	1.700	0.800
0.65889	0.02698	0.62284	1.18996	1.700	0.900
0.56859	0.02796	0.53927	1.24224	1.700	1.000
0.47461	0.02650	0.45279	1.30141	1.700	1.100
0.38214	0.02316	0.36708	1.36590	1.700	1.200
0.29446	0.01888	0.28465	1.43425	1.700	1.300
0.21287	0.01458	0.20671	1.50547	1.700	1.400
0.13716	0.01100	0.13352	1.57912	1.700	1.500
0.06652	0.00865	0.06479	1.65515	1.700	1.600
0.00000	0.00783	0.00000	1.73354	1.700	1.700

UZ(Z,R)	UR(Z,R)	T(Z,R)	RO(Z,R)	Z	R
0.96635	0.00000	0.93320	1.02636	1.800	0.000
0.96397	0.00107	0.93510	1.02824	1.800	0.100
0.95643	0.00246	0.92557	1.03253	1.800	0.200
0.94285	0.00440	0.90893	1.04009	1.800	0.300
0.92175	0.00708	0.88417	1.05155	1.800	0.400
0.89120	0.01059	0.85010	1.06774	1.800	0.500
0.84934	0.01481	0.80570	1.08961	1.800	0.600
0.79472	0.01934	0.75043	1.11810	1.800	0.700
0.72709	0.02348	0.68472	1.15399	1.800	0.800
0.64797	0.02638	0.61019	1.19758	1.800	0.900
0.56089	0.02737	0.52758	1.24860	1.800	1.000
0.47044	0.02630	0.44525	1.30612	1.800	1.100
0.38093	0.02362	0.36329	1.36890	1.800	1.200
0.29522	0.02009	0.28299	1.43578	1.800	1.300
0.21450	0.01644	0.20621	1.50595	1.800	1.400
0.13981	0.01330	0.13363	1.57900	1.800	1.500
0.06756	0.01107	0.06502	1.65488	1.800	1.600
0.00000	0.01002	0.00000	1.73384	1.800	1.700

UZ(Z,R)	UR(Z,R)	T(Z,R)	RO(Z,R)	Z	R
0.95934	0.00000	0.92688	1.03193	1.900	0.000
0.95663	0.00124	0.92356	1.03343	1.900	0.100
0.94844	0.00279	0.91342	1.03804	1.900	0.200
0.93375	0.00487	0.89588	1.04610	1.900	0.300
0.91126	0.00763	0.87008	1.05918	1.900	0.400
0.87936	0.01111	0.83511	1.07592	1.900	0.500
0.83647	0.01518	0.79022	1.09744	1.900	0.600
0.78155	0.01943	0.73517	1.12624	1.900	0.700
0.71471	0.02323	0.67058	1.16201	1.900	0.800
0.63758	0.02590	0.59805	1.20500	1.900	0.900
0.55334	0.02690	0.52006	1.25491	1.900	1.000
0.46594	0.02616	0.43748	1.31102	1.900	1.100
0.37904	0.02403	0.35897	1.37233	1.900	1.200
0.29512	0.02110	0.28046	1.43790	1.900	1.300
0.21534	0.01800	0.20207	1.50705	1.900	1.400
0.13985	0.01521	0.13324	1.57941	1.900	1.500
0.06826	0.01309	0.06497	1.65494	1.900	1.600
0.00000	0.01186	0.00000	1.73334	1.900	1.700

UZ(Z,R)	UR(Z,R)	T(Z,R)	RO(Z,R)	Z	R
0.95171	0.00000	0.91493	1.03735	2.000	0.000
0.94882	0.00141	0.91143	1.03895	2.000	0.100
0.93995	0.00312	0.90078	1.04334	2.000	0.200
0.92425	0.00532	0.88249	1.05234	2.000	0.300
0.90051	0.00814	0.85589	1.06406	2.000	0.400
0.86754	0.01159	0.82026	1.08234	2.000	0.500
0.82367	0.01550	0.77510	1.10520	2.000	0.600
0.76887	0.01950	0.72044	1.13420	2.000	0.700
0.70290	0.02303	0.65599	1.16983	2.000	0.800
0.62762	0.02552	0.58533	1.21225	2.000	0.900
0.54590	0.02655	0.51067	1.26120	2.000	1.000
0.46115	0.02606	0.43254	1.31609	2.000	1.100
0.37566	0.02439	0.35425	1.37610	2.000	1.200
0.29435	0.02197	0.27752	1.44048	2.000	1.300
0.21552	0.01931	0.20342	1.50853	2.000	1.400
0.14037	0.01683	0.13245	1.58024	2.000	1.500
0.06869	0.01480	0.06470	1.65525	2.000	1.600
0.00000	0.01341	0.00000	1.73354	2.000	1.700

UZ(Z,R)	UR(Z,R)	T(Z,R)	RO(Z,R)	Z	R
0.92836	0.00000	0.88051	1.05327	2.200	0.000
0.92505	0.00241	0.87672	1.05505	2.200	0.100
0.91488	0.00516	0.86526	1.06048	2.200	0.200
0.89731	0.00843	0.84588	1.06978	2.200	0.300
0.87153	0.01232	0.81824	1.08334	2.200	0.400
0.83669	0.01679	0.78207	1.10161	2.200	0.500
0.79218	0.02160	0.73737	1.12506	2.200	0.600
0.73790	0.02631	0.68454	1.15409	2.200	0.700
0.67460	0.03035	0.62453	1.18894	2.200	0.800
0.60395	0.03315	0.55867	1.22957	2.200	0.900
0.52839	0.03426	0.48952	1.27560	2.200	1.000
0.45074	0.03342	0.41869	1.32632	2.200	1.100
0.37371	0.03050	0.34852	1.38071	2.200	1.200
0.29965	0.02522	0.28093	1.43749	2.200	1.300
0.23041	0.01695	0.21751	1.49519	2.200	1.400
0.16745	0.00446	0.15950	1.55217	2.200	1.500
0.11180	-0.01406	0.10770	1.60684	2.200	1.600
0.06378	-0.04083	0.06230	1.65804	2.200	1.700
0.02975	-0.05135	0.02932	1.69732	2.200	1.800
0.00000	-0.04783	0.00000	1.73384	2.200	1.900

UZ(Z,R)	UR(Z,R)	T(Z,R)	RU(Z,R)	Z	R
0.90927	0.00000	0.85357	1.06607	2.400	0.000
0.90572	0.00210	0.84969	1.06704	2.400	0.100
0.89490	0.00438	0.83803	1.07360	2.400	0.200
[illegible]	0.00693	0.81844	1.08324	2.400	0.300
0.85001	0.00977	0.79081	1.09714	2.400	0.400
0.81475	0.01283	0.75510	1.11564	2.400	0.500
0.77053	0.01593	0.71154	1.13907	2.400	0.600
0.71754	0.01879	0.66071	1.16768	2.400	0.700
0.65666	0.02108	0.60361	1.20159	2.400	0.800
0.58949	0.02247	0.54169	1.24066	2.400	0.900
0.51814	0.02273	0.47672	1.28448	2.400	1.000
0.44517	0.02175	0.41058	1.33239	2.400	1.100
0.37270	0.01951	0.34510	1.38348	2.400	1.200
0.30289	0.01614	0.28184	1.43670	2.400	1.300
0.23710	0.01186	0.22203	1.49031	2.400	1.400
0.17645	0.00705	0.16657	1.54499	2.400	1.500
0.12170	0.00224	0.11603	1.59779	2.400	1.600
0.07333	-0.00213	0.07076	1.64825	2.400	1.700
0.03401	-0.00389	0.03317	1.69264	2.400	1.800
0.00000	-0.00362	0.00000	1.73364	2.400	1.900

UZ(Z,R)	UR(Z,R)	T(Z,R)	RO(Z,R)	Z	R
0.88910	0.00000	0.82607	1.07946	2.600	0.000
0.88540	0.00233	0.82217	1.08139	2.600	0.100
0.87421	0.00480	0.81046	1.08722	2.600	0.200
0.85527	0.00749	0.79090	1.09709	2.600	0.300
0.82824	0.01040	0.76353	1.11122	2.600	0.400
0.79234	0.01347	0.72849	1.12933	2.600	0.500
0.74906	0.01653	0.68617	1.15317	2.600	0.600
0.69732	0.01937	0.63726	1.18138	2.600	0.700
0.63859	0.02172	0.58280	1.21445	2.600	0.800
0.57441	0.02332	0.52415	1.25219	2.600	0.900
0.50673	0.02397	0.46293	1.29418	2.600	1.000
0.43767	0.02357	0.40080	1.33978	2.600	1.100
0.36927	0.02208	0.33933	1.38817	2.600	1.200
0.30322	0.01954	0.27986	1.43843	2.600	1.300
0.24083	0.01608	0.22340	1.48953	2.600	1.400
0.18291	0.01191	0.17062	1.54091	2.600	1.500
0.12986	0.00738	0.12183	1.59155	2.600	1.600
0.08171	0.00310	0.07708	1.64102	2.600	1.700
0.03900	0.00061	0.03695	1.68807	2.600	1.800
0.00000	0.00056	0.00000	1.73384	2.600	1.900

UZ(Z,R)	UR(Z,R)	T(Z,R)	RO(Z,R)	Z	R
0.86813	0.00000	0.79835	1.09332	2.800	0.000
0.86433	0.00252	0.79446	1.09528	2.800	0.100
0.85290	0.00516	0.78235	1.10121	2.800	0.200
0.83368	0.00794	0.76355	1.11120	2.800	0.300
0.80650	0.01087	0.73571	1.12541	2.800	0.400
0.77130	0.01387	0.70261	1.14399	2.800	0.500
0.72828	0.01679	0.66174	1.16709	2.800	0.600
0.67800	0.01943	0.61487	1.19475	2.800	0.700
0.62150	0.02156	0.56303	1.22691	2.800	0.800
0.56024	0.02297	0.50752	1.26333	2.800	0.900
0.49593	0.02350	0.44976	1.30359	2.800	1.000
0.43046	0.02308	0.39121	1.34710	2.800	1.100
0.36564	0.02172	0.33322	1.39317	2.800	1.200
0.30277	0.01952	0.27688	1.44104	2.800	1.300
0.24293	0.01668	0.22301	1.48999	2.800	1.400
0.18686	0.01347	0.17212	1.53940	2.800	1.500
0.13464	0.01024	0.12443	1.58877	2.800	1.600
0.08625	0.00739	0.07791	1.63779	2.800	1.700
0.04166	0.00562	0.03866	1.68600	2.800	1.800
0.00000	0.00520	0.00000	1.73384	2.800	1.900

UZ(Z,R)	UR(Z,R)	T(Z,R)	RO(Z,R)	Z	R
0.84656	0.00000	0.77057	1.10755	3.000	0.000
0.84272	0.00270	0.76676	1.10953	3.000	0.100
0.83119	0.00547	0.75537	1.11550	3.000	0.200
0.81191	0.00834	0.73651	1.12552	3.000	0.300
0.78485	0.01128	0.71039	1.13970	3.000	0.400
0.75012	0.01422	0.67740	1.15813	3.000	0.500
0.70807	0.01702	0.63810	1.18088	3.000	0.600
0.65937	0.01952	0.59329	1.20793	3.000	0.700
0.60505	0.02151	0.54397	1.23917	3.000	0.800
0.54649	0.02285	0.49135	1.27435	3.000	0.900
0.48526	0.02340	0.43669	1.31305	3.000	1.000
0.42298	0.02314	0.38128	1.35477	3.000	1.100
0.36114	0.02210	0.32625	1.39891	3.000	1.200
0.30096	0.02039	0.27255	1.44435	3.000	1.300
0.24326	0.01820	0.22085	1.49203	3.000	1.400
0.18860	0.01575	0.17158	1.53994	3.000	1.500
0.13709	0.01331	0.12491	1.58825	3.000	1.600
0.08865	0.01115	0.08085	1.63674	3.000	1.700
0.04312	0.00962	0.03933	1.68520	3.000	1.800
0.00000	0.00890	0.00000	1.73384	3.000	1.900

UZ(Z,R)	UR(Z,R)	T(Z,R)	RO(Z,R)	Z	R
0.77542	0.00000	0.69468	1.15390	3.500	0.000
0.76080	0.00801	0.67142	1.16153	3.500	0.200
0.71756	0.01587	0.63208	1.18444	3.500	0.400
0.64813	0.02293	0.57015	1.22239	3.500	0.600
0.55813	0.02799	0.49133	1.27432	3.500	0.800
0.45630	0.02975	0.40356	1.33759	3.500	1.000
0.35284	0.02732	0.31509	1.40823	3.500	1.200
0.25706	0.02007	0.23330	1.48039	3.500	1.400
0.17555	0.00699	0.16332	1.54827	3.500	1.600
0.11182	-0.01397	0.10774	1.60650	3.500	1.800
0.07037	-0.02929	0.07043	1.64803	3.500	2.000
0.04622	-0.03363	0.04743	1.67553	3.500	2.200
0.02962	-0.04090	0.03033	1.69548	3.500	2.400
0.01742	-0.04338	0.01829	1.71088	3.500	2.600
0.00795	-0.04241	0.00831	1.72333	3.500	2.800
0.00000	-0.03875	0.00000	1.73334	3.500	3.000

UZ(Z,R)	UR(Z,R)	T(Z,R)	RO(Z,R)	Z	R
0.70584	0.00000	0.60625	1.19998	4.000	0.000
0.69271	0.00840	0.59491	1.20693	4.000	0.200
0.65438	0.01625	0.56202	1.22756	4.000	0.400
0.59406	0.02280	0.51088	1.26106	4.000	0.600
0.51749	0.02705	0.44576	1.30575	4.000	0.800
0.43232	0.02310	0.37613	1.35879	4.000	1.000
0.34684	0.02540	0.30553	1.41630	4.000	1.200
0.26805	0.01894	0.24027	1.47395	4.000	1.400
0.20047	0.00926	0.18371	1.52786	4.000	1.600
0.14591	-0.00252	0.13708	1.57536	4.000	1.800
0.10434	-0.01421	0.10043	1.61483	4.000	2.000
0.07322	-0.02280	0.07192	1.64692	4.000	2.200
0.04908	-0.02829	0.04897	1.67369	4.000	2.400
0.02972	-0.03096	0.03002	1.69647	4.000	2.600
0.01367	-0.03120	0.01394	1.71628	4.000	2.800
0.00000	-0.02941	0.00000	1.73384	4.000	3.000

UZ(Z,R)	UR(Z,R)	T(Z,R)	RO(Z,R)	Z	R
0.63993	0.00000	0.53594	1.24442	4.500	0.000
0.62869	0.00645	0.52670	1.25050	4.500	0.200
0.59587	0.01612	0.49999	1.26843	4.500	0.400
0.54480	0.02228	0.45369	1.29720	4.500	0.600
0.48065	0.02614	0.40713	1.33499	4.500	0.800
0.40973	0.02715	0.35055	1.37923	4.500	1.000
0.33355	0.02516	0.29318	1.42635	4.500	1.200
0.27209	0.02049	0.23938	1.47477	4.500	1.400
0.21355	0.01389	0.19125	1.52044	4.500	1.600
0.16410	0.00638	0.14965	1.56228	4.500	1.800
0.12339	-0.00090	0.11441	1.59955	4.500	2.000
0.09003	-0.00691	0.08463	1.63245	4.500	2.200
0.06226	-0.01130	0.05917	1.66169	4.500	2.400
0.03867	-0.01395	0.03705	1.68795	4.500	2.600
0.01817	-0.01489	0.01751	1.71185	4.500	2.800
0.00000	-0.01417	0.00000	1.73384	4.500	3.000

UZ(Z,R)	UR(Z,R)	T(Z,R)	RO(Z,R)	Z	R
0.59638	0.00000	0.49105	1.27455	5.000	0.000
0.58645	0.00577	0.48321	1.27997	5.000	0.200
0.55767	0.01093	0.46052	1.29590	5.000	0.400
0.51299	0.01495	0.42540	1.32135	5.000	0.600
0.45692	0.01741	0.38143	1.35406	5.000	0.800
0.39479	0.01809	0.33266	1.39363	5.000	1.000
0.33179	0.01704	0.28293	1.43574	5.000	1.200
0.27204	0.01456	0.23523	1.47861	5.000	1.400
0.21811	0.01120	0.19143	1.52027	5.000	1.600
0.17108	0.00752	0.15237	1.55947	5.000	1.800
0.13086	0.00405	0.11812	1.59553	5.000	2.000
0.09664	0.00119	0.08824	1.62839	5.000	2.200
0.06735	-0.00090	0.06207	1.65830	5.000	2.400
0.04197	-0.00220	0.03899	1.68561	5.000	2.600
0.01974	-0.00276	0.01845	1.71068	5.000	2.800
0.00000	-0.00269	0.00000	1.73384	5.000	3.000

UZ(Z,R)	UR(Z,R)	T(Z,R)	RO(Z,R)	Z	R
0.55520	0.00000	0.44387	1.30351	5.500	0.000
0.54546	0.00565	0.44318	1.30834	5.500	0.200
0.52121	0.01074	0.42382	1.32252	5.500	0.400
0.49201	0.01451	0.39379	1.34513	5.500	0.600
0.43277	0.01754	0.35503	1.37468	5.500	0.800
0.37804	0.01873	0.31385	1.40926	5.500	1.000
0.32203	0.01842	0.27034	1.44631	5.500	1.200
0.26829	0.01686	0.22795	1.48537	5.500	1.400
0.21883	0.01440	0.18827	1.52338	5.500	1.600
0.17477	0.01146	0.15207	1.55978	5.500	1.800
0.13595	0.00843	0.11753	1.59402	5.500	2.000
0.10204	0.00564	0.09144	1.62593	5.500	2.200
0.07217	0.00329	0.06437	1.65563	5.500	2.400
0.04563	0.00154	0.04088	1.68334	5.500	2.600
0.02175	0.00052	0.01954	1.70933	5.500	2.800
0.00000	0.00029	0.00000	1.73384	5.500	3.000

UZ(Z,R)	UR(Z,R)	T(Z,R)	RO(Z,R)	Z	R
0.51675	0.00000	0.41232	1.33108	6.000	0.000
0.50912	0.00544	0.40663	1.33536	6.000	0.200
0.48707	0.01033	0.39013	1.34793	6.000	0.400
0.45285	0.01427	0.36448	1.36776	6.000	0.600
0.40975	0.01696	0.33204	1.39414	6.000	0.800
0.36154	0.01827	0.29548	1.42438	6.000	1.000
0.31177	0.01824	0.25731	1.45845	6.000	1.200
0.26325	0.01710	0.21953	1.49327	6.000	1.400
0.21781	0.01516	0.18349	1.52808	6.000	1.600
0.17635	0.01278	0.14993	1.56199	6.000	1.800
0.13903	0.01029	0.11910	1.59448	6.000	2.000
0.10557	0.00795	0.09096	1.62535	6.000	2.200
0.07545	0.00595	0.06527	1.65459	6.000	2.400
0.04813	0.00442	0.04174	1.68231	6.000	2.600
0.02312	0.00344	0.02007	1.70867	6.000	2.800
0.00000	0.00304	0.00000	1.73384	6.000	3.000

UZ(Z,R)	UR(Z,R)	T(Z,R)	RO(Z,R)	Z	R
0.48087	0.00000	0.37799	1.35734	6.500	0.000
0.47426	0.00520	0.37315	1.36112	6.500	0.200
0.45509	0.00990	0.35908	1.37224	6.500	0.400
0.42525	0.01375	0.33711	1.38978	6.500	0.600
0.38751	0.01644	0.30915	1.41322	6.500	0.800
0.34495	0.01793	0.27734	1.44063	6.500	1.000
0.30057	0.01825	0.24371	1.47050	6.500	1.200
0.25663	0.01760	0.20990	1.50242	6.500	1.400
0.21476	0.01624	0.17709	1.53443	6.500	1.600
0.17578	0.01445	0.14598	1.56607	6.500	1.800
0.13907	0.01251	0.11639	1.59655	6.500	2.000
0.10722	0.01063	0.08990	1.62654	6.500	2.200
0.07721	0.00895	0.06489	1.65503	6.500	2.400
0.04957	0.00758	0.04171	1.68235	6.500	2.600
0.02394	0.00659	0.02014	1.70859	6.500	2.800
0.00000	0.00599	0.00000	1.73384	6.500	3.000

UZ(Z,R)	UR(Z,R)	T(Z,R)	RO(Z,R)	Z	R
0.44745	0.00000	0.34649	1.38235	7.000	0.000
0.44173	0.00496	0.34236	1.38570	7.000	0.200
0.42506	0.00947	0.33034	1.39554	7.000	0.400
0.39908	0.01320	0.31148	1.41126	7.000	0.600
0.36600	0.01593	0.28730	1.43194	7.000	0.800
0.32840	0.01758	0.25951	1.45647	7.000	1.000
0.28968	0.01820	0.22977	1.48367	7.000	1.200
0.24881	0.01795	0.19945	1.51246	7.000	1.400
0.21018	0.01705	0.16957	1.54196	7.000	1.600
0.17359	0.01572	0.14079	1.57148	7.000	1.800
0.13937	0.01419	0.11348	1.60055	7.000	2.000
0.10754	0.01262	0.08777	1.62892	7.000	2.200
0.07794	0.01115	0.06368	1.65644	7.000	2.400
0.05032	0.00987	0.04110	1.68307	7.000	2.600
0.02442	0.00884	0.01993	1.70835	7.000	2.800
0.00000	0.00811	0.00000	1.73384	7.000	3.000

UZ(Z,R)	UR(Z,R)	T(Z,R)	RO(Z,R)	Z	R
0.41631	0.00000	0.31748	1.40622	7.500	0.000
0.41134	0.00473	0.31394	1.40919	7.500	0.200
0.39687	0.00906	0.30363	1.41791	7.500	0.400
0.37419	0.01269	0.28737	1.43188	7.500	0.600
0.34519	0.01545	0.26633	1.45033	7.500	0.800
0.31182	0.01725	0.24202	1.47235	7.500	1.000
0.27621	0.01815	0.21565	1.49695	7.500	1.200
0.23996	0.01826	0.18341	1.52324	7.500	1.400
0.20431	0.01776	0.16119	1.55044	7.500	1.600
0.16999	0.01683	0.13462	1.57795	7.500	1.800
0.13740	0.01567	0.10903	1.60534	7.500	2.000
0.10669	0.01440	0.08476	1.63231	7.500	2.200
0.07769	0.01314	0.06174	1.65870	7.500	2.400
0.05036	0.01197	0.03999	1.68441	7.500	2.600
0.02454	0.01094	0.01944	1.70945	7.500	2.800
0.00000	0.01008	0.00000	1.73334	7.500	3.000

UZ(Z,R)	UR(Z,R)	T(Z,R)	RO(Z,R)	Z	R
0.38719	0.00000	0.29062	1.42907	8.000	0.000
0.38287	0.00451	0.28758	1.43170	8.000	0.200
0.37023	0.00867	0.27870	1.43945	8.000	0.400
0.35045	0.01222	0.26462	1.45189	8.000	0.600
0.32483	0.01500	0.24632	1.46841	8.000	0.800
0.29527	0.01695	0.22490	1.48822	8.000	1.000
0.26327	0.01808	0.20146	1.51053	8.000	1.200
0.23028	0.01850	0.17696	1.53456	8.000	1.400
0.19736	0.01835	0.15219	1.55965	8.000	1.600
0.16523	0.01777	0.12772	1.58526	8.000	1.800
0.13431	0.01692	0.10394	1.61096	8.000	2.000
0.10477	0.01590	0.08108	1.63648	8.000	2.200
0.07664	0.01481	0.05925	1.66160	8.000	2.400
0.04988	0.01373	0.03343	1.68622	8.000	2.600
0.02438	0.01269	0.01875	1.71030	8.000	2.800
0.00000	0.01173	0.00000	1.73384	8.000	3.000

UZ(Z,R)	UR(Z,R)	T(Z,R)	RO(Z,R)	Z	R
0.35986	0.00000	0.26563	1.45100	8.500	0.000
0.35610	0.00431	0.26301	1.45334	8.500	0.200
0.34512	0.00831	0.25532	1.46024	8.500	0.400
0.32773	0.01179	0.24309	1.47136	8.500	0.600
0.30516	0.01460	0.22708	1.48618	8.500	0.800
0.27878	0.01667	0.20819	1.50405	8.500	1.000
0.24995	0.01801	0.18731	1.52431	8.500	1.200
0.21989	0.01871	0.16527	1.54630	8.500	1.400
0.18952	0.01886	0.14275	1.56943	8.500	1.600
0.15947	0.01853	0.12028	1.59321	8.500	1.800
0.13025	0.01800	0.09824	1.61725	8.500	2.000
0.10202	0.01720	0.07687	1.64125	8.500	2.200
0.07490	0.01628	0.05533	1.66501	8.500	2.400
0.04890	0.01527	0.03567	1.68840	8.500	2.600
0.02395	0.01423	0.01791	1.71135	8.500	2.800
0.00000	0.01319	0.00000	1.73384	8.500	3.000

UZ(Z,R)	UR(Z,R)	T(Z,R)	RO(Z,R)	Z	R
0.33411	0.00000	0.24227	1.47212	9.000	0.000
0.33085	0.00413	0.24000	1.47420	9.000	0.200
0.32121	0.00800	0.23332	1.48037	9.000	0.400
0.30592	0.01142	0.22266	1.49033	9.000	0.600
0.28593	0.01424	0.20861	1.50365	9.000	0.800
0.26237	0.01642	0.19191	1.51980	9.000	1.000
0.23637	0.01795	0.17330	1.53822	9.000	1.200
0.20395	0.01887	0.15348	1.55833	9.000	1.400
0.18094	0.01928	0.13305	1.57962	9.000	1.600
0.15294	0.01927	0.11248	1.60164	9.000	1.800
0.12539	0.01892	0.09214	1.62403	9.000	2.000
0.09855	0.01832	0.07229	1.64649	9.000	2.200
0.07257	0.01753	0.05309	1.66882	9.000	2.400
0.04749	0.01650	0.03463	1.69067	9.000	2.600
0.02332	0.01556	0.01694	1.71235	9.000	2.800
0.00000	0.01444	0.00000	1.73384	9.000	3.000

UZ(Z,R)	UR(Z,R)	T(Z,R)	RO(Z,R)	Z	R
0.30973	0.00000	0.22034	1.49251	9.500	0.000
0.30685	0.00298	0.21837	1.49437	9.500	0.333
0.29340	0.00773	0.21255	1.49989	9.500	0.667
0.28490	0.01109	0.20322	1.50883	9.500	1.000
0.26714	0.01394	0.19087	1.52042	9.500	1.333
0.24606	0.01620	0.17609	1.53543	9.500	1.667
0.22257	0.01789	0.15950	1.55217	9.500	2.000
0.19756	0.01902	0.14169	1.57034	9.500	2.333
0.17175	0.01965	0.12319	1.59009	9.500	2.667
0.14572	0.01986	0.10444	1.61042	9.500	3.000
0.11987	0.01972	0.08577	1.63118	9.500	3.333
0.09449	0.01929	0.06744	1.65208	9.500	3.667
0.06975	0.01862	0.04762	1.67292	9.500	4.000
0.04574	0.01776	0.03242	1.69355	9.500	4.333
0.02250	0.01673	0.01588	1.71387	9.500	4.667
0.00000	0.01555	0.00000	1.73384	9.500	5.000

UZ(Z,R)	UR(Z,R)	T(Z,R)	RO(Z,R)	Z	R
0.28652	0.00000	0.19968	1.51224	10.000	0.000
0.29399	0.00385	0.19796	1.51392	10.000	0.333
0.27653	0.00750	0.19237	1.51836	10.000	0.667
0.26456	0.01081	0.18470	1.52689	10.000	1.000
0.24877	0.01367	0.17382	1.53769	10.000	1.333
0.22986	0.01602	0.16074	1.55090	10.000	1.667
0.20863	0.01784	0.14596	1.56609	10.000	2.000
0.18583	0.01914	0.13000	1.58284	10.000	2.333
0.16209	0.01996	0.11330	1.60075	10.000	2.667
0.13794	0.02037	0.09627	1.61943	10.000	3.000
0.11379	0.02040	0.07923	1.63858	10.000	3.333
0.08991	0.02011	0.06241	1.65791	10.000	3.667
0.06651	0.01955	0.04599	1.67723	10.000	4.000
0.04369	0.01875	0.03009	1.69639	10.000	4.333
0.02152	0.01772	0.01475	1.71527	10.000	4.667
0.00000	0.01649	0.00000	1.73384	10.000	5.000

UZ(Z,R)	UR(Z,R)	T(Z,R)	RO(Z,R)	Z	R
0.26432	0.00000	0.18016	1.53138	10.500	0.000
0.26206	0.00374	0.17865	1.53288	10.500	0.333
0.25549	0.00731	0.17421	1.53731	10.500	0.667
0.24488	0.01058	0.16703	1.54452	10.500	1.000
0.23077	0.01346	0.15746	1.55424	10.500	1.333
0.21379	0.01587	0.14589	1.56617	10.500	1.667
0.19460	0.01780	0.13275	1.57993	10.500	2.000
0.17383	0.01924	0.11847	1.59516	10.500	2.333
0.15204	0.02023	0.10347	1.61148	10.500	2.667
0.12972	0.02079	0.08808	1.62857	10.500	3.000
0.10725	0.02098	0.07261	1.64613	10.500	3.333
0.08492	0.02082	0.05728	1.66390	10.500	3.667
0.06292	0.02035	0.04226	1.68163	10.500	4.000
0.04140	0.01960	0.02768	1.69932	10.500	4.333
0.02042	0.01858	0.01359	1.71672	10.500	4.667
0.00000	0.01732	0.00000	1.73384	10.500	5.000

UZ(Z,R)	UR(Z,R)	T(Z,R)	RO(Z,R)	Z	R
0.24298	0.00000	0.16167	1.54995	11.000	0.000
0.24100	0.00365	0.16036	1.55129	11.000	0.333
0.23515	0.00716	0.15647	1.55526	11.000	0.667
0.22572	0.01039	0.15018	1.56172	11.000	1.000
0.21312	0.01328	0.14177	1.57046	11.000	1.333
0.19787	0.01574	0.13155	1.58120	11.000	1.667
0.18053	0.01776	0.11990	1.59362	11.000	2.000
0.16164	0.01933	0.10719	1.60740	11.000	2.333
0.14172	0.02045	0.09376	1.62222	11.000	2.667
0.12115	0.02115	0.07994	1.63776	11.000	3.000
0.10036	0.02146	0.06599	1.65376	11.000	3.333
0.07959	0.02141	0.05212	1.66997	11.000	3.667
0.05906	0.02102	0.03850	1.68620	11.000	4.000
0.03890	0.02031	0.02524	1.70231	11.000	4.333
0.01921	0.01930	0.01240	1.71821	11.000	4.667
0.00000	0.01801	0.00000	1.73384	11.000	5.000

UZ(Z,R)	UR(Z,R)	T(Z,R)	RO(Z,R)	Z	R
0.22238	0.00000	0.14416	1.56797	11.500	0.000
0.22062	0.00358	0.14301	1.56916	11.500	0.333
0.21545	0.00703	0.13961	1.57271	11.500	0.667
0.20704	0.01024	0.13412	1.57849	11.500	1.000
0.19573	0.01313	0.12673	1.58631	11.500	1.333
0.18210	0.01564	0.11775	1.59594	11.500	1.667
0.16646	0.01773	0.10746	1.60710	11.500	2.000
0.14935	0.01939	0.09620	1.61951	11.500	2.333
0.13116	0.02063	0.08426	1.63287	11.500	2.667
0.11234	0.02144	0.07193	1.64691	11.500	3.000
0.09320	0.02186	0.05944	1.66137	11.500	3.333
0.07401	0.02190	0.04699	1.67604	11.500	3.667
0.05498	0.02157	0.03474	1.69074	11.500	4.000
0.03625	0.02091	0.02279	1.70532	11.500	4.333
0.01791	0.01991	0.01120	1.71970	11.500	4.667
0.00000	0.01860	0.00000	1.73384	11.500	5.000

UZ(Z,R)	UR(Z,R)	T(Z,R)	RO(Z,R)	Z	R
0.20242	0.00000	0.12755	1.58544	12.000	0.000
0.20086	0.00352	0.12656	1.58650	12.000	0.333
0.19625	0.00692	0.12360	1.58965	12.000	0.667
0.18879	0.01011	0.11881	1.59479	12.000	1.000
0.17875	0.01300	0.11237	1.60176	12.000	1.333
0.16649	0.01555	0.10450	1.61035	12.000	1.667
0.15243	0.01770	0.09547	1.62032	12.000	2.000
0.13696	0.01944	0.08556	1.63141	12.000	2.333
0.12047	0.02077	0.07502	1.64337	12.000	2.667
0.10332	0.02167	0.06410	1.65595	12.000	3.000
0.08583	0.02218	0.05302	1.66891	12.000	3.333
0.06823	0.02229	0.04195	1.68206	12.000	3.667
0.05073	0.02202	0.03103	1.69524	12.000	4.000
0.03347	0.02139	0.02037	1.70831	12.000	4.333
0.01655	0.02040	0.01002	1.72119	12.000	4.667
0.00000	0.01908	0.00000	1.73384	12.000	5.000

UZ(Z,R)	UR(Z,R)	T(Z,R)	RO(Z,R)	Z	R
0.18302	0.00000	0.11183	1.60234	12.500	0.000
0.18164	0.00347	0.11097	1.60318	12.500	0.400
0.17755	0.00683	0.10842	1.60606	12.500	0.800
0.17094	0.00999	0.10427	1.61061	12.500	1.200
0.16201	0.01289	0.09867	1.61677	12.500	1.600
0.15107	0.01546	0.09184	1.62437	12.500	2.000
0.13343	0.01766	0.08397	1.63320	12.500	2.400
0.12457	0.01946	0.07531	1.64303	12.500	2.800
0.10971	0.02085	0.06609	1.65364	12.500	3.200
0.09419	0.02133	0.05651	1.66480	12.500	3.600
0.07832	0.02241	0.04677	1.67631	12.500	4.000
0.06231	0.02258	0.03703	1.68797	12.500	4.400
0.04535	0.02235	0.02741	1.69956	12.500	4.800
0.03061	0.02175	0.01800	1.71124	12.500	5.200
0.01514	0.02078	0.00885	1.72255	12.500	5.600
0.00000	0.01945	0.00000	1.73334	12.500	6.000

UZ(Z,R)	UR(Z,R)	T(Z,R)	RO(Z,R)	Z	R
0.16414	0.00000	0.09599	1.61864	13.000	0.000
0.16295	0.00342	0.09625	1.61946	13.000	0.400
0.15933	0.00675	0.09405	1.62190	13.000	0.800
0.15347	0.00989	0.09049	1.62588	13.000	1.200
0.14556	0.01278	0.08568	1.63128	13.000	1.600
0.13585	0.01536	0.07978	1.63794	13.000	2.000
0.12464	0.01759	0.07299	1.64569	13.000	2.400
0.11223	0.01944	0.06551	1.65431	13.000	2.800
0.09893	0.02089	0.05752	1.66362	13.000	3.200
0.08501	0.02193	0.04921	1.67341	13.000	3.600
0.07073	0.02255	0.04075	1.68350	13.000	4.000
0.05631	0.02277	0.03227	1.69373	13.000	4.400
0.04192	0.02259	0.02389	1.70396	13.000	4.800
0.02768	0.02201	0.01570	1.71410	13.000	5.200
0.01370	0.02105	0.00772	1.72407	13.000	5.600
0.00000	0.01972	0.00000	1.73334	13.000	6.000

UZ(Z,R)	UR(Z,R)	T(Z,R)	RO(Z,R)	Z	R
0.14574	0.00000	0.08302	1.63428	13.500	0.000
0.14468	0.00338	0.08239	1.63479	13.500	0.400
0.14152	0.00667	0.08052	1.63710	13.500	0.800
0.13633	0.00978	0.07749	1.64055	13.500	1.200
0.12942	0.01256	0.07340	1.64523	13.500	1.600
0.12087	0.01525	0.06838	1.65100	13.500	2.000
0.11097	0.01750	0.06258	1.65771	13.500	2.400
0.09990	0.01937	0.05619	1.66518	13.500	2.800
0.08819	0.02085	0.04936	1.67324	13.500	3.200
0.07583	0.02193	0.04224	1.68171	13.500	3.600
0.06312	0.02260	0.03499	1.69043	13.500	4.000
0.05027	0.02285	0.02772	1.69927	13.500	4.400
0.03745	0.02270	0.02053	1.70811	13.500	4.800
0.02473	0.02215	0.01349	1.71685	13.500	5.200
0.01224	0.02120	0.00664	1.72544	13.500	5.600
0.00000	0.01988	0.00000	1.73394	13.500	6.000

UZ(Z,R)	UR(Z,R)	T(Z,R)	RO(Z,R)	Z	R
0.12782	0.00000	0.06994	1.64919	14.000	0.000
0.12690	0.00333	0.06941	1.64950	14.000	0.400
0.12415	0.00658	0.06785	1.65160	14.000	0.800
0.11968	0.00966	0.06531	1.65454	14.000	1.200
0.11362	0.01252	0.06187	1.65854	14.000	1.600
0.10615	0.01510	0.05765	1.66346	14.000	2.000
0.09751	0.01735	0.05279	1.66918	14.000	2.400
0.08790	0.01924	0.04740	1.67555	14.000	2.800
0.07756	0.02074	0.04165	1.68242	14.000	3.200
0.06671	0.02185	0.03565	1.68963	14.000	3.600
0.05555	0.02254	0.02954	1.69705	14.000	4.000
0.04425	0.02282	0.02340	1.70456	14.000	4.400
0.03296	0.02269	0.01733	1.71206	14.000	4.800
0.02177	0.02216	0.01139	1.71947	14.000	5.200
0.01073	0.02124	0.00561	1.72674	14.000	5.600
0.00000	0.01992	0.00000	1.73334	14.000	6.000

UZ(Z,R)	UR(Z,R)	T(Z,R)	RO(Z,R)	Z	R
0.11046	0.00000	0.05780	1.66329	14.500	0.000
0.10960	0.00328	0.05736	1.66330	14.500	0.400
0.10723	0.00647	0.05608	1.66531	14.500	0.800
0.10340	0.00952	0.05398	1.66778	14.500	1.200
0.09817	0.01234	0.05115	1.67112	14.500	1.600
0.09176	0.01490	0.04767	1.67524	14.500	2.000
0.08431	0.01713	0.04365	1.68003	14.500	2.400
0.07602	0.01902	0.03920	1.68536	14.500	2.800
0.06709	0.02053	0.03445	1.69109	14.500	3.200
0.05772	0.02164	0.02949	1.69711	14.500	3.600
0.04807	0.02235	0.02443	1.70330	14.500	4.000
0.03829	0.02265	0.01936	1.70955	14.500	4.400
0.02852	0.02254	0.01434	1.71579	14.500	4.800
0.01884	0.02203	0.00942	1.72194	14.500	5.200
0.00932	0.02112	0.00464	1.72796	14.500	5.600
0.00000	0.01983	0.00000	1.73384	14.500	6.000

UZ(Z,R)	UR(Z,R)	T(Z,R)	RO(Z,R)	Z	R
0.09352	0.00000	0.04663	1.67647	15.000	0.000
0.09283	0.00321	0.04628	1.67669	15.000	0.400
0.09086	0.00634	0.04525	1.67812	15.000	0.800
0.08761	0.00932	0.04355	1.68014	15.000	1.200
0.08320	0.01210	0.04127	1.68287	15.000	1.600
0.07777	0.01461	0.03846	1.68625	15.000	2.000
0.07146	0.01682	0.03522	1.69016	15.000	2.400
0.06443	0.01869	0.03163	1.69451	15.000	2.800
0.05687	0.02018	0.02779	1.69918	15.000	3.200
0.04892	0.02129	0.02379	1.70409	15.000	3.600
0.04074	0.02200	0.01971	1.70912	15.000	4.000
0.03245	0.02231	0.01562	1.71420	15.000	4.400
0.02416	0.02222	0.01156	1.71925	15.000	4.800
0.01596	0.02173	0.00760	1.72423	15.000	5.200
0.00790	0.02085	0.00374	1.72910	15.000	5.600
0.00000	0.01958	0.00000	1.73384	15.000	6.000

APPENDIX C

ANALYTICAL SOLUTION OF AXIAL TEMPERATURE AND VELOCITY DECAY

The present analysis is based on the assumption that the rising air is in the turbulent motion, the turbulence being generated by the motion in the column itself, and is confined to conditions of no wind so that the axis of the column is aligned with the force of buoyance. The process taken into account are the buoyance of the column, its spreading and the entrainment of air into it, and the loss of momentum and heat by lateral diffusion.

Considering a ring-shaped volume of air as shown in Figure 2-2, in steady state yields an equation of continuity

$$\frac{\partial}{\partial z}(r u_z \rho) + \frac{\partial}{\partial r}(r u_r \rho) = 0 \qquad \text{(C-1)}$$

an equation of verticle motion

$$\frac{\partial}{\partial z}(r u_z^2 \rho) + \frac{\partial}{\partial r}(r u_z u_r \rho) = r \frac{\Delta t}{t_a} \rho g + \frac{\partial}{\partial r}(r \tau) \qquad \text{(C-2)}$$

nad an equation of heat conservation.

$$\frac{\partial}{\partial z}(r u_1 t \rho) + \frac{\partial}{\partial r}(r u_z t \rho) = \frac{1}{c_p} \frac{\partial}{\partial r}(r F) \qquad \text{(C-3)}$$

All the quantities relate to mean values for the ring, and the verticle turbulent mixing has been neglected in comparision with the horizontal. The pressure is auumed to be undisturbed, the density is treated as constant except in so far as it affects the buoyance.

From Equation (C-1) and (C-2) may be derived the kinetic energy equation

$$\frac{\partial}{\partial z}\left(\frac{1}{2} r u_z^3 \rho\right) + \frac{\partial}{\partial r}\left(\frac{1}{2} r u_r u_z^2 \rho\right) = r u_z \frac{\Delta t}{t_a} \rho g + u_z \frac{\partial}{\partial r}(r\tau) \qquad \text{(C-4)}$$

and from Equation (C-1) and (C-3), yield

$$\frac{\partial}{\partial z}(r u_z \Delta t \rho) + \frac{\partial}{\partial r}(r u_r \Delta t \rho) = -\frac{1}{c_p}\frac{\partial}{\partial r}(rF) - r u_z \rho \frac{\partial t_a}{\partial z} \qquad \text{(C-5)}$$

Equations (C-2), (C-4), and (c-5) are integrated from r=0 to r=∞ with the boundary conditions given in Chapter III which implies that at a sufficient radial distance, there will be no momentum transfer and heat flow. The Equations become,

$$\frac{d}{dz}\int_0^\infty r u_z^2 \rho \, dr = \int_0^\infty r \frac{\Delta t}{t_a} \rho g \, dr \qquad \text{(C-6)}$$

$$\frac{d}{dz}\int_0^\infty \frac{1}{2} r u_z^3 \rho \, dr = \int_0^\infty r u_z \frac{\Delta t}{t_a} \rho g \, dr - \int_0^\infty r\tau \frac{\partial u_z}{\partial r} dr \qquad \text{(C-7)}$$

$$\frac{d}{dz}\int_0^\infty r u_z \Delta t \rho \, dr = -\int_0^\infty r u_z \rho \frac{\partial t_a}{\partial z} dr \qquad \text{(C-8)}$$

Equation (C-6) states that the verticle gradient of momentum flux is equal to the buoyance of a horizontal stratum of unit thickness. Equation (C-7) states that the verticle gradient of flux of kinetic energy is equal to the rate at which work is done by buoyant force less that rate which work is done by the turbulent shear. Equation (C-8) expresses the incremental weight flux past all successives planes; when the ambient air is constant, neutral condition, i.e., $\frac{\partial t_a}{\partial z}=0$, the increment is constant.

In order to solve the equations analytically, it is assumed that the shearing stress is a quadratic function of the relative velocity, i.e.,

$$\tau = 1/2 \ \rho u_{zm}^2 j(\frac{r}{R}) \tag{C-9}$$

and the similarity hypothesis is good for the radial profiles of Δt and u_z. Following the argument of Sutton [10] that the profiles are Gaussian and the measures of dispersion are approximately at least, the same for Δt and u_z, for which experimental confirmation in the laboratory had been provided by Rouse et al. [9] and by Railston [5], Δt and u_z are taking as

$$\Delta t = \Delta t_m \exp\left(-\frac{r^2}{2R_m^2}\right) \tag{C-10}$$

$$u_z = u_{zm} \exp\left(-\frac{r^2}{2R_m^2}\right) \tag{C-11}$$

Substituting Equation (C-9), (C-10), and (C-11) into (C-6), (C-7), and (C-8) and then integrating gives

$$\frac{d}{dz}(R_m^2 u_{zm}^2) = 2R_m^2 \frac{\Delta t_m}{t_a} g \tag{C-12}$$

$$\frac{d}{dz}(R_m^2 u_{zm}^2) = 3R_m^2 u_{zm} \frac{\Delta t_m}{t_a} g - \alpha R_m u_{zm}^3 \tag{C-14}$$

No assumption has been made about the form of the function j, i.e. the value of α; to the extent that is justifiable to assume that the relation between τ and u_{zm}^2 is independent of the stability of the enviroment, α becomes a universal constant. Multiplying Equation (C-12) by $3u_{zm}$ and (C-13) by 2 and subtracting it follows immediately that

$$\frac{dR_m}{dz} = \alpha \qquad \text{or } R_m = \alpha z' \tag{C-15}$$

where $z' = z + z_o$. Further Δt_m and u_{zm} are solved by integrating factor method from the equations, the final form are:

$$\Delta t_m = \frac{A_1}{\alpha^2 z'^2} \left[\frac{3}{2} \frac{A_1 g}{t_a \alpha^2 z'} + \frac{A_2}{z'^3} \right]^{-1/3} \tag{C-16}$$

$$u_{zm} = \left[\frac{3}{2} \frac{A_1 g}{t_a \alpha^2 z'} + \frac{A_2}{z'^3} \right]^{1/3} \tag{C-17}$$

APPENDIX D

NON-LINEAR LEAST SQUARE FIT PROGRAM AND RESULT FOR THE SPREADING COEFFICIENT

The program set up is based on Scraborough's [23] non-linear least square fit method. Equation (3-33) is the key equation to solve for the spreading coefficient, α , of the free jet from the experimental data of axial temperature and velocity decay. An iterative procedure was used until the absolute difference of the new α and the old α is less than 5% of the new α.

```
$$WATFIV
C      CALCULATE THE SPREADING COEFFICIENT OF FREE JET
C      BY SCARBOROUGH'S NON-LINEAR SQUARE FIT METHOD
       REAL M1,M2,M3,M4,M5
       DIMENSION UZ(20),T(20),Z(20),UYA(20),UYC(20)
      1, TYA(20),TYC(20),DUY(20), DTY(20),ZT(20),ZU(20),
      3ZTA(20),ZUA(20),TC(20),UZC(20)
       READ (5,100) N, U0,T0,TA, D, ZCV, ZCT, AFO
 100   FORMAT (I10,7F10.3)
       READ (5,101)    (Z(I), I=1,N)
       READ (5,101) (UZ(I),I=1,N)
       READ (5,101) (T(I),     I=1,N)
 101   FORMAT(8F10.3)
       DT=T0-TA
       R0=0.5*D
       M1=0.25*D**2*U0*DT
       M2=0.375*D**2*U0*DT*32.2/TA
       M3=0.125*D**3
       M4=U0**3
       M5=0.75*D*U0*DT*32.2/TA
       TAFO=AFO
       NN=0
   20  ST=0.
       STD=0.
       DO 10 I=1,N
       TYA(I)= M1**3/((T(I)-TA)**3)
       ZT(I)=Z(I)-ZCT
       ZTA(I)=R0+ ZT(I)*TAFO
       TYC(I)=M2*ZTA(I)**5./TAFO +M3*M4*ZTA(I)**3.
      1-M3*M5*ZTA(I)**3/TAFO
       WRITE (6,52) ZTA(I),ZT(I), TAFO
  52   FORMAT (3F10.3)
       DTY(I)=-M2*ZTA(I)**5/TAFO*TAFO
      1 +5.*ZT(I)*M2*ZTA(I)**4./TAFO
      1+3.*M3*M4*ZT(I)*ZTA(I)**2+M3*M5*ZTA(I)**3/TAFO*TAFO
      3-2*M3*M5*ZT(I)*ZTA(I)**2/TAFO
       ST=ST+(TYC(I)-TYA(I))*DTY(I)
       STD= STD+ DTY(I)*DTY(I)
   10  CONTINUE
       TAF=TAFO+ ST/STD
        TDA= ABS((TAF-TAFO)/TAFO)
       IF (TDA.LE.0.05) GO TO 30
       NN=NN+1
       TAFO=TAF
       IF (NN.GE.15) GO TO 31
       GO TO 20
   31  WRITE (6,102) NN
  102  FORMAT(20X,'NN=',I3)
   30  L=0
       UAFO=AFO
   40  SU=0.
       SUD=0.
       DO 50 I=1,N
       UYA(I)=UZ(I)**3.
        ZU(I)=Z(I)-ZCV
       ZUA(I)=R0+ZU(I)*UAFO
       WRITE (6,52) ZU(I),ZUA(I), UAFO
       UYC(I)=M2/(UAFO*ZUA(I))+M3*(M4-M5/UAFO)/(ZUA(I)**3.)
       DUY(I)=-M2*(2.*UAFO*ZU(I)+R0)/(UAFO*ZUA(I) *
      6UAFO*ZUA(I))
      1-M3*M5/(UAFO*UAFO
      1                   *ZUA(I)**3)-3*M3*(M4-M5/UAFO)*ZU(I)/
      2ZUA(I)**4.
        SU=SU+(UYC(I)-UYA(I))*DUY(I)
        SUD=SUD+DUY(I)*DUY(I)
   50  CONTINUE
       UAF=UAFO+SU/SUD
       UDA= ABS((TAF-TAFO)/TAFO)
       IF (UDA.LE.0.05) GO TO 60
       L=L+1
```

```
      UAFO=UAF
      IF (L.GE.15) GO TO 41
      GO TO 40
   41 WRITE (6,99) L
   99 FORMAT (20X,'L=',I3)
   60 WRITE(6,110) UO,TO,TA,D
  110 FORMAT(1H1,/////,30X,'CALCULATE THE SPREADING
     1COEFFICIENT OF FREE JET',
     1/,20X,'BY NON-LINEAR LEAST SQUARE FIT METHOD',
     3//, 30X, 'EXIT VELOCITY, FT/SEC=',F10.5,/,
     430X,'EXIT PLUME TEMPERATURE, DEG. R =',F10.5,/,
     530X,'AMBIENT TEMPERATURE, DEG. R=',F10.5,/,
     630X,'DIAMETER OF THE STACK, FT =',F10.5,/)
      WRITE (6,999) UAF, TAF
  999 FORMAT (/,30X, 'SPREADING COEFFICIENT FOR VEL.',
     1'DECAY=',F6.3,/,
     230X,'SPREADING COEFFICIENT FOR TEMP. DECAY=',F6.3)
      WRITE (6,120)
  120 FORMAT(///,10X,'Z',10X,'UZ(Z)',8X,'UZ(Z) CAL.',
     16X,'T(Z)',6X,'T(Z) CAL.')
      SDT=0.
      SDU=0.
      ADT=0.
      ADU=0.
      DO 70 I=1,N
      TC(I)=M1/(TYC(I)*0.333)-TA
      UZC(I)=UYC(I)**0.3333
      SDT= (ABS(TC(I)-T(I)))*2 +SDT
      SDU=(ABS(UZC(I)-UZ(I)))**2. +SDU
      ADT=ABS((TC(I)-T(I))/T(I))+ADT
      ADU=ABS ((UZC(I)-UZ(I))/UZ(I))+ADU
      WRITE (6,130) Z(I),UZ(I),UZC(I),T(I),TC(I)
  130 FORMAT (5F15.2)
   70 CONTINUE
      SDT=(SDT/N)**0.5
      ADT=ADT/N*100.
      SDU=(SDU/N)**0.5
      ADU= (ADU/N )*100.
      WRITE (6,140) SDU,ADU,SDT,ADT
  140 FORMAT(//,30X,'AXIAL DECAY OF VELOCITY',/,
     130X,'STD. DEVIATION=',F6.2,/,
     230X,'AVG. PERCENT DEVIATION=',F6.2,//,
     330X,' AXIAL DECAY OF TEMPERATURE',/,
     430X,'STD.DEVIATION=',F6.2,/,
     530X,'AVG. PERCENT DEVIATION=',F6.2)
      STOP
      END
```

CALCULATE THE SPREADING COEFICIENT OF FREE JET
BY NON-LINEAR LEAST SQUARE FIT METHOD

EXIT VELOCITY, FT/SEC= 37.30
EXIT TEMPERATURE,DEG. R = 912.00
AMBIENT TEMPERATURE, DEG. R= 526.00
DIAMETER OF THE JET,FI= 0.340E 01

SPREADING COEFFICIENT FOR VEL.DECAY= 0.145
SPREADING COEFFICIENT FOR TEMP. DECAY= 0.141

Z	UZ(Z)	UZ(Z) CAL.	T(Z)	T(Z) CAL.
2.00	35.40	36.17	879.20	870.37
2.50	33.90	33.00	850.20	845.96
3.00	31.30	31.11	823.20	811.07
4.00	26.50	26.23	761.50	763.78
5.00	22.40	21.37	722.90	730.01
6.00	19.40	17.89	688.10	694.56
7.00	16.40	14.72	665.00	672.88
8.00	13.80	12.10	641.80	655.92
9.00	11.90	9.23	622.50	637.40
10.00	10.40	8.35	603.20	618.54

AXIAL DECAY OF VELOCITY
STD. DEVIATION= 2.11
AVG. PERCENT DEVIATION= 4.51

AXIAL DECAY OF TEMPERATURE
STD.DEVIATION= 12.73
AVG. PERCENT DEVIATION= 5.39

CALCULATE THE SPREADING COEFICIENT OF FREE JET
BY NON-LINEAR LEAST SQUARE FIT METHOD

EXIT VELOCITY, FT/SEC= 35.60
EXIT TEMPERATURE,DEG. R = 916.20
AMBIENT TEMPERATURE, DEG. R= 526.00
DIAMETER OF THE JET,FT= 0.340E 01

SPREADING COEFFICIENT FOR VEL.DECAY= 0.150
SPREADING COEFFICIENT FOR TEMP. DECAY= 0.147

Z	UZ(Z)	UZ(Z) CAL.	T(Z)	T(Z) CAL.
2.00	34.18	35.11	877.00	865.12
2.50	32.04	31.37	845.10	837.53
3.00	29.90	28.82	814.60	810.47
4.00	24.92	24.00	760.00	755.57
5.00	21.36	21.20	724.90	720.31
6.00	18.15	19.51	689.80	692.87
7.00	15.66	16.68	662.50	670.35
8.00	12.82	13.99	643.00	655.20
9.00	11.04	13.05	623.50	640.10
10.00	9.26	11.48	611.80	632.19

AXIAL DECAY OF VELOCITY
STD. DEVIATION= 2.02
AVG. PERCENT DEVIATION= 4.28

AXIAL DECAY OF TEMPERATURE
STD.DEVIATION= 11.20
AVG. PERCENT DEVIATION= 4.43

CALCULATE THE SPREADING COEFICIENT OF FREE JET
BY NON-LINEAR LEAST SQUARE FIT METHOD

EXIT VELOCITY, FT/SEC= 78.00
EXIT TEMPERATURE,DEG. R =1058.00
AMBIENT TEMPERATURE, DEG. R= 523.80
DIAMETER OF THE JET,FT= 0.830E-01

SPREADING COEFFICIENT FOR VEL.DECAY= 0.105
SPREADING COEFFICIENT FOR TEMP. DECAY= 0.097

Z	UZ(Z)	UZ(Z) CAL.	T(Z)	T(Z) CAL.
4.00	75.60	76.44	1004.50	983.00
5.00	70.20	68.64	940.47	919.23
6.00	62.40	59.28	881.70	871.03
7.00	54.80	53.04	822.95	833.63
8.00	46.80	48.36	790.90	801.58
9.00	42.12	42.90	764.19	769.53
10.00	37.40	39.01	737.51	748.16
11.00	32.00	34.32	710.77	726.79
12.00	30.42	32.76	694.74	705.43
13.00	27.30	29.64	684.06	694.74

AXIAL DECAY OF VELOCITY
STD. DEVIATION= 6.20
AVG. PERCENT DEVIATION= 6.43

AXIAL DECAY OF TEMPERATURE
STD.DEVIATION= 20.50
AVG. PERCENT DEVIATION= 4.90

CALCULATE THE SPREADING COEFICIENT OF FREE JET
BY NON-LINEAR LEAST SQUARE FIT METHOD

EXIT VELOCITY, FT/SEC= 822.00
EXIT TEMPERATURE,DEG. R =1413.00
AMBIENT TEMPERATURE, DEG. R= 527.40
DIAMETER OF THE JET,FT= 0.208E-01

SPREADING COEFFICIENT FOR VEL.DECAY= 0.082
SPREADING COEFFICIENT FOR TEMP. DECAY= 0.070

Z	UZ(Z)	UZ(Z) CAL.	T(Z)	T(Z) CAL.
6.00	715.14	731.58	1218.40	1227.26
7.00	657.60	674.04	1147.53	1151.96
8.00	591.84	600.06	1094.38	1085.52
9.00	534.00	526.08	1058.94	1041.22
10.00	484.98	493.02	1005.79	996.93
11.00	443.88	460.10	970.35	961.49
12.00	402.78	411.09	926.06	918.97
13.00	345.27	394.56	899.48	897.71

AXIAL DECAY OF VELOCITY
STD. DEVIATION= 10.20
AVG. PERCENT DEVIATION= 5.50

AXIAL DECAY OF TEMPERATURE
STD.DEVIATION= 28.00
AVG. PERCENT DEVIATION= 3.80

APPENDIX E

COMPUTER PROGRAM FOR IRRS SIGNAL PROCESSING

The first program, 'Experimental Spectrogram of CO' recalls the experimental data of Mahagaokar [14] and print it out in the way as it was digitised in the tape. The second program, 'Simulated Spectrogram of CO' generates the P-R structure of CO and also the spectrogram that resembles the way as it was obtained from experiment.

```
      DIMENSION YSPEC(2100),NFILE(20),
     1 N(20),   TEMP(20),NPK(20)
      DIMENSION Y(126) ,X(126)
      DIMENSION IXUNT(6), IYUNT(6), LIST(8)
      DATA IXUNT/'WAVE',' NUM','BER ','CM- ',' ',' '/
      DATA IYUNT/'SPEC','TRUM',' INT','ENSI','TY V','ALUE'/
      DATA LIST/'    ','    ','    ','    ','    ','    ',
     1'    ','    '/
      DATA N/312,322/
      DATA NFILE/1,5/
      DATA NPK/256,118/
       DATA TEMP/510.,510./
      DO 1000 I=1,2
      WRITE (6,104) N(I),NFILE(I),NPK(I)
  104 FORMAT(1H1,10X,'WAVE-NUMBER VS SPECTROGRAM VALUE',/,
     110X,'RUN # =',
     1I3,10X,'FILE # =',I3,20X,'NPK=',I3)
      READ (1,102) (YSPEC(J),J=1,2046)
  102 FORMAT (11F12.5)
      NNPK=NPK(I)
      READ (1,102) (YSPEC(J),J=1,NNPK)
      READ (1,102)          (YSPEC(J),J=1,2048)
    1 READ(1,102,END=103)
      WRITE (6,111)
  111 FORMAT (1X, 'DUMMY')
      GO TO 1
  103 CONTINUE
      SV=0.
      DO 998 J= 1067,1151
      SV=SV+ YSPEC(J)
  998 CONTINUE
      WRITE (6,11) SV
   11 FORMAT (20X,'SV=', F10.5)
      DO 999 J=1036,1162
      ANU=1.92781*J
      JJ=J-1035
      Y(JJ)=YSPEC(J)/SV
      X(JJ)=ANU
      WRITE (6,105) J, ANU,YSPEC(J),Y(JJ)
  999 CONTINUE
  105 FORMAT (20X,I5,3(5X,F12.5) )
      VMAX=3.830*(SQRT(0.180527*TEMP(I)) +0.5)
      PVMAX=2143.26- VMAX
      RVMAX=2143.26 + VMAX
      WRITE(6,112) TEMP(I),PVMAX,RVMAX
  112 FORMAT (1H1,20X,'TEMP,K=' ,F10.5,/,20X,'PVMAX=',
     1F10.5,/,20X,'RVMAX=',F10.5)
      CALL PLOT1 ( 1997.2107,1.9278,Y,126,0.,0.,1,LIST,
     11.,IYUNT,IXUNT)
 1000 CONTINUE
      END
```

```
      DIMENSION F(3,150), E(3,150) , FF(150)
      DIMENSION XX(200), A(200), RS(200)
      DIMENSION  TEMP(100), V(10), Y(100), X(200)
      DIMENSION IXUNT(6), IYUNT(6), LIST(8)
      DATA LIST/'    ','    ','    ','    ','    ','    ','
     1'    ','    '/
      DATA IXUNT/'    ','    ','    ','    ','    ','    '/
      DATA IYUNT/'    ','    ','    ','    ','    ','    '/
      TEMP(1)=510.
      V(1)=0.
      V(2)=1.
      HC=1.98768E-23
      B=1.92
      W0=2143.28
      RK=1.38054E-23
      I=1
      DO 998 K=1,2
      WRITE (6,1) TEMP (I)
    1 FORMAT (1H1,10X,'TEMP,K',F10.2,/,20X, 'J',15X,'E(V,J)',
     122X,'F(V,J)')
      DO 997 J=1,40
      M=J-1
       E(K,J)=HC*B*M*(M+1)
      F(K,J)=(2*M +1) * EXP(- E(K,J)/(RK*TEMP(I)))
      WRITE (6,5) M, E(K,J), F(K,J)
    5 FORMAT (20X,I3,13X,E12.5,10X,E12.5)
  997 CONTINUE
  998 CONTINUE
      FF(40)=0.
      DO 995  J=1,39
      J2=41-J
      J1=40-J
      JR=80-J
      FF(J)=F(1,J2)
      FF(JR)=FF(J)
  995 CONTINUE
      SFT=0.
      DO 5354 N=1,79
      SFT=SFT+FF(N)
 5354 CONTINUE
      DO 996 N=1,79
      Y(N)=FF(N)/SFT
      X(N)=1993.20+ (N-1)*3.84
      WRITE (6,10)  N, X(N), Y(N), FF(N)
   10 FORMAT ( 30X,I3,20X,F10.5,10X,E10.5,10X,E10.5)
  996 CONTINUE
      SF1=0.
      DO 5355 N=18,60
      SF1=SF1+Y(N)
 5355 CONTINUE
      SF2=0.
      DO 5356 N=25,55
      SF2=SF2+Y(N)
 5356 CONTINUE
      WRITE (6,11) SFT, SF1, SF2
   11 FORMAT (///,20X,'SFT=',F10.5,/,20X,'SF1=',F10.5,/,
     520X,'SF2=',F10.5)
      CALL PLOT1 (1993.20,3.84    ,Y, 79,0.0,0.0,1,LIST,
     11.,IYUNT,IXUNT)
       DO 679 III=11,21,2
      DO 600  J=1033,1185
      NN=J-1032
      XX(NN)=1.9287*J-0.1*III
      XX1=XX(NN)-2.
      XX2=XX(NN)+2.
      XN=(XX(NN)-1993.20)/3.84 +1.
      N=IFIX(XN)
      K=N+1
```

```
          X(N)  =1993.20 + (N-1)*3.84
          X1= X(N)- 0.227
          X2= X(N) + 0.227
          XA1= X1+3.8
          XA2= X2+3.80
          IF (XX1.LT.X1.AND.XX2.LT.XA1) GO TO 500
          IF (XX1.LT.X1.AND.XX2.GT.XA1) GO TO 701
          IF (X1.LT.XX1.AND.XX2.LT.XA2) GO TO 501
          IF (XX1.LT.X2.AND.XX2.GT.XA2) GO TO 702
          IF (XX2. GE.XA2) GO TO 502
    500   A(NN)=0.227*Y(N)
          GO TO 600
    701   A(NN)=0.227*Y(N) +0.5*((XX2-XA1)**2)*Y(N+1)/0.227
           GO TO 600
    501   DA1= (XX1-X1)/0.227
          IF (DA1-1.)  550,550,551
    550   A1=0.227*Y(N)-Y(N)*DA1*(XX1-X1)*0.5
          GO TO 552
    551   A1= (DA1-1.)*Y(N)*(X2-XX1)
    552   DA2= (XA2-XX2)/0.227
          IF (DA2-1.)560,560,561
    560   A2=0.227*Y(K)-Y(K)*DA2*(XA2-XX2)*0.5
          GO TO 570
    561   A2= (DA2-1.)*Y(K) *(XX2-XA1)
    570   A(NN)=A1+ A2
          GO TO 600
    702    A(NN)=0.227*Y(N+1) +0.5*((X2-XX1)**2)*Y(N)/0.227
           GO TO 600
    502   A(NN)=0.227*Y(K)
    600   CONTINUE
          ASFT=0.
          DO 601 NN=1,152
          ASFT=ASFT+A(NN)
    601   CONTINUE
          ASF1=0.
           DO 5359  NN=35,117
          ASF1=ASF1+A(NN)
   5359   CONTINUE
          ASF2=0.
           DO 5360 NN=47,107
          ASF2=ASF2+A(NN)
   5360   CONTINUE
          WRITE (6,12)   ASFT,ASF1,ASF2
     12   FORMAT (///,20X,'ASFT=',F10.5,/,20X,'ASF1=',F10.5,/,
         120X,'ASF2=',F10.5)
          DO 602 NN=1, 152
          RS(NN)=A(NN)/ASFT
          WRITE(6,10)  NN,XX(NN), A(NN), RS(NN)
    602   CONTINUE
          CALL PLOT1 (1993.20,1.9278,RS,152,0.,0.,1,LIST,1.,
         2IYUNT,IXUNT)
    679   CONTINUE
          STOP
          END
```